# BEHAVIOR AND ANALYSIS OF A MODEL SOIL - ICE BARRIER

Thesis for the Degree of Ph. D.
MICHIGAN STATE UNIVERSITY
DAVID L. WARDER
1969



# This is to certify that the

#### thesis entitled

"Behavior and Analysis of a Model Soil-Ice Barrier"

# presented by

David L. Warder

has been accepted towards fulfillment of the requirements for

Ph. D. degree in Civil Engineering

O.B. Unlevelan

Date August 5, 1969

de

#### ABSTRACT

# BEHAVIOR AND ANALYSIS OF A MODEL SOIL-ICE BARRIER

By

# David L. Warder

The strength and impermeability of frozen soil render it useful as a temporary barrier in certain types of engineering construction. In this study, the use of artificially frozen soil as a barrier around the periphery of a model shaft was investigated with regard to the stress-deformation characteristics of the soil-ice cylinder. Two analyses are proposed and are compared with results of an experimental program.

The first analysis involves the extension of a creep equation proposed by AlNouri (1969). After making certain simplifying assumptions, this constitutive relationship was solved together with the equation of equilibrium, the compatibility equation, and the straindisplacement definitions. This analysis gives expressions for stresses, strain rates, and displacement rates which are applicable to the steady state portion of the creep curve. The second approach is based on the use of time dependent strength parameters, concepts from the

Mohr-Coulomb failure theory, and the conditions for plastic equilibrium in the frozen soil.

The experimental program consisted of loading hollow, cylindrical, frozen soil models by an outside pressure in a special test cell. Radial deformation at the inner surface was measured at various time intervals after application of the load. The axial force on the cylinder was also measured using a load cell mounted in the base of the test cell. The low temperatures necessary were maintained by submerging the entire apparatus in a cooled ethylene glycol-water solution. Tests were conducted on a sand-ice material and a frozen Ontonagon clay.

Measured displacement rates at the inner surface were compared with those predicted by the analysis.

Additional parameters were introduced in order to obtain agreement. A comparison of the measured and calculated values of axial force provided reasonably good agreement in most instances.

The behavior of the two soil types studied was found to be vastly different. The sand-ice material showed very little deformation during primary creep and rapidly approached a well defined steady deformation state. The axial force in the sample was noted to increase at a decreasing rate with time. This reflects the stiff nature of the material and its delay in reaching a final stress state. By contrast, the frozen

clay exhibited relatively large deformations during primary creep and a greater delay before approaching a more poorly defined steady state creep. Due to this greater ability to flow and a tendency to reach a final stress state quickly, the measured total axial force was found to reach a constant value almost immediately after loading.

# BEHAVIOR AND ANALYSIS OF A MODEL SOIL-ICE BARRIER

Ву

David L. Warder

# A THESIS

Submitted to
Michigan State University
in partial fulfillment of the requirements
for the degree of

DOCTOR OF PHILOSOPHY

Department of Civil Engineering

7-17-70 854401

#### ACKNOWLEDGMENTS

The writer wishes to express his sincere appreciation to Dr. O. B. Andersland, Professor of Civil Engineering, under whose direction this research was performed, for his patience, guidance, and encouragement throughout the preparation of this thesis. Thanks are also due the other members of the writer's guidance committee: Dr. C. E. Cutts, Chairman and Professor of Civil Engineering, Dr. W. A. Bradley, Professor of Applied Mechanics, and Dr. J. W. Trow, Professor of Geology. writer owes a debt of gratitude to Dr. R. R. Goughnour, Associate Professor of Civil Engineering, for his many worthwhile suggestions, and to Mr. R. W. Laza for his assistance in the laboratory. To Mr. Leo Szafranski and Mr. Don Childs of the Division of Engineering Research Machine Shop, special thanks for their cooperation in the fabrication of experimental equipment.

In addition to those acknowledged above, the writer wishes to thank the National Science Foundation and the Division of Engineering Research at Michigan State University for the financial assistance which made this research possible.

# TABLE OF CONTENTS

F	age
ACKNOWLEDGMENTS	ii
LIST OF TABLES	v
LIST OF FIGURES	vii
LIST OF APPENDICES	ix
NOTATIONS	х
CHAPTER	
I. INTRODUCTION	1
II. LITERATURE REVIEW	6
2.1 Field Practice	6 11 18 21
III. SOILS STUDIED AND SAMPLE PREPARATION	23
3.1 Soils Studied	23 24 24
Samples	27 28
IV. TESTING EQUIPMENT AND PROCEDURES	31
4.1 Equipment	31 31
Apparatus	34 35 37 38 38 39
V. THEORETICAL CONSIDERATIONS	42
5.1 Formulation of the Problem	42 46

CHAPTE	R			Page
	5.3	Analysis Based on Time Dependent Strength Parameters	•	51
VI.	EXPERI	MENTAL RESULTS	•	57
	6.2	General	•	57 60 60 64 69
VII.	DISCUS	SION AND INTERPRETATION OF RESULTS	•	73
	•	General		73 75
	7.3	Equation Analysis	•	75 89 92
VIII.		SIONS AND RECOMMENDATIONS FOR FURTHER CH	•	99
	8.1 8.2	Summary of Conclusions Suggestions for Further Research		99 102
BIBLIO	GRAPHY		•	104
APPEND	TCES .			107

# LIST OF TABLES

Table		Page
3.1	Index properties of Ontonagon clay	. 25
3.2	Mineralogical properties of Ontonagon clay .	. 25
6.1	Summary of sand-ice tests	. 61
6.2	Sand-ice displacement rate results	. 65
6.3	Summary of frozen clay tests	. 66
6.4	Frozen clay displacement rate results	. 66
7.1	Summary of displacement rate comparisons using Equation (5.23'), sand-ice	. 78
7.2	Summary of displacement rate comparisons using Equation (5.23"), sand-ice	. 82
7.3	Results of total axial force calculations .	. 87
7.4	Values of $\alpha$ (From AlNouri, 1969)	. 90
7.5	Data for c-¢ analysis	. 91
7.6	Summary of comparisons for $c-\phi$ analysis	• 93
A-1	Test data, SA-4	. 108
A-2	Test data, SA-6	. 111
A-3	Test data, SA-7	. 113
A-4	Test data, SA-8	. 116
A-5	Test data, SA-9	. 119
<b>A-</b> 6	Test data, SA-11	. 122
A-7	Test data, SA-12	. 125
A-8	Test data, SA-14	. 128
A-9	Test data, SA-16	. 130
A-10	Test data, SA-18	. 132
A-11	Test data, C-3	. 134
A-12	Test data, C-4	. 136

Table		Page
A-13	Test data, C-5	138
B-1	Calibration data for deformation measuring device	142
B-2	Calibration data for load cell	145
C-1	Values of $u_m$ and $\epsilon_{\theta m}$	149

# LIST OF FIGURES

Figure	Pa	zе
2.1	Typical Creep Curve for Frozen Soil	15
2.2	Elasto-Plasto-Viscous Model	15
3.1	Preparation Mold and Drilling Accessories	26
3.2	Preparation Mold and Accessories for Varying Sample Size	29
3.3	Preparation of Clay Sample	29
4.1	Test Cell Detail	32
4.2	Test Cell	33
4.3	Deformation Measuring Device	36
4.4	Pressure System	36
4.5	Clay Sample Mounted in Test Cell	40
4.6	Test Set-Up	40
5.1	Sketch of Model Soil-Ice Barrier	43
5.2	Distribution of $\dot{u}$ and $\dot{\epsilon}_{\theta}$ for a unit rate of displacement at inner surface	52
5.3	Mohr Circle Representation	53
6.1	Time-Displacement Plot for Test SA-9	52
6.2	Time-Displacement Plot for Test SA-11	63
6.3	Time-Displacement Plot for Test C-4	67
6.4	Time-Axial Force Plot for Test SA-11	70
6.5	Time-Axial Force Plot for Test SA-12	71
6.6	Time-Axial Force Plot for Test C-5	72
6.7	Time-Axial Force Plot for Test C-4	72
7.1	Range of Strain Rates, Sand-Ice	74
7.2	Range of Strain Rates, Frozen Clay	74
7.3	Graphical Comparison, Sand-Ice, Equation (5.23')	80

Figure		Page
7.4	Graphical Comparison, Sand-Ice, Equation (5.23') (Modified)	81
7.5	Graphical Comparison, Sand-Ice, Equation (5.23")	83
7.6	Graphical Comparison, Sand-Ice, Equation (5.23") (Modified)	85
7.7	Distribution of $\sigma_r$ and $\sigma_\theta$ According to Equations (5.22a) and (5.22b)	86
7.8	Sketch Showing Development of Radial Stress Distribution	87
7.9	Plot of ε vs α	90
7.10	Distribution of $\sigma_n$ and $\sigma_\theta$ According to Equations (5.28) and (5.25')	94
7.11	Graphical Comparison, Frozen Clay, Equation (5.23') (Modified)	96
B-1	Calibration Curve for Deformation Measuring Device	143
B-2	Calibration Curve for Load Cell	146

Append

A

В

C

# LIST OF APPENDICES

Appendix																				Page
A	Test Da	ata .	•	•	•	•	•	•	•	•	•	•	•	•	•	•	•	•	•	107
В	Calibra	ation	Da	ta	Ļ	•	•	•	•	•	•	•	•	•	•	•	•	•	•	140
С	Sample	Calc	ula	ıti	on	s											•			147

#### NOTATIONS

a = inner radius of hollow, circular cylinder

 $A,m_1$  = experimental parameters (Vialov, 1965b)

b = outer radius of hollow, circular cylinder

 $B,C_1$  = experimental parameters (Andersland and Akili, 1967)

c = time dependent cohesion

C,N,m = experimental parameters (AlNouri, 1969)

 $F_z$  = total axial force

h = height of cylinder

 $k_1, k_2, k_3$  = constants of integration

 $K_1, K_2, n_1, n_2$  = experimental parameters (Goughnour and Andersland, 1968)

 $N = \tan (45^{\circ} + \frac{9}{2})$ 

p = radial pressure on cylinder

$$Q = \sqrt{3/2} N - m/2$$

Q' = XN-m/2

$$Q'' = \sqrt{3/2} N - Ym/2$$

 $r, \theta, z$  = orthogonal coordinates in the radial, circumferential and axial directions

t = time

T = intensity of tangential stresses (Vialov, 1965b)

u = displacement in radial direction

 $\dot{\mathbf{u}}$  = time derivative of  $\mathbf{u}$ 

x,y,z = orthogonal rectangular coordinates

X = parameter which varies derivatoric stress
 component

Y = parameter which varies hydrostatic stress component

 $\alpha = c \cos \phi$ 

 $\delta$  = thickness of cylinder, b-a

 $\varepsilon$  = direct strain

 $\dot{\varepsilon}$  = time derivative of direct strain

 $\varepsilon_r, \varepsilon_{\theta}, \varepsilon_z$  = direct strains on the r,  $\theta$ , and z planes

 $\varepsilon_x$ ,  $\varepsilon_v$  = direct strains on the x and y planes

 $\varepsilon_{\rm p}$  = plastic direct strain

 $\dot{\epsilon}_{n}$  = time derivative of plastic direct strain

 $\frac{\cdot}{\epsilon}$  = effective strain rate

 $\gamma$  = shear strain

 $\gamma_{r\theta}, \gamma_{\theta z}, \gamma_{zr},$ 

 $\gamma_{xy}, \gamma_{yz}, \gamma_{zx}$  = shear strain on the plane of the first subscript in the direction of the second subscript

 $\Gamma$  = intensity of shearing deformation (Vialov, 1965b)

 $\phi$  = time dependent friction angle

 $\sigma$  = direct stress

 $\sigma_{\mathbf{r}}, \sigma_{\theta}, \sigma_{\mathbf{z}}$  = direct stresses on the r,  $\theta$ , and z planes

 $\sigma_{x}, \sigma_{y}$  = direct stresses on the x and y planes

 $\sigma_1$  = major principal stress

 $\sigma_3$  = minor principal stress

 $\sigma_m$  = mean or hydrostatic stress

 $\bar{\sigma}$  = effective stress

 $\tau$  = shear stress

 $\tau_{r\theta}, \tau_{\theta z}, \tau_{zr},$ 

τ<sub>xy</sub>,τ<sub>yz</sub>,τ<sub>zx</sub> = shear stress on the plane of the first subscript in the direction of the second subscript

# CHAPTER I

# INTRODUCTION

Frozen soil, because of its strength and impermeability, may be used to advantage in certain types of engineering construction. High strength of soil-ice barriers can eliminate the necessity for temporary supports; and its impervious nature prevents ground water from entering the construction area. Thus, the method of artificially freezing soil to form a temporary barrier is gaining increasing acceptance in construction situations where more conventional methods are not practical.

This technique was first employed in the late 1800's in Europe as an aid to shaft sinking by the mining industry. A method developed by F.H. Poetsch (Sanger, 1968) was among the first used and with minor modifications is still the most widely used today. This method involves sinking pipes, closed at the bottom, around the periphery of the shaft to be sunk. Smaller diameter pipes, open at the bottom, are then placed inside them. A coolant from a refrigeration plant is then pumped down the inner pipes and up through the annular region between the pipes. As the coolant circulates, it extracts heat

from the ground and a frozen cylinder of soil is formed around each freeze pipe. As the size of each frozen soil cylinder increases, the desired soil-ice barrier is completed.

Although this method has been used successfully in many cases, it has been used sparingly and only in situations where unusual circumstances have caused other methods to fail or to appear impractical. The major disadvantages are the excessive cost of installing freeze pipes and operating refrigeration equipment and the time required to freeze the soil. Freezing time has been measured in weeks or even months before excavation of the shaft could even begin.

Due to the large expense involved, it appears important that there be a more reliable means of determining the minimum dimensions of the soil-ice barrier that has the necessary strength and deformation characteristics.

At present, only empirical and rule of thumb design procedures exist. In the past, frozen soil barriers have been designed using the false assumption that frozen soil is an elastic material or by applying a very large factor of safety. It is the purpose of this study to contribute knowledge toward the understanding of the behavior of a soil-ice cylinder subjected to an outside pressure.

The primary reason for the difficulty in describing the behavior of a soil-ice barrier is the complex nature of the frozen soil itself. Its stress-strain properties depend upon temperature, soil structure, water and ice content and are also time dependent. Frozen soil has been described as an elasto-plasto-viscous material. Models containing these various elements have been proposed to describe its stress-deformation behavior. However, none have had wide spread applicability and, thus, this behavior is still not well understood.

Any method of designing a soil-ice barrier must consider the limiting conditions of strength and deformation. If the strength of the barrier is exceeded, ground water would be permitted to flow into the excavated region and the safety of workmen would be endangered. Less obvious, but also detrimental, are the consequences of excessive deformation. This could cause large deflections and even failure in the freeze pipes, as well as difficulties in the installation of permanent supports. Due to the stress relaxation and creep properties of frozen soil, each of these limiting conditions must be carefully considered.

In this study, certain assumptions and simplifications are made in order to solve the problem. A hollow, thick-walled cylinder of frozen soil is considered under conditions of plane strain. The loading is assumed to be a radial, uniform, compressive pressure applied to the outside surface of the cylinder. The validity of such a representation is dependent upon construction procedures. In some cases, shafts have been sunk to great depths before permanent supports have been installed. In such cases, the

plane strain and uniform pressure assumptions probably closely approximate the actual conditions in the shaft at points 3 to 4 diameters or greater from its ends (Vialov, 1965b). In other excavations, where permanent supports have been installed as the digging proceeds, the end effects cannot be neglected and the plane strain assumption may not be realistic. A further simplification is that no attempt is made to describe the "primary creep" portion of the deformation. It is reasoned that this deformation occurs during excavation and can be compensated for at that time. It is the "secondary" or "steady state" creep occurring after excavation which, if not properly accounted for, will present difficulties in lining the shaft.

Two separate analyses are studied in order to describe stress-deformation behavior. First, the boundary value problem is formulated using the equations of equilibrium and compatibility along with a constitutive equation similar to one predicted by the rate process theory. In the second analysis, strength parameters c and  $\phi$ , corresponding to a given creep rate and temperature, are used to relate the dimensions of the cylinder and the pressure to the creep rate. Both methods use experimental results given by AlNouri (1969).

Finally, the results of an experimental program used to check the analyses as well as to gain additional insight are reported. Frozen clay and sand-ice cylinders

were prepared and loaded in a testing cell which was designed and fabricated specifically for this study. The radial displacement at the inner surface and the axial force in the sample were measured.

#### CHAPTER II

#### LITERATURE REVIEW

# 2.1 Field Practice

The method of artificially freezing soll to form a barrier around a shaft has been used in mining for more than a century (Brace, 1904). Not until recently has it been widely used by the construction industry. The usual procedure is to place water tight freezing tubes, approximately 4 to 10 inches in diameter, around the periphery of the proposed shaft. These tubes, closed at the bottom, are usually spaced at 3 to 4 foot intervals. Smaller circulating pipes, open at the bottom, are then placed inside the freezing tubes. The circulating pipes are joined together by a circulating ring. Similarly, the freezing tubes are joined by a collector ring. A circuit is completed as the circulating and collector rings are connected to a refrigeration plant. The coolant is pumped down through the circulating pipes, up through the freezing tubes to the collector ring, and back to the refrigeration plant. While a brine solution is most commonly used as the coolant, liquid nitrogen at a much lower temperature has been used in at least one case (Cross, 1964).

A frozen soil cylinder is thus formed around each freezing tube. In most cases, these frozen soil cylinders have been allowed to expand until the entire region of the proposed shaft is frozen, forming one large solid cylinder of frozen soil. The frozen soil is then excavated out of the center of the cylinder. Brace (1904) reports that this material is about as difficult to excavate as soft limestone. The frozen soil is usually loosened by jack hammers or blasting and then removed by clam shells.

In some cases, the excavation continues to the entire depth of the shaft, with the hollow frozen soil cylinder providing temporary support. The permanent lining is then begun at the bottom and continued upward. In other cases, the excavation is carried out in 20 or 30 foot sections. The permanent lining is then completed for each section before proceding to the next.

According to Brace (1904), the first example of artificial soil freezing as an aid to excavation was in England in 1852, where brine was circulated through freeze pipes to stabilize a bed of quicksand in sinking a well.

F.H. Poetsch introduced the method described above in 1883 at Saxony when quicksand was encountered at a depth of 111.5 feet during excavation of the Archibald shaft.

Eighteen feet of quicksand was frozen and the excavation continued. There were several other examples of this method being used in Germany, Prussia, Sweden, and Belgium in the 1880's. The first application in the United States

appears to have been at a shaft at the Chapin Mine, Iron Mountain, Michigan in 1887. Freezing pipes were placed around the periphery of a 15½ by 16½ foot rectangular shaft in order to freeze an unstable sand.

Tsytovich and Khakimov (1961) report the use of an artificial soil-ice barrier in the excavation of an underground railway station in Moscow in 1949. The excavation took place adjacent to the construction of a high frame building. The authors claim that the absence of temporary supports permitted mechanization of the construction and thus speeded construction time.

Artificial freezing was used in a shaft for a salt mine near Windsor, Ontario in 1954. The 16 foot diameter shaft was sunk to a depth of 1100 feet. Only the first 720 feet, however, required freezing. Six inch freezing tubes with two inch circulating pipes were placed on a circle of 32 foot diameter. A brine cooled to -12° F. in a 200 ton refrigeration plant was pumped through the pipes. Approximately three months freezing time was required. After each 28 feet of excavation, reinforcing steel and forms for concrete were placed and concrete poured for the lining before beginning excavation of the next section. Approximately 154 hours and 44 construction workers were required for each 28 foot section.

Latz (1952) reports the sinking of a 15 foot diameter, 1000 foot deep shaft to a potash bed in Carlsbad, New Mexico. When exploratory borings revealed the presence of

several horizons of quicksand in the first 350 feet, it was decided to freeze the soil to that depth. Twenty eight freeze pipes were placed on a diameter of 31 feet and chilled brine was circulated. Drilling of freeze holes began July 15, 1950, the refrigeration plant began operating on November 19, and sinking of the shaft began January 19, 1951. Concrete lining was placed in 25 feet sections as excavation proceeded. The shaft lining was completed on September 19, 1951.

When the City of New York had to sink a 318 foot shaft as part of a system carrying sewage under the East River, the most obvious method of keeping the excavation dry was to lower the ground water table by pumping. This, however, had to be ruled out since it would have resulted in excessive ground water depletion and possible differential settlement and damage to nearby buildings which were as close as 56 feet from the shaft. Therefore, freeze pipes were placed around the outside of the 14.5 foot diameter shaft to a depth of 123 feet and the material was frozen before excavation began. Silinsh (1960) reports that the entire cost of the shaft was approximately \$6.5 million.

Low (1960) gives an account of artificial soil freezing used in Montreal in 1960 in a railway tunnel when track rearrangement dictated that a single concrete arch replace the existing double arch system. The tunnel was located directly beneath a busy street and between two

buildings. Thus, an open cut was impossible since it would have cut through too many services and required heavy bracing to support the soil pressure due to the buildings. Vertical freeze pipes were placed along the entire length of the tunnel and a cooled methanol solution was circulated through them. After the material was frozen, it was excavated by drilling and blasting. While steel liner plates and ribs were used as temporary supports in the tunnel, Low concludes that they were not necessary and could be omitted from future jobs. There was an upward heave of the street of about 5 inches causing cracking and it had to be replaced.

In 1962, the City of New York was faced with the problem of sinking shafts at either end of a 25,000 foot water supply tunnel under the New York harbor from Brooklyn to Staten Island. Stewart et al.(1963) reports that on the Brooklyn side, lowering of the water table could have caused movement to nearby factories which contained precision equipment. Thus, the first 118 feet to bedrock of the 965 foot deep shaft was frozen using 28 freeze pipes on a 30 foot diameter. Freezing was completed 42 days after the freezing plant was put into operation. The 20 foot diameter shaft was sunk to its entire depth before concrete lining was begun at the bottom and proceeded upward.

Cross (1964) describes a slightly different method of using artificially frozen soil in the construction of a four mile sewer tunnel in Milwaukee in 1964. While digging

an 18 foot diameter, 90 foot deep shaft to begin the tunnel, soft clay and running silt were encountered on one side. Six freeze pipes were placed horizontallly in the wall of the shaft and liquid nitrogen was circulated through them. Although liquid nitrogen is relatively expensive, its low temperature (-320° F.) permitted a section of the wall to be frozen in a day and a half; whereas, a brine solution would probably have taken several weeks. Cross warns that extreme caution must be used when using nitrogen since it is heavier than air and could, thus, endanger the safety of workmen in the bottom of the shaft if leakage were to occur.

# 2.2 Mechanical Properties of Frozen Soil

Mechanical properties of unfrozen soil depend primarily on internal friction and on cohesion due to internal interparticle bonds. When soil is frozen, other factors and parameters must be considered. These include temperature, ice content, and characteristics of ice crystals, all of which affect ice cementation of particles (Yong, 1963).

Of the factors governing the mechanical properties of frozen soil, ice cementation bonds are probably the most important (Tsytovich, 1963). These bonds appear to be the strongest as well as the most sensitive to external temperature change. According to Tsytovich, "The mechanical properties of frozen soil depend mainly on the number and properties of these bonds." In all frozen soil, a portion of the pore water remains in a liquid state. Tsytovich

theorizes that frozen soils are characterized by a dynamic equilibrium between the frozen and unfrozen water. An external load causes weakening due to melting and slippage. Simultaneously, strengthening occurs due to denser packing of mineral particles and refreezing of water. Damped or undamped creep results depending on whether strengthening or weakening predominates.

Vialov (1965a) describes frozen soil as an elastoplasto-viscous material. The presence of the viscous
property is exemplified by the strong time dependence of
its stress-deformation characteristics. Experience has
shown that frozen soil exhibits both creep, or growth of
deformation with time under a constant stress, and a reduction in strength with time.

Deformations in frozen soil can be divided into those that are recoverable and those that are irrecoverable (Vialov, 1965a). Recoverable deformations include elastic and structurally reversible deformations. Elastic deformation is associated with elastic changes in the crystal lattice of the ice and mineral particles and elastic compression of air and unfrozen water. This disappears immediately when the load is removed and is usually small enough to ignore in most considerations. Structurally reversible deformation arises from the change in thickness of water films between particles. This may be considered a visco-elastic response since it grows with time and gradually diminishes when the load is removed.

Part of the irrecoverable deformation consists of structurally irreversible deformations associated with consolidation. These include squeezing out air, regrouping of particles, and breaking up of bonds. They increase with time and are completely irrecoverable. Plastic deformation is the other part of the irrecoverable portion. This represents the irreversible displacement of solid particles and the flow of ice.

A typical creep curve for frozen soil under constant stress is given in Figure 2.1. While this representation is usually associated with uniaxial compression, creep curves for other stress states are similar (Sanger, 1968). Section OA represents the instantaneous response which may be entirely elastic or elasto-plastic (Vialov, 1965b). Section AB corresponds to the first stage of creep where the deformation grows at a decreasing rate. Deformation during this stage is only partially recovered when the load is removed. The first stage continues until the slope reaches some minimum value at which time the process enters the second, or steady flow stage. Sanger (1968) states that most deformation in practice occurs during the second stage of creep. As the deformation continues, the third or progressive flow stage (CD) is reached. During this stage, deformation continues at an increasing rate. Point C is often considered as corresponding to failure.

There is considerable disagreement regarding the relationship between stress and strain in frozen soil. While it is generally agreed that such a relationship for a particular frozen soil at a constant temperature is time dependent, it is not well understood how stress, strain, and time are related.

Various mechanical models such as the one shown in Figure 2.2 proposed by Vialov (1965a), can qualitatively describe the various components of the deformation process. Springs represent elastic qualities, dashpots viscous qualities, and the friction element represents plastic qualities. However, due to the many peculiarities involved in the actual deformation process, all such models have failed to quantitatively describe the process over a wide range of stresses.

Vialov (1965a) reports that stress-strain curves can be expressed by the power law

$$\sigma = A(t) \varepsilon^{m_1} \tag{2.1}$$

where  $\sigma$  is stress,  $\varepsilon$  is strain, t is time, A(t) is the modulus of total deformation, and  $m_1$  is known as the strengthening factor. A(t) can be determined using the Botzmann-Volterra theory of hereditary creep and is both temperature and time dependent. The strengthening factor is a positive number equal to or less than one and depends on neither time nor temperature. Vialov suggests determining this relationship for a simplified stress state such as uniaxial compression. It can then be extended to complex stress conditions by using the intensity of tangential stresses,

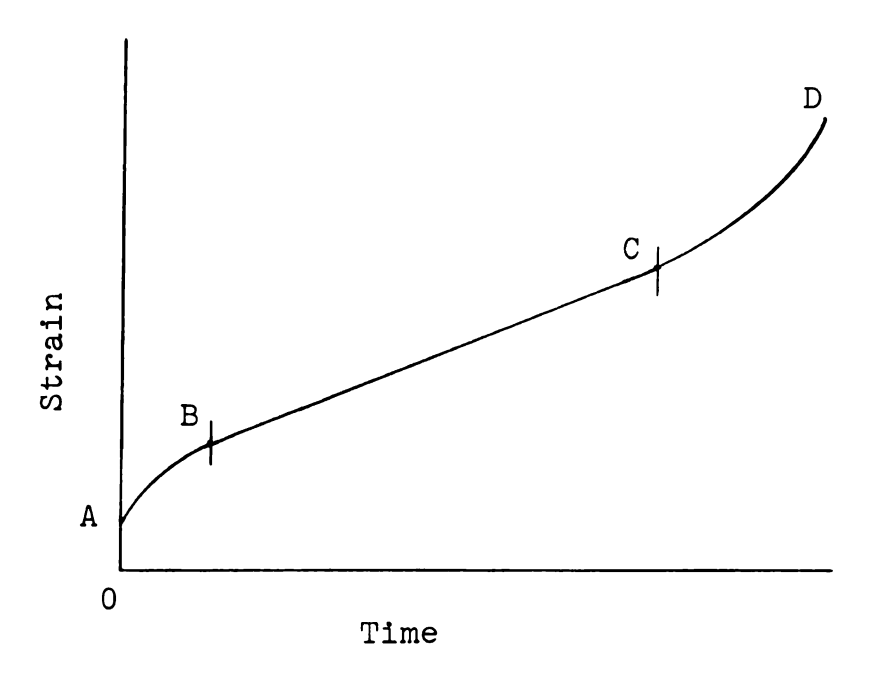


Figure 2.1. Typical Creep Curve for Frozen Soil

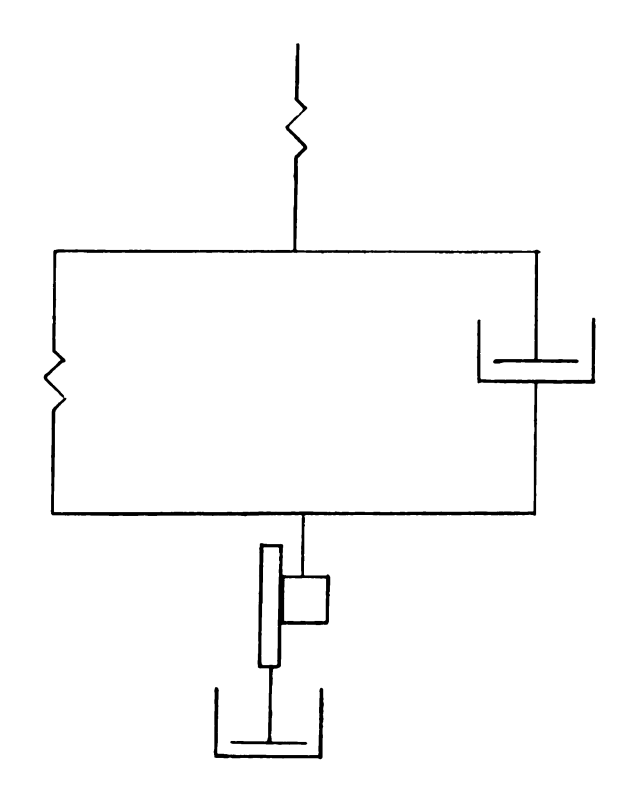


Figure 2.2. Elasto-Plasto-Viscous Model

$$T = \sqrt{1/6 \left[ (\sigma_{x} - \sigma_{y})^{2} - (\sigma_{y} - \sigma_{z})^{2} - (\sigma_{z} - \sigma_{x})^{2} \right] + \tau_{xy}^{2} + \tau_{yz}^{2} + \tau_{zx}^{2}} \quad (2.2)$$

and the intensity of shearing deformation,

$$\Gamma = \sqrt{\frac{2}{3}\left[\left(\varepsilon_{x}-\varepsilon_{y}\right)^{2}-\left(\varepsilon_{y}-\varepsilon_{z}\right)^{2}-\left(\varepsilon_{z}-\varepsilon_{x}\right)^{2}\right]+\gamma_{xy}^{2}+\gamma_{yz}^{2}+\gamma_{zx}^{2}}.(2.3)$$

Subscripted  $\sigma$ 's and  $\epsilon$ 's represent direct stresses and strains, respectively and  $\tau$ 's and  $\gamma$ 's are shear stresses and strains. Thus, Equation (2.1) can be written

$$T = A(t)\Gamma^{m}1. (2.4)$$

Goughnour and Andersland (1968) found that the following equation fit the behavior of polycrystalline ice:

$$\varepsilon_{p} = K_{1} \exp(-n_{1}\varepsilon_{p}) + K_{2} \exp(n_{2} \int \sigma d\varepsilon_{p}).$$
(2.5)

Andersland and Akili (1967) propose that creep in frozen soil is a thermally activated process and suggest an equation of the form

$$\dot{\varepsilon} = C_1 \exp (B\sigma)$$
 (2.6)

to describe it. This is based on the results of a series of uniaxial compression tests on a frozen clay at different temperatures. B and C are determined experimentally and are temperature dependent. Equation (2.6) was found to describe the steady state portion of the creep curve.

AlNouri (1969) extended this approach by performing a series of differential creep tests on two frozen soils under triaxial stress conditions. He was thus able to include the effect of the hydrostatic part of the stress as well as the derivatoric. Alnouri's equation for a frozen soil at a constant temperature takes the form

$$\dot{\varepsilon} = C \exp \left[ N(\sigma_1 - \sigma_3) \right] \cdot \exp(-m\sigma_m). \tag{2.7}$$

C, N, and m are experimentally determined parameters,  $\sigma_{m}$  is the mean stress, and  $\sigma_{1}$  and  $\sigma_{3}$  are the major and minor principal stresses, respectively. Equation (2.7) predicted the axial strain rate during steady state creep for a frozen clay and a sand-ice material under a constant axial load with varying confining pressures.

AlNouri (1969) further showed how Equation (2.7) can be used to give the cohesion (c) and angle of internal friction (\$\phi\$) for a given strain rate and temperature. He found that different combinations of stresses produced the same axial strain rate. After sketching the Mohr circle corresponding to each set of stresses, he showed that a

straight line could be drawn tangent to each of the circles. Defining the line by the intercept, c, and the slope,  $\phi$ , a relationship can be established between these parameters and the principal stresses for a particular strain rate. It was found that the angle of internal friction appeared to remain constant for the Ottawa sand and was independent of temperature but that the cohesion varied with strain rate and temperature.

## 2.3 Existing Methods of Analysis

Until recently, methods used in designing soil-ice retaining structures have failed to account for the time-dependent behavior of frozen soil. For example, the formula

$$\delta = a \sqrt{\frac{\sigma_d}{\sigma_d - 2p}} - 1$$

has been used to determine the wall thickness,  $\delta$ , of a frozen soil cylinder of inner radius a, loaded by an outside pressure, p.  $\sigma_d$  is the maximum permissive compressive stress of the frozen soil. This formula is based on Lamé's solution for an elastic material. Since frozen soil does not behave elastically, Equation (2.8) could not be expected to give results which are consistent with the actual behavior. Further, this formula only considers the strength of the frozen soil. It does not provide for the determination of deformations which often control the design of such a structure. Other empirical formulas have also

been proposed but none have proved to have widespread applicability.

The only attempt to incorporate the creep and strength reduction properties of frozen soil in the analysis of soil-ice cylinders was made by Vialov (1965b). The results of his work are briefly outlined in the following paragraphs.

Vialov points out that any analysis of a frozen soil barrier must take into account two limiting conditions—strength and deformation. Stress must not be allowed to exceed the shear strength of the soil. Neither can excessive deformations be permitted. Experience has shown that intolerable deformations can occur at stresses well below those necessary to produce failure.

Vialov considers a thick-walled frozen soil cylinder of inner radius a and outer radius b loaded by a uniform outside pressure, p. He assumes that a plane strain condition exists in the cylinder. For the strength limiting condition, Vialov simultaneously solves the equation of equilibrium and a yield criterion for the portion of the cylinder where the yield strength has been exceeded. This produces expressions for stresses in the "plastic zone". He then uses the Lame' solution for the zone in which the stresses are less than the yield strength. Since the radial stress,  $\sigma_{\mathbf{r}}$ , must be the same on either side of the "elastic-plastic boundary", the two expressions for  $\sigma_{\mathbf{r}}$  are

equated. The limiting condition is when the stresses in the entire section have exceeded the yield strength. Vialov solves the problem for several different yield criteria. In each case, he arrives at an expression which relates the strength parameters and the geometry of the cylinder to the outside pressure. Thus, for a given soil and outside pressure, the required wall thickness can be calculated for a fixed inner diameter.

In considering deformation, Vialov uses one stressstrain relationship for the instantaneous case and a
second relationship for deformation during creep. In both
cases, he uses the equation of equilibrium, the incompressibility condition, the strain-displacement definitions,
Hencky's equations, and a constitutive equation to arrive
at a result. For the instantaneous case, he uses the constitutive equation given in Equation (2.1), using the value
of A at t = 0. The result is

$$u_a = \left(\frac{m_1 p}{A}\right)^{\frac{1}{m}} \cdot \frac{a}{2\left[1 - \left(\frac{a}{b}\right) 2m_1\right]^{\frac{1}{m}}}$$
 (2.9)

This equation gives the instantaneous deformation at the inner surface,  $u_a$ , in terms of the pressure, the dimensions of the cylinder, and the experimental parameters A and  $m_1$ .

For the condition during creep, Equation (2.1) is again used, this time using the law of hereditary creep. The resulting equation is

$$\frac{a}{b} = \left\{ 1 - \frac{m_1 p}{A(t) \left[ \frac{2u_a(t)}{a} \right]^{m_1}} \right\}^{\frac{1}{2m}} 1.$$
 (2.10)

## 2.4 Previous Experimental Work

Due to the specialized equipment and techniques required in a study of this type, experimental work in this area has been very limited. A testing program conducted in the USSR (Vialov, 1965b) is apparently the only one reported in the literature where cylindrical frozen soil models have been used. Information is also lacking from actual construction projects. Contracting companies using this method "have much proprietary information which cannot be published" (Sanger, 1968). Soil properties and other valuable data are often omitted from reports.

In order to determine the relationship between parameters in the prototype and a model, Vialov (1965b) uses the criteria of similitude. Based on this, he finds that the following relationships must hold:

$$\frac{b_1}{a_1} = \frac{b_m}{a_m} \tag{2.11}$$

$$\frac{\mathbf{h_1}}{\mathbf{a_1}} = \frac{\mathbf{h_m}}{\mathbf{a_m}} \tag{2.12}$$

$$\frac{\mathbf{u_1}}{\mathbf{a_1}} = \frac{\mathbf{u_m}}{\mathbf{a_m}} \tag{2.13}$$

a and b are as defined above, h is the height of the cylinder, and u is the radial displacement. The subscripts i and m indicate "in situ" and model, respectively. He further points out that since the properties of the material must be preserved, any parameters which describe material behavior must be the same in the prototype and model. That is, the same material should be used. In addition, pressure, temperature, and time must be the same in each to insure similarity.

Vialov indicates that if the criteria of similitude outlined above is satisfied, the Reynolds' criterion is automatically satisfied. This makes it impossible to satisfy the Froude criterion. Vialov points out that this causes no significant error since it only indicates that the soil weight has been neglected.

Vialov used a testing cell similar to the one used in the current study to test frozen soil cylinders. The model was placed inside a rubber sheath and loaded by an outside pressure. Deformation was measured using a lever device and dial gages.

Tests were performed on a sandy loam and a clay material at various temperatures. Various dimensions were used and pressures varied from 20 to 80 kilograms per square centimeter. The results are given only in terms of total displacement at a fixed time after loading. Thus, strain rates are not available.

#### CHAPTER III

#### SOILS STUDIED AND SAMPLE PREPARATION

#### 3.1 Soils Studied

In an attempt to arrive at results which have applicability for all soils, two soil types were used in this study: one cohesive and one cohesionless. The cohesive soil was an Ontonagon clay which occurs naturally in Northern Michigan. This soil was taken from a roadside site midway between Rudyard and Kinross, Michigan at a depth of approximately 24 inches. The soil was air dried and then ground to a fine powder. The index properties of this material are given in Table 3.1.

The clay content of the Ontonagon soil was about 70%. The clay fraction was found to contain the following clay minerals in the approximate amounts indicated:

Illite	45%
Vermiculite	20%
Kaolinite	15%
Chlorite	10%

The remaining 10% is made up of montmorillonite, quartz, feldspar, and amorphous material. The illite, vermiculite,

and chlorite appeared to be randomly interstratified within the soil. This data was derived from x-ray diffraction, differential thermal analysis, infrared absorption, and various other tests performed on the clay fraction. Further data on the clay fraction are given in Table 3.2.

The cohesionless soil studied was a standard Ottawa sand purchased from Soiltest, Inc. (CN-501 Density Sand). Only that portion which passed a No. 20 sieve and was retained on a No. 30 sieve was used.

## 3.2 Sample Preparation

## 3.2.1 Equipment

Preparation techniques differed for the two soil types studied and will be discussed separately. The basic apparatus, common to both, consisted of a split cylindrical mold used to form the outside of the cylindrical soil samples (See Figure 3.1). It was cut from a steel pipe (5 3/4" outer diameter, 5" inner diameter) which was split lengthwise and then machined to preserve a cylindrical shape. punched steel flanges were welded to each half so that they could be joined using 1/4" bolts. The split portion of the mold was 12 inches long. Unsplit extensions, 3 inches long, which fit into grooves in the split part were provided for the top and bottom of the mold. In order to study samples of different diameters, liners of varying sizes were placed inside the mold. These were cut from steel pipe of appropriate sizes, split, and machined in the same manner as the outside of the mold (See Figure 3.2).

Table 3.1 Index properties of Ontonagon clay

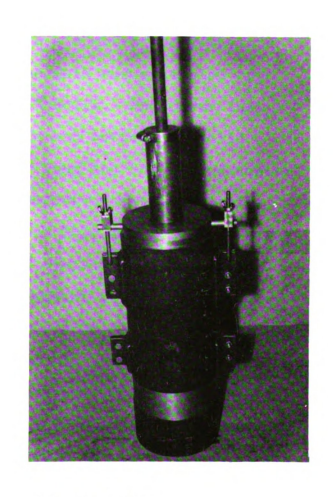
:	Plastic Limit	23.6%
1	Liquid Limit	60.5%
:	Plasticity Index	36.9%

Table 3.2 Mineralogical properties of Ontonagon clay

Surface Area	215m <sup>2</sup> /g
Cation Exchange Capacity	
Ca/Mg K/NH <sub>4</sub>	48.5 meq/100g 17.7 meq/100g
Potassium Content	3.7%



(a) Disassembled



(b) Assembled

Figure 3.1. Preparation Mold and Drilling Accessories

## 3.2.2 Preparation of Cohesive Samples

A weighed amount of air dried clay was first placed in a metal pan. Enough distilled water was then added to bring the water content to 27%. The water was added slowly and carefully mixed by hand. When it appeared that the water had been uniformly distributed throughout the clay, the mixture was placed in an airtight container until used.

The inside of the split mold was lubricated with a thin coat of oil and covered with a sheet of polyethylene in order to reduce friction. The mold was assembled by joining the flanges with the 1/4" bolts. The three inch extensions were placed at the top and bottom. A solid cylindrical metal plug, 3 inches long and the same diameter as the mold was placed inside the bottom extension. The clay was then placed in the mold. This was done by placing small amounts at a time and then compacting by hand to guard against void spaces. The amount of soil added was that necessary to give a density of 100 pounds per cubic foot for the prescribed volume of the sample. Both density and water content were chosen to agree with AlNouri (1969).

The clay was then statically compacted to the desired density using a Tinius Olsen testing machine. A three inch solid cylindrical plug was attached to the driving head of the machine to compact the sample from the top. By suspending the bottom of the mold, compaction from the bottom plug was also achieved, thus assuring a more uniform density.

After compaction, the sample was in the form of a solid cylinder. A hole was then drilled in the center using a 1 1/2" auger. This was done by first placing a one inch thick circular plate on top of the mold. It fit into a groove and was secured by tie rods from studs in the plate to the flanges of the mold. A six inch long pipe with a 1 1/2" inside diameter was threaded vertically into the center of the plate. This served as a guide for the auger (See Figure 3.1). The auger was placed in the guide and rotated to make the center hole in the sample. It was necessary to withdraw the auger frequently to clean the loose soil from it. The mold was then stripped by removing the bolts. Figure 3.3 shows a clay sample which had been prepared in this manner.

## 3.2.3 Preparation of Cohesionless Samples

A thin coat of lubricating oil was applied to the inside of the mold and covered with a polyethylene sheet. In the bottom of the mold was placed a 13/16 inch thick, circular, stainless steel plate with a smoothly machined 1 1/2 inch hole in the center. A smoothly machined 1 1/2 inch stainless steel round bar, 18 inches long, was placed into the hole in the plate. The bar was tapered one ten thousandth of an inch over its length in order to permit its removal after the sample had frozen. A thin coat of oil and polyethylene sheets were also applied to the plate and bar. As the mold was assembled, vacuum grease was applied to all joints to seal them against leakage.

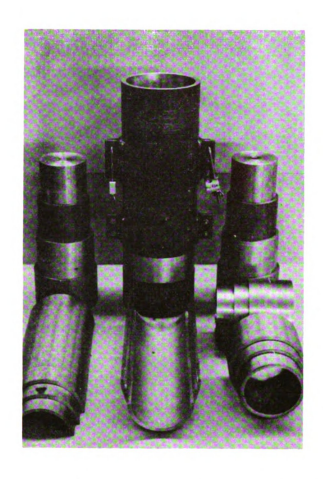


Figure 3.2. Preparation Mold and Accessories for Varying Sample Size



Figure 3.3. Preparation of Clay Sample

The dry sand was placed in the mold in four layers, each layer being tamped 25 times. The amount of sand used was that necessary to give 64% sand by volume, using 2.65 as its specific gravity. This is in agreement with AlNouri (1969). Distilled water was then added slowly from the top until the sample was saturated. It was then placed in a freezer at -18° C. for 48 hours.

After freezing, the center rod was removed by placing the mold in the Tinius Olsen testing machine and extruding it with a hydraulic jack. The mold was then returned to the freezer and stripped from the sample by removing the bolts. Since an irregular cap of ice usually formed at the top of the sample, it was necessary to smooth the top using coarse sand paper until the end was square.

#### CHAPTER IV

#### TESTING EQUIPMENT AND PROCEDURES

# 4.1 Equipment

## 4.1.1 Test Cell

A cross sectional sketch of the test cell is shown in Figure 4.1 and photographs of it are given in Figure 4.2. The cell consists of a hollow cylinder which, at its ends, fits into grooves cut into square plates. Rubber 0- rings are placed in the grooves in order to seal the cell. The plates are held by tie rods at their corners which are tightened using nuts at each end. A pedestal, upon which the soil sample rests, is built into the bottom plate. The base of the pedestal is connected to a flat load cell which measures the axial force in the sample. Calibration data for the load cell are given in Appendix B.

At the top of the sample is a piston which fits through the top plate. The purpose of the piston in this study was to enforce a plane strain condition by permitting no axial movement of the sample. With minor modification it could be used to transmit an axial load to the sample. A third square plate at the top is fixed by 8 nuts to

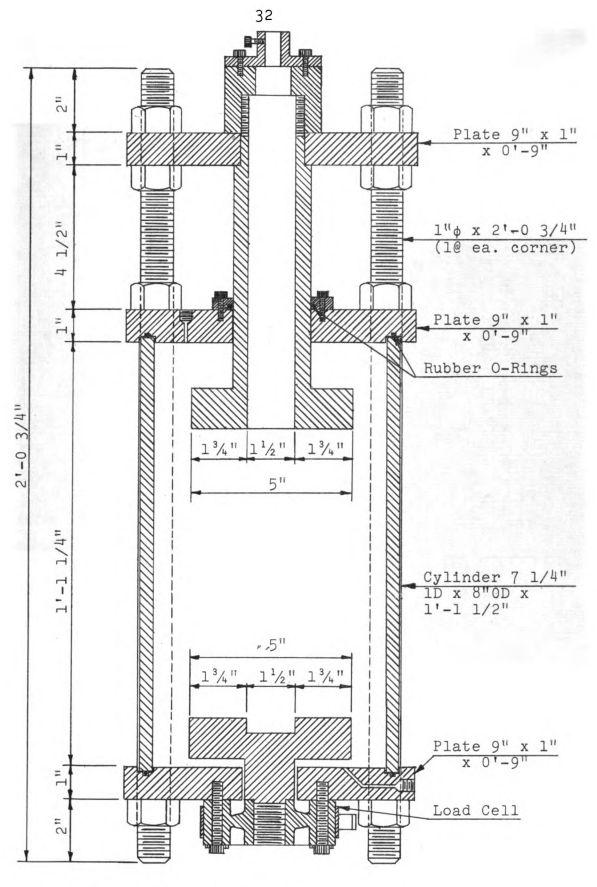
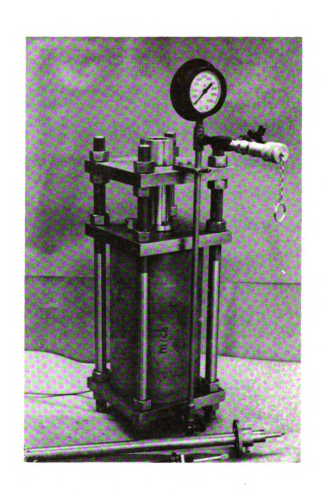


Figure 4.1. Test Cell Detail



(a) Disassembled



(b) Assembled

rigidly hold the piston. A collar containing a rubber 0ring is fastened to the top plate at the point where the
piston fits through the plate to seal it at that point. The
cell is made entirely of stainless steel and was fabricated
in the Division of Engineering Research Machine Shop at
Michigan State University. Dimensions are as given in Figure 4.1.

# 4.1.2 <u>Deformation Measuring Apparatus</u>

A sketch of the device used to measure the deformation of the inner surface of the frozen soil cylinders is shown in Figure 4.3. It was made of thin steel strips pinned together to form an unstable, trapezoidally shaped structure. At the bottom of the trapezoid, the steel strips are extended and equipped with rounded brass pieces which are pinned at their ends. The brass pieces rest against the inner surface of the sample. At the top of the trapezoid is pinned a round bar which was placed parallel to the axis of the cylinder. A steel pipe encases the round bar and has a collar at its top which is fastened to the top of the piston by 4 screws. The collar is equipped with a set screw so that the position of the steel pipe can be adjusted. discs which act as guides for the round bar are located inside the pipe at the top and bottom.

This device was placed through the center hole of the piston and sample and then secured. As the inner surface of the sample moved radially inward, the rounded brass pieces were displaced, thus causing an upward movement of the round

bar. The top of the round bar was connected to a linear differential transformer which measured its vertical movement. The linear differential transformer and the load cell in the base of the testing cell were electronically connected to a two channel recorder which recorded the displacement of the bar and the force on the load cell.

Due to the nonlinearity of the relationship between the inward movement of the brass pieces and the vertical movement of the round bar, it was necessary to calibrate the device over the range of its use. This was done by mounting the device in a vertical position and placing a micrometer, secured in a vise, over the brass pieces. Then by adjusting the micrometer and noting the recorder reading, the relationship was obtained. Calibration data are given in Appendix B.

# 4.1.3 Pressure System

Figure 4.4 shows a sketch of the pressure system. The source of the pressure was a cylinder of compressed nitrogen. The pressure in the cylinder was reduced to the desired pressure by the use of a high pressure regulator placed at the cylinder outlet. This pressure was applied to the top of a liquid in a high pressure cell which served as a reservoir for the fluid in the test cell. The high pressure cell consisted of two flat steel plates at either end of a hollow steel cylinder. The plates were held tightly by tie rods at the four corners. A valve was located near the inlet to the high pressure cell in order to

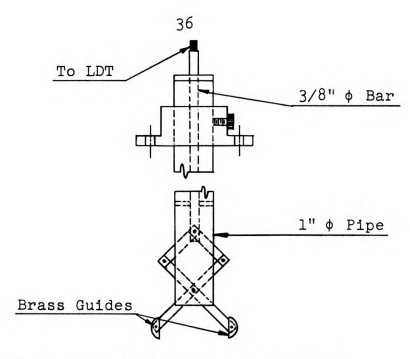


Figure 4.3. Deformation Measuring Device

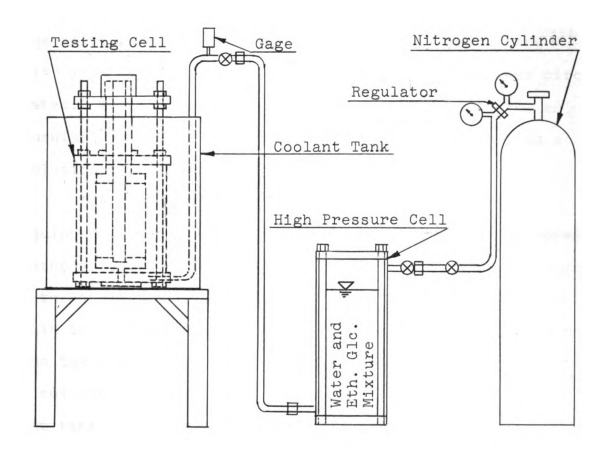


Figure 4.4. Pressure System

transmitted the pressure from the pressure cell to the test cell. The pressure entered the test cell through a hole in the bottom plate. A gage placed near the inlet to the testing cell was used to determine the pressure in the cell. Pressures ranging from 100 to 900 pounds per square inch were used in this study. The liquid used in the system was a mixture of 50% water and 50% ethylene glycol.

## 4.1.4 Cooling System

In order to maintain the frozen soil samples at the low temperatures required, the entire test cell was submerged in a coolant maintained at the desired temperature. The testing cell was placed in a galvanized steel tank (14" x 14" x 1'-9 1/2") through which the coolant was circulated. The tank was open at the top and covered with an insulating material (styrofoam). The coolant used was a solution of 50% water and 50% ethylene glycol.

The fluid was cooled in a low temperature bath equipped with a thermoregulator. By setting the thermoregulator at the desired temperature, the low temperature bath alternately heated and cooled the fluid in order to maintain it at that temperature. The fluid was circulated from the low temperature bath into the bottom of the galvanized steel tank and then back into the bath through the top of the tank. Temperature control of 0.1° C. was easily attainable using this apparatus.

## 4.2 Procedures

# 4.2.1 Cohesive Soil

In order to reduce friction at the ends of the sample, a thin coat of oil was applied to the top of the pedestal and the bottom of the piston. A sheet of polyethylene, cut to the required annular shape, was then placed over the pedestal and piston.

Due to the stiffness of the clay used, it was not necessary to freeze the sample prior to mounting it in the testing cell. Thus, the hollow cylindrical sample, prepared as described in Chapter III, was placed on the pedestal and the piston placed on top of the sample. Two rubber membranes were then placed over the sample and stretched over the pedestal and piston. Circular clamps were tightened around the pedestal and piston to seal the sample. Strips of heavy rubber were placed between the clamps and the outer membrane in order to protect the membrane. A photograph taken at this stage of preparation is shown in Figure 4.5.

Since the weight of the fully assembled testing cell made handling difficult, it was placed in the galvanized steel tank at this point. The stainless steel cylinder was then positioned, followed by the top plate. After the top plate was secured by tightening the nuts, the collar on the outside of the piston was placed and the plug in the top plate tightened. The remainder of the cell was then assembled and the temperature of the fluid was brought to -18°C.



This temperature was maintained for approximately 48 hours. Twenty four hours before loading the sample, the temperature was raised to  $-12^{\circ}$ C. This temperature history was used in order to agree with AlNouri (1969).

Thirty minutes before beginning the test, the deformation measuring device, which had been precooled to eliminate the possibility of thawing where it contacted the sample, was positioned and secured. The linear differential transformer was then assembled and the recorder balanced. The pressure was applied to the sample by opening the nitrogen cylinder valve and adjusting the regulator to the desired pressure. A pressure of 100 pounds per square inch was initially applied in most tests. The pressure was increased in increments of 100 p.s.i. Each increment was applied until the steady state portion of the creep curve was determined. For each increment, the deformation and the force on the load cell were recorded on the two channel recorder.

At the end of the test, the pressure was released and any recovery of deformation noted. The cell was then disassembled and the sample examined. Figure 4.6 shows a photograph of the test set-up.

# 4.2.2 <u>Cohesionless Soil</u>

Since the cohesionless samples were frozen before being placed in the testing cell, a slightly different procedure was used. The pedestal and piston were kept in the freezer at -18°C. for several hours before mounting to guard against the sample thawing at points of contact. Friction



Figure 4.5 Clay Sample Mounted in Test Cell



Figure 4.6. Test Set-Up

reducers, as described for the clay samples, were placed on the pedestal and piston. The sample was mounted and membranes placed while the apparatus remained in the freezer. In early tests, it was found that there was a greater occurrence of membrane failures in the sand-ice samples. Therefore, between four and six membranes were used on each sample.

After the clamps were tightened at the ends, the cell was transferred to the cooling tank which had been cooled to a temperature of -18°C. The pump was temporarily turned off to lower the level of the liquid in order to allow placement of the testing cell. The remainder of the assembly and testing procedure are as described above for the cohesive soil.

#### CHAPTER V

#### THEORETICAL CONSIDERATIONS

## 5.1 Formulation of the Problem

Vialov (1965b) indicates that the limiting strength condition for soil-ice barriers can be adequately handled by solving the equation of equilibrium together with the Mohr-Coulomb failure criterion and the appropriate boundary conditions. The strength parameters can be determined from a series of triaxial tests on undisturbed soil samples frozen to the desired temperature. It is the objective of this study to gain additional insight into the deformation characteristics of frozen soil barriers, thus contributing knowledge toward the understanding of their limiting deformation condition.

By way of approximating the actual conditions in a soil-ice barrier surrounding a circular shaft, consider a thick-walled cylinder of inner diameter 2a and outer diameter 2b, loaded at the outside surface by a uniform compressive pressure, p (See Figure 5.1). The inner surface is unloaded. The following assumptions and simplifications are made:

- (1) A plane strain condition exists in the section being considered. Thus, the strain in the vertical direction must be everywhere zero; and all other strains and stresses must be independent of the vertical coordinate. This approximation is reasonable at sections distant from the ends of the shaft.
- (2) There is no volume change in the frozen soil during deformation. Thus,

$$\varepsilon_{\mathbf{r}} + \varepsilon_{\theta} = 0,$$
 (5.1)

where  $\varepsilon_{r}$  and  $\varepsilon_{\theta}$  represent the direct strains in the radial and tangential directions, respectively. It follows from the incompressibility condition that Poisson's ratio is equal to 0.5. Experiments on frozen soils have shown that this is valid "for sufficiently developed creep deformations" (Vialov, 1965b). Therefore, it is necessary that

$$\sigma_{z} = \frac{1}{2} (\sigma_{r} + \sigma_{\theta}), \qquad (5.2)$$

where the subscripted  $\sigma$ 's denote direct stresses in the indicated orthogonal directions. Taking compressive stresses as positive,  $\sigma_\theta$  is the major principal stress,  $\sigma_r$  the minor, and  $\sigma_z$  the intermediate.

- (3) Displacements are small enough that the initial dimensions and coordinates can be used throughout the deformation process.
- (4) Only the steady state portion of the creep curve need be considered. Adjustments for deformation occurring

during primary creep can be made during excavation.

Stresses necessary to produce progressive flow during the construction period may be ruled out by the limiting strength condition. However, the results of this study are not sufficient to insure this. Therefore, care should be taken in this regard.

Due to assumption (1) and the radial symmetry involved, the equilibrium equations reduce to the following single equation for this case.

$$\frac{d\sigma_{\mathbf{r}}}{d\mathbf{r}} + \frac{\sigma_{\mathbf{r}} - \sigma_{\theta}}{\mathbf{r}} = 0. \tag{5.3}$$

Similarly, the compatibility relationship becomes

$$\frac{d\varepsilon_{\theta}}{dr} + \frac{\varepsilon_{\theta} - \varepsilon_{r}}{r} = 0 \tag{5.4}$$

The strain -displacements relationships are

$$\varepsilon_{\theta} = \frac{\mathbf{u}}{\mathbf{r}}$$
 (5.5)

and

$$\varepsilon_r = \frac{du}{dr} \tag{5.6}$$

where u is the radial displacement and is considered positive in the inward direction. The boundary conditions on stresses are

$$\sigma_{\mathbf{r}} = 0 \quad \text{at} \quad \mathbf{r} = \mathbf{a} \tag{5.7}$$

and

$$\sigma_{\mathbf{r}} = \mathbf{p} \quad \text{at} \quad \mathbf{r} = \mathbf{b}. \tag{5.8}$$

The solution involves using the conditions given above along with a constitutive relationship for the material. This is done in the following paragraphs for frozen soil using two relationships given by AlNouri (1969).

## 5.2 Analysis Based on a Creep Equation

While it has often been assumed that the mean normal stress has no effect on creep in frozen soil, AlNouri (1969) has shown that the following equation appears to describe the creep behavior for two frozen soil types:

$$\dot{\varepsilon}_1 = C \cdot \exp \left[ N(\sigma_1 - \sigma_3) \right] \cdot \exp(-m\sigma_m). \tag{2.7}$$

The mean normal stress,  $\sigma_m$ , is equal to one-third the sum of the direct stresses, while C, N, and m are parameters which must be determined experimentally. N and m were found to vary only with soil structure, while C depends on both temperature and soil structure for the range of stresses and temperatures studied by AlNouri. Equation (2.7) is based on the results of differential creep tests, during which the hydrostatic pressure was varied in increments while the applied axial stress remained constant. Tests were conducted in a standard triaxial testing cell.

Since Equation (2.7) was derived for a uniform stress condition in which two of the principal stresses were always equal, it is necessary to modify it in order to apply it to a more general stress situation. It is proposed that Equation (2.7) be extended as follows:

$$\stackrel{\cdot}{\varepsilon} = C \cdot \exp(N\sigma) \cdot \exp(-m\sigma_m) \tag{5.9}$$

where  $\bar{\sigma}$  is the effective stress given by

$$\bar{\sigma} = \left\{ \frac{1}{2} \left[ (\sigma - \sigma_{\theta})^{2} + (\sigma_{\theta} - \sigma_{z})^{2} + (\sigma_{z} - \sigma_{r})^{2} \right] + 3(\tau_{rz}^{2} + \tau_{z\theta}^{2} + \tau_{r\theta}^{2}) \right\} \frac{1}{2}.$$
 (5.10)

This expression seems a reasonable one to use for the derivatoric portion of the stress since it reduces to  $(\sigma_1 - \sigma_3)$  for the stress condition used in deriving Equation (2.7)

(i.e. 
$$\sigma_z = \sigma_1$$
,  $\sigma_r = \sigma_\theta = \sigma_\theta$ , all  $\tau$ 's = 0).

Similarly,  $\dot{\tilde{\epsilon}}$  is the effective strain rate given by

$$\dot{\vec{\epsilon}} = \left\{ 2/9 \left[ (\dot{\epsilon}_{\mathbf{r}} - \dot{\epsilon}_{\theta})^2 + (\dot{\epsilon}_{\theta} - \dot{\epsilon}_{\mathbf{z}})^2 + (\dot{\epsilon}_{\mathbf{z}} - \dot{\epsilon}_{\mathbf{r}})^2 \right] + 3(\dot{\gamma}_{\mathbf{rz}}^2 + \dot{\gamma}_{\mathbf{z}\theta}^2 + \dot{\gamma}_{\mathbf{r}\theta}^2) \right\} 1/2.$$
(5.11)

For the case of  $\dot{\epsilon}_r = \dot{\epsilon}_\theta$ ,  $\dot{\epsilon}_r + \dot{\epsilon}_\theta + \dot{\epsilon}_z = 0$ ,  $\dot{\epsilon}_z = \dot{\epsilon}_1$ , and all

shear strains equal to zero,  $\dot{\epsilon}$  becomes  $\dot{\epsilon_1}$ , thus making it a

reasonable choice for the strain rate element. The mean normal stress is

$$\sigma_{\rm m} = \frac{1}{3} \quad (\sigma_{\rm r} + \sigma_{\theta} + \sigma_{\rm z}). \tag{5.12}$$

Using Equations (5.2), (5.3), and (5.10) to calculate  $\bar{\sigma}$  for the thick-walled cylinder, it becomes

$$= \sqrt{3/2} r \frac{d\sigma_{\mathbf{r}}}{d\mathbf{r}}.$$
 (5.13)

Similarly, based on the plane strain assumption ( $\epsilon_z$  = 0) and the incompressibility condition (5.1), the effective strain rate is

$$\frac{\dot{\epsilon}}{\epsilon} = (2\sqrt{3}/3)\dot{\epsilon}_{\theta}. \tag{5.14}$$

The calculation of  $\sigma_{_{\boldsymbol{m}}}$  yields

$$\sigma_{\rm m} = \sigma_{\rm r} + \frac{\rm r}{2} \frac{\rm d\sigma_{\rm r}}{\rm dr}. \tag{5.15}$$

Substituting the strain-displacement relationships (5.5) and (5.6) into Equation (5.4) and taking the time derivative, the equation

$$\frac{d\dot{u}}{dr} + \frac{\dot{u}}{r} = 0 \tag{5.16}$$

is obtained. Solving Equation (5.16),

$$\dot{\mathbf{u}} = \frac{\mathbf{k}_1}{\mathbf{r}} \tag{5.17}$$

$$\dot{\varepsilon}_{\theta} = \frac{k_1}{r^2} \tag{5.18}$$

and substituting this for  $\dot{\epsilon}_{\theta}$  into Equation (5.14),

$$\frac{\dot{\epsilon}}{\epsilon} = \frac{2\sqrt{3}}{3} \frac{k_1}{r^2}.$$
 (5.19)

The governing differential equation is formed by substituting expressions (5.13), (5.15), and (5.19) into Equation (5.9). After doing this, taking the natural logarithm of both sides, and rearranging terms, the differential equation becomes

$$\frac{d\sigma_{\mathbf{r}}}{d\mathbf{r}} - \left(\frac{\mathbf{m}}{\mathbf{Q}\mathbf{r}}\right)\sigma_{\mathbf{r}} = \frac{1}{\mathbf{Q}\mathbf{r}} \ln\left(\frac{2\sqrt{3}\mathbf{k}_{1}}{3\mathbf{C}\mathbf{r}^{2}}\right)$$
 (5.20)

where  $Q = \sqrt{3}N - \frac{m}{2}$ . Solving Equation (5.20) for  $\sigma_r$ ,

$$\sigma_{r} = -\frac{1}{m} \ln \left( \frac{2\sqrt{3}k_{1}}{3Cr^{2}} \right) + \frac{2Q}{m^{2}} + k_{2}(r)^{\frac{m}{Q}}$$
 (5.21)

Using boundary conditions (5.7) and (5.8) to solve for the constants of integration,  $k_1$  and  $k_2$ , they are found to be

$$k_{1} = \frac{\sqrt{3}Ca^{2}exp}{2} \left\{ \frac{2Q}{m} + \left[ \frac{pm + 2 \ln \left( \frac{a}{b} \right)}{\frac{m}{Q} - \frac{m}{Q}} \right] \right\}$$

and

$$k_2 = \frac{p + \frac{2}{m} \ln \left(\frac{a}{b}\right)}{\frac{m}{Q} \frac{m}{Q}}$$

$$(b) - (a)$$

The expressions for stresses, radial displacement rate, and strain rates are then

$$\sigma_{\mathbf{r}} = -\frac{1}{m} \ln \left(\frac{\mathbf{a}}{\mathbf{r}}\right)^{2} + \left[\left(\frac{\mathbf{r}}{\mathbf{a}}\right)^{2} - 1\right] \left[\frac{\mathbf{p} + \frac{2}{m} \ln \left(\frac{\mathbf{a}}{\mathbf{b}}\right)}{\frac{m}{Q} - \frac{m}{Q}}\right]$$
(5.22a)

$$\sigma_{\theta} = \frac{2}{m} - \frac{1}{m} \ln \left(\frac{\underline{a}}{r}\right)^{2} + \left[\left(\frac{\underline{r}}{\underline{a}}\right)^{\frac{m}{Q}} \left(1 + \frac{\underline{m}}{Q}\right) - 1\right] \underbrace{\begin{bmatrix} p + \frac{2}{m} \ln \left(\frac{\underline{a}}{\underline{b}}\right) \\ \frac{\underline{m}}{Q} & -\frac{\underline{m}}{Q} \\ (b) & (a) & -1 \end{bmatrix}}_{(5.22b)}$$

$$\sigma_{z} = \frac{1}{m} \left[ 1 - \ln \left( \frac{a}{r} \right)^{2} \right] + \left[ \left( \frac{r}{a} \right)^{\frac{m}{Q}} \left( 1 - \frac{m}{2Q} \right) - 1 \right] = \left[ \frac{p + \frac{2}{m} \ln \left( \frac{a}{b} \right)}{\frac{m}{Q} - \frac{m}{Q}} \right]$$

$$(5.22c)$$

$$\dot{u} = \frac{\sqrt{3}Ca^2}{2r} \exp \left\{ \frac{2Q}{m} + \left[ \frac{pm + 2\ln\left(\frac{a}{b}\right)}{\frac{m}{Q} - \frac{m}{Q}} \right] \right\}$$

$$(5.23)$$

$$\dot{\varepsilon}_{\theta} = \frac{\sqrt{3}\text{Ca}^2}{2\text{r}^2} \exp \left\{ \frac{2Q}{m} + \left[ \frac{pm + 2\ln\left(\frac{a}{b}\right)}{\frac{m}{Q} - \frac{m}{Q}} \right] \right\}$$

$$(5.24a)$$

$$\dot{\varepsilon}_{r} = -\frac{\sqrt{3}Ca^{2}}{2r^{2}} \exp \left\{ \frac{2Q}{m} + \begin{bmatrix} \frac{pm + 2\ln{\frac{a}{b}}}{\frac{m}{Q}} \\ \frac{m}{Q} & -\frac{m}{Q} \\ (b) & (a) & -1 \end{bmatrix} \right\}$$
(5.24b)

The variation of u and  $\varepsilon$  across the section is shown in Figure 5.2 for a unit rate of displacement at r = a.

Equation (5.23) can be used to predict the deformation of a cylindrical soil-ice barrier which satisfies the preceding assumptions at any time after the initiation of secondary creep. Therefore, the dimensions of the shaft could be determined to fit the size of the permanent supports at the time of their placement. The parameters C, N, and m could be determined by conducting differential creep tests on undisturbed samples frozen to several different temperatures. Based on this, the temperature and the size of the soil-ice barrier could be chosen so that displacements would remain within tolerable limits.

Stresses calculated according to Equations (5.22) can be used to check the strength of the barrier. Stress combinations must be compared with the failure criterion (e.g. Mohr-Coulomb) to insure that conditions necessary to produce failure exist nowhere in the barrier.

# 5.3 Analysis Based on Time Dependent Strength Parameters

AlNouri (1969) reports that time dependent strength parameters cohesion, c, and angle of internal friction,  $\phi$ , can be used to describe creep behavior in cylindrical sandice samples. Using the results of differential creep tests, AlNouri plotted Mohr circles for various stress conditions, each of which produced the same strain rate (See Figure 5.3). He showed that for a sand-ice material one straight



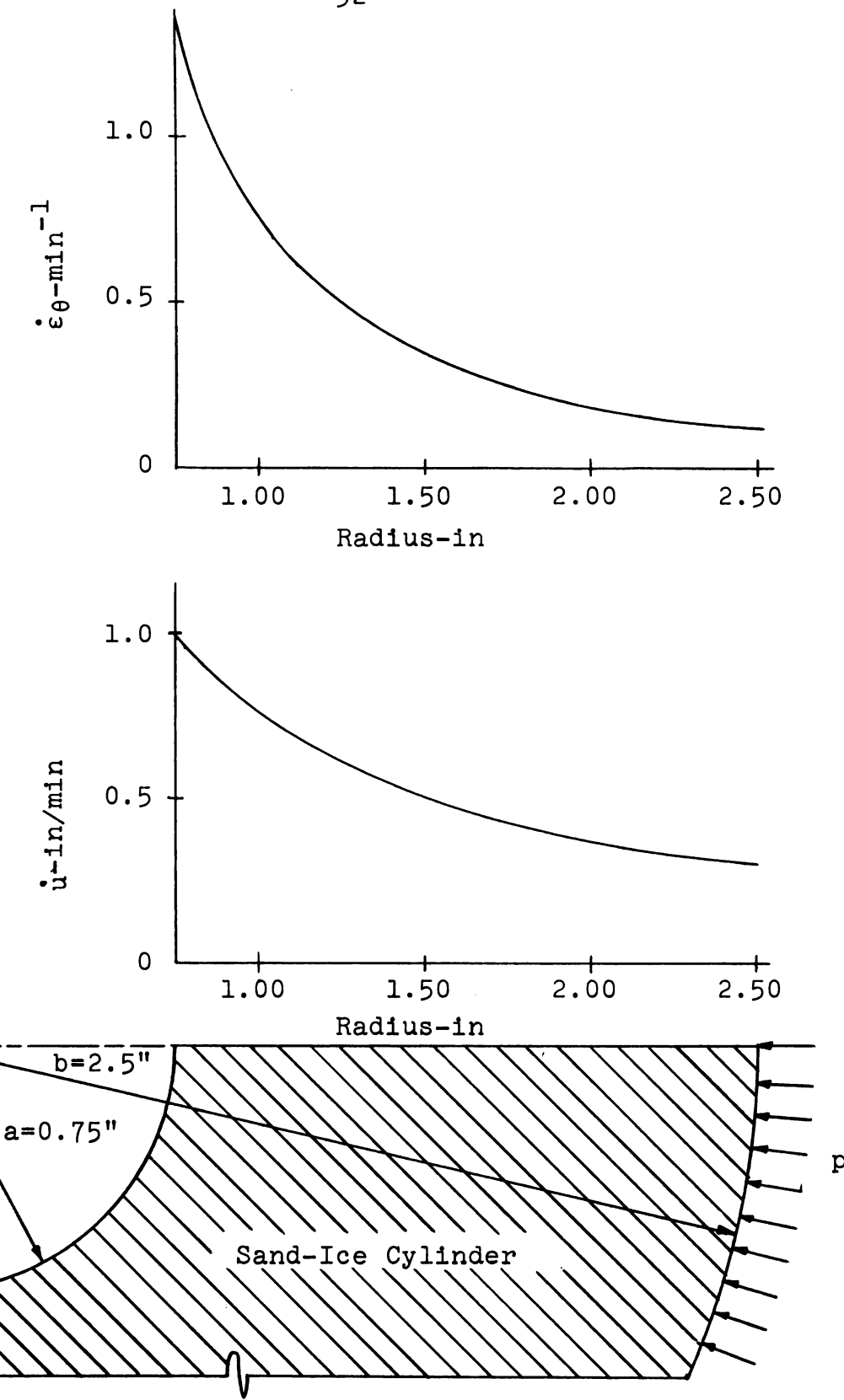


Figure 5.2. Distribution of  $\dot{u}$  and  $\dot{\epsilon}_{\theta}$  for a Unit Rate of Displacement at Inner Surface

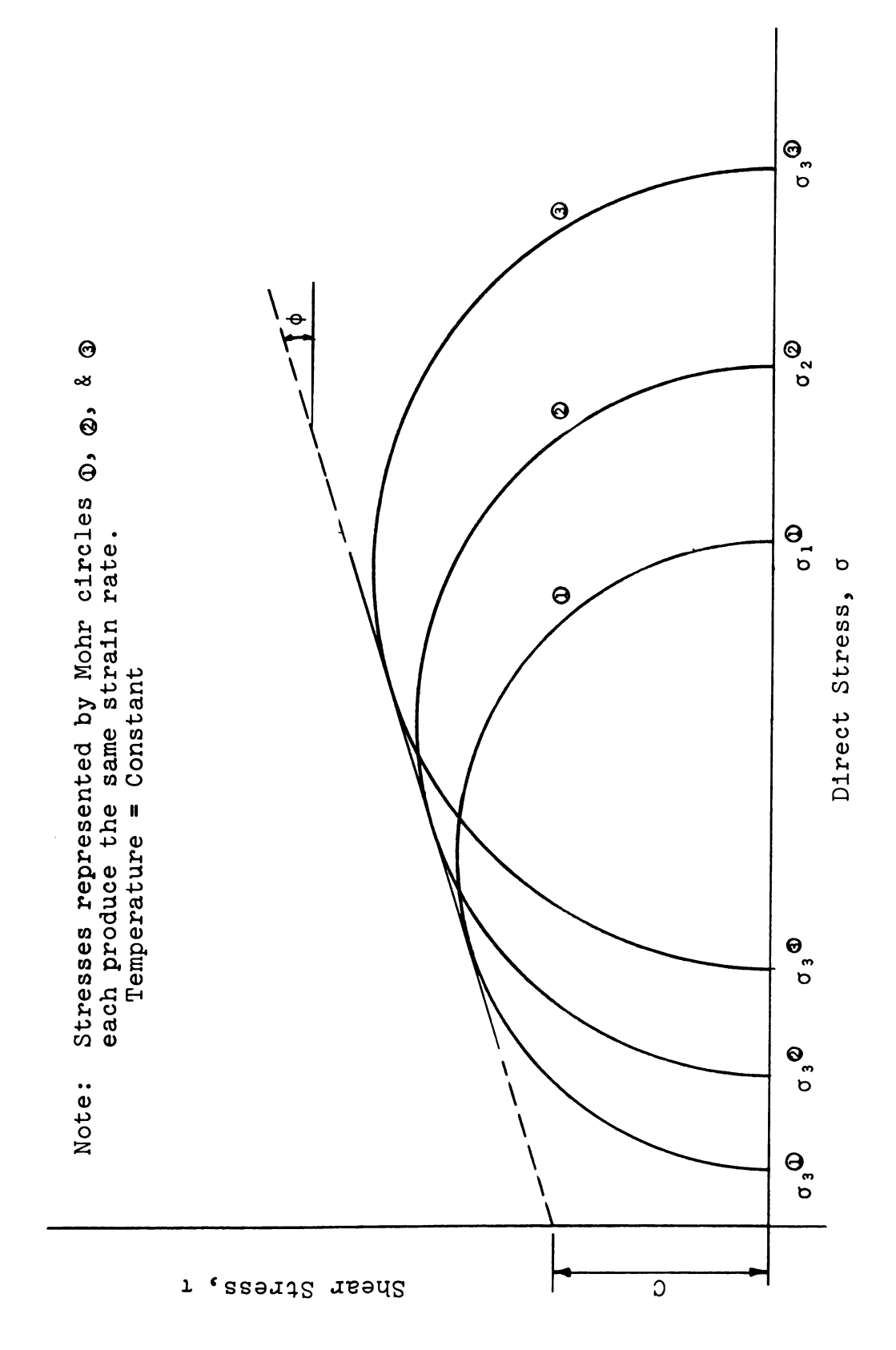


Figure 5.3. Mohr Circle Representation

line could be drawn tangent to each of the circles. Thus, this straight line, defined by its intercept d, and slope angle  $\phi$ , is characteristic of a given strain rate.

The use of such a geometrical representation immediately suggests an analogy to the Mohr-Coulomb failure criterion. It should be noted here, however, that the straight line described above is not related to failure in the conventional sense. Rather, it defines stress combinations necessary to produce a particular strain rate. Failure need not be approached anywhere in the soil-ice mass.

By considering the geometry of the Mohr plot, the principal stresses can be related to the time dependent strength parameters as follows:

$$\sigma - N^2 \sigma = 2eN.$$
 (5.25)

 $\sigma_1$  and  $\sigma_3$  are the major and minor principal stresses, respectively, and N = tan (45° +  $\phi/2$ ). As noted above,  $\sigma_{\theta}$  corresponds to  $\sigma_1$  and  $\sigma_r$  to  $\sigma_3$  in the problem under consideration. Thus, after rearranging terms, Equation (5.25) can be rewritten

$$\sigma_{\theta} = N^2 \sigma_{\mathbf{r}} + 2 c N. \qquad (5.25')$$

Substituting this expression for  $\sigma_{\theta}$  into the equation of equilibrium (5.3), the resulting differential equation is

$$\frac{d\sigma_{\mathbf{r}}}{d\mathbf{r}} + \frac{\sigma_{\mathbf{r}}(1-N^2)}{\mathbf{r}} = \frac{2\sigma N}{\mathbf{r}}.$$
 (5.26)

Solving Equation (5.26) for  $\sigma_{p}$ ,

$$\sigma_{\mathbf{r}} = \frac{1}{N^2 - 1} \left[ -2cN + (k_3 r)^{N^2 - 1} \right]$$
 (5.27)

where  $k_3$  is a constant of integration. The value of  $k_3$  can be determined by using the boundary condition that  $\sigma_n = 0$  at r = a.

$$k_3^{N^2-1} = \frac{2cN}{(a)^{N^2-1}}$$

Thus,

$$q_{r} = \frac{2cN}{N^{2}-1} \left[ \frac{r}{a} \right]^{N^{2}-1} -1$$
 (5.28)

Since the pressure, p, is applied at r = b, the following relationship results:

$$p = \frac{2cN}{N^2 - 1} \left[ \left( \frac{b}{a} \right)^{N^2 - 1} - 1 \right]. \tag{5.29}$$

Equation (5.29) relates the outside pressure and the geometry of the soil-ice barrier to the time dependent strength parameters.

The use of Equation (5.29) is complicated by a difficulty in obtaining reliable values for c and  $\phi$ . Little is known regarding the nature of these time dependent parame-By using a trial and error method, it would be necessary to conduct a large number of creep tests in order to determine them for a range of strain rates. However, AlNouri's (1969) work indicates that only a few tests are needed to evaluate the constants C, N, and m. Then Equation (2.7) can be used for the determination of C and  $\phi$ . For a particular strain rate, various values of  $\sigma_{\gamma}$  could be specified and the resulting values for  $\boldsymbol{\sigma}_{\gamma}$  calculated according to Equation (2.7). Thus, a series of Mohr circles could be drawn and the strength parameters would then be determined by drawing the straight line tangent to them. A further limitation is that it is not known whether this approach is applicable to a wide range of soil types. Available data (AlNouri, 1969) are only for a sand-ice system.

Assuming that satisfactory values of c and \$\phi\$ could be obtained, Equation (5.29) would be a useful tool for designing frozen soil barriers. The radius of the shaft, a, would be fixed in most cases and the pressure could be estimated based on earth pressure theory. The size of the barrier necessary to limit the strain rate to an acceptable value at a given temperature could then be determined by calculating the outer radius, b, from Equation (5.29).

#### CHAPTER VI

#### EXPERIMENTAL RESULTS

## 6.1 General

The experimental program consisted of 18 tests on the sand-ice material and 6 on frozen clay. In each test (with two exceptions), a lateral load of 100 pounds per square inch was initially applied to the model. This produced little or no deformation in the sand-ice samples but served to account for any seating difficulty caused by shifting of the sample. After a brief period of time, the load was increased to 200 p.s.i. and then in 100 p.s.i. increments for the remainder of the test. Each load increment was allowed to remain until the steady state portion of the creep curve was established. The only exception to this was at low stress levels in the sand-ice samples where such stresses produced insignificant deformation. The rate of deformation for each load increment was then calculated by using the calibration information for the deformation measuring device (See Appendix B).

Due to the new design of the testing equipment and procedures, a number of difficulties were encountered in the

experimental work. The results of early tests are probably questionable since preparation techniques and testing procedures were being formulated, and it was uncertain exactly what methods would provide the desired effect. These tests served to define the capabilities and limitations of the equipment as well as to establish procedures. Modifications in both the equipment and techniques were made throughout the entire testing program in order to produce more reliable results.

In addition, mechanical problems eliminated results from several tests and rendered results invalid on others. Five tests were aborted due to failure of the membranes encasing the samples. This allowed leakage of the ethylene glycol into the sample, causing an immediate loss of pressure in the system and melting of the sample. Membrane failure was believed to be related to difficulty in obtaining flat, square ends, particularly in the sand-ice samples. This caused small gaps between the sample and the piston, thus allowing the membranes to be punctured as they were stretched into these irregularities by higher pressures. Greater care was exercised during sample preparation and more membranes were used on each sample to correct this. However, the problem was not completely solved.

The deformation measuring device was the source of another difficulty. The brass pieces had a tendency to rotate approximately 90° as the device was installed. This caused the wrong side of the brass pieces to be in contact

with the sample and, thus produced erroneous readings on several tests. When this problem was recognized, restraints which limited the range of rotation of the brass pieces were placed on them.

Lateral shifting of the sample both during the preparation and during testing created difficulties in aligning the center hole of the model with the hole in the piston. To rectify this problem during preparation, a precooled steel rod, 24 inches long and 1 7/16 inches in diameter, was placed through the center hole of the model and into the hole in the pedestal. The piston was then guided into place by sliding it over the steel rod. The rod remained in place until the cell was assembled and placed in the cooling tank. To eliminate shifting of the sample during testing, a styrofoam plug was placed in the hole in the pedestal and allowed to extend 1/2 inch into the center hole of the sample. This stabilized the sample but did not interfere with its deformation.

The two piece piston was initially fabricated by "force fitting" the bottom, flat cylindrical portion onto the shaft portion. It was soon discovered that the downward force due to the pressure on the flat portion was causing it to slip slightly on the shaft. A single 1/8 inch pin was then placed through the two pieces and it was later replaced by three, 1/4 inch pins. This slipping induced an axial load in the sample in excess of that necessary to enforce the plane strain condition. It also appeared that a small

amount of ethylene glycol leaked into the sample through the area of contact between the two pieces. This caused weakening of the sample and excessive deformation in several tests. A silicon rubber sealer was placed at the interface to eliminate leakage. Both the slippage and leakage appeared to occur in the samples with a 5 inch outer diameter and at high pressure. This condition created the greatest downward force on the piston.

Thus, while a total of 24 tests were conducted, only a somewhat smaller number can be considered valid. All results are reported in the following sections. Comments are made regarding the relative validity of them.

### 6.2 Deformation Results

## 6.2.1 Sand-Ice

A summary of the tests conducted on sand-ice samples is given in Table 6.1. An attempt was made to determine displacement rates for various pressures and wall thicknesses. Using an inner diameter of 1 1/2 inches, samples with outer diameters of 3 1/2, 4, 4 1/2, and 5 inches were tested. The length of nearly all samples was approximately 9 inches. The only exception was Test SA-10 where damage near the end of the sample caused its length to be reduced to 7 1/2 inches.

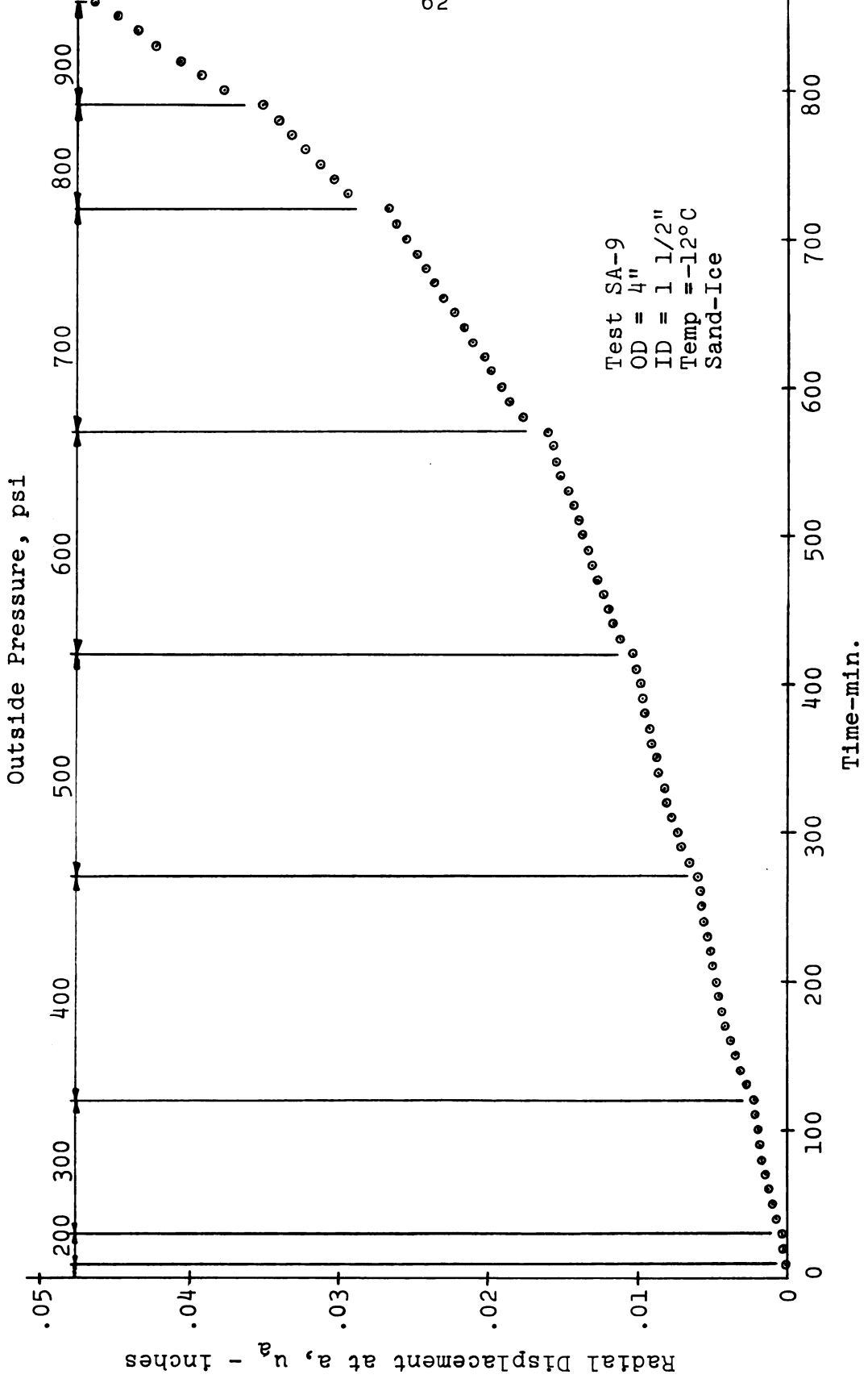
Typical displacement results are given for two tests in Figures 6.1 and 6.2 in the form of time vs. radial displacement at the inner surface plots. These results show

Table 6.1 Summary of sand-ice tests

Test Designation	Outer Diameter (inches)	Height (inches)	Water Content (%)	Remarks
SA-1 SA-2	5 5	9	21.0 18.5	Membrane failed Membrane failed. Reused sand changed proper- ties.
SA-3	5	9	21.6	Low pressures used produced insignificant deformation.
SA-4	4	9 5/16	20.6	
SA-5	3 1/2	9 5/16 9	20.2	Poor alignment of sample and piston
SA-6	3 1/2	9	20.2	Contaminated sand used
SA-7 SA-8	3 1/2 4	9 1/8 9 5/16	21.0 21.6	Cooled to -25.4°C prior to test
SA-9 SA-10	4 3 <b>1/</b> 2	9 3/16 <b>7 1/</b> 2	21.2 20.7	Brass piece ro-
SA-11 SA-12 SA-13 SA-14	3 1/2 4 1/2 3 1/2 5	9 1/8 9 3/16 9 1/8 9 1/4	21.4 21.0 20.8 21.6	Sample shifted Piston slipped. Ethylene glycol may have reached sample.
SA-15 SA-16	3 1/2 5	9 9 1/4	21.3	Membrane failed Small amount of ethylene glycol may have reached sample.
SA-17 SA-18	3 1/2 5	9	21.8 21.4	Membrane failed Small amount of ethylene glycol may have reached sample.

Note: Data on all samples
Inner diameter 1 1/2 inches
Test temperature -12.0°C
Sand density 64% by volume





Time-Displacement Plot for Test SA-9

Figure 6.1.

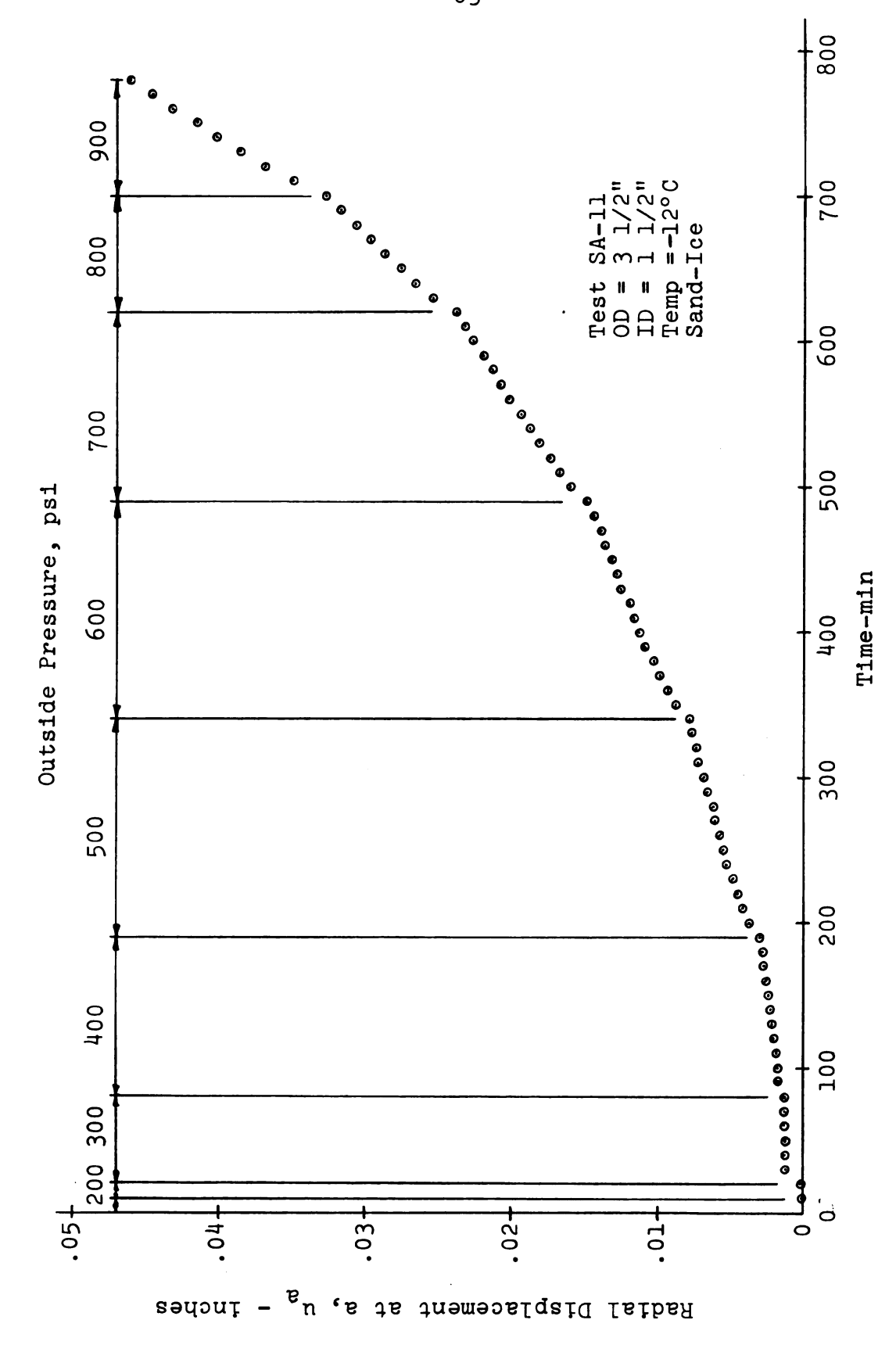


Figure 6.2. Time-Displacement Plot for Test SA-11

that the steady state portion of the curve was well established after a brief period of primary creep following the application of each load increment. The length of time for primary creep seldom exceeded 10 or 20 minutes. Thus, a linear relationship between displacement and time appears to be a valid assumption for the major portion of the deformation process for this material.

Table 6.2 summarizes the steady state strain rates for those tests for which they could be calculated. There are no results on Tests SA-1, 2, 15, and 17 due to membrane failures. Alignment problems eliminated strain rate results on Tests SA-5, 10, and 13, while SA-3 showed very little deformation due to low pressures used. Several of the samples with a 5 inch outer diameter (SA-14, 16, and 18) showed indications that a small amount of ethylene glycol may have leaked into the sample. This probably accounts for the consistantly large deformations in these tests.

# 6.2.2 Frozen Clay

Six tests were conducted on frozen clay samples. Each sample had an outside diameter of 5 inches, an inside diameter of 1 1/2 inches, and was approximately 9 inches in height. The temperature for all tests was -12.0°C. Table 6.3 summarizes the frozen clay testing program. Displacement rates at the inner surface are given in Table 6.4, while Figure 6.3 shows a plot of time vs. displacement for a typical test.

TABLE 6.2 Sand-ice displacement rate results

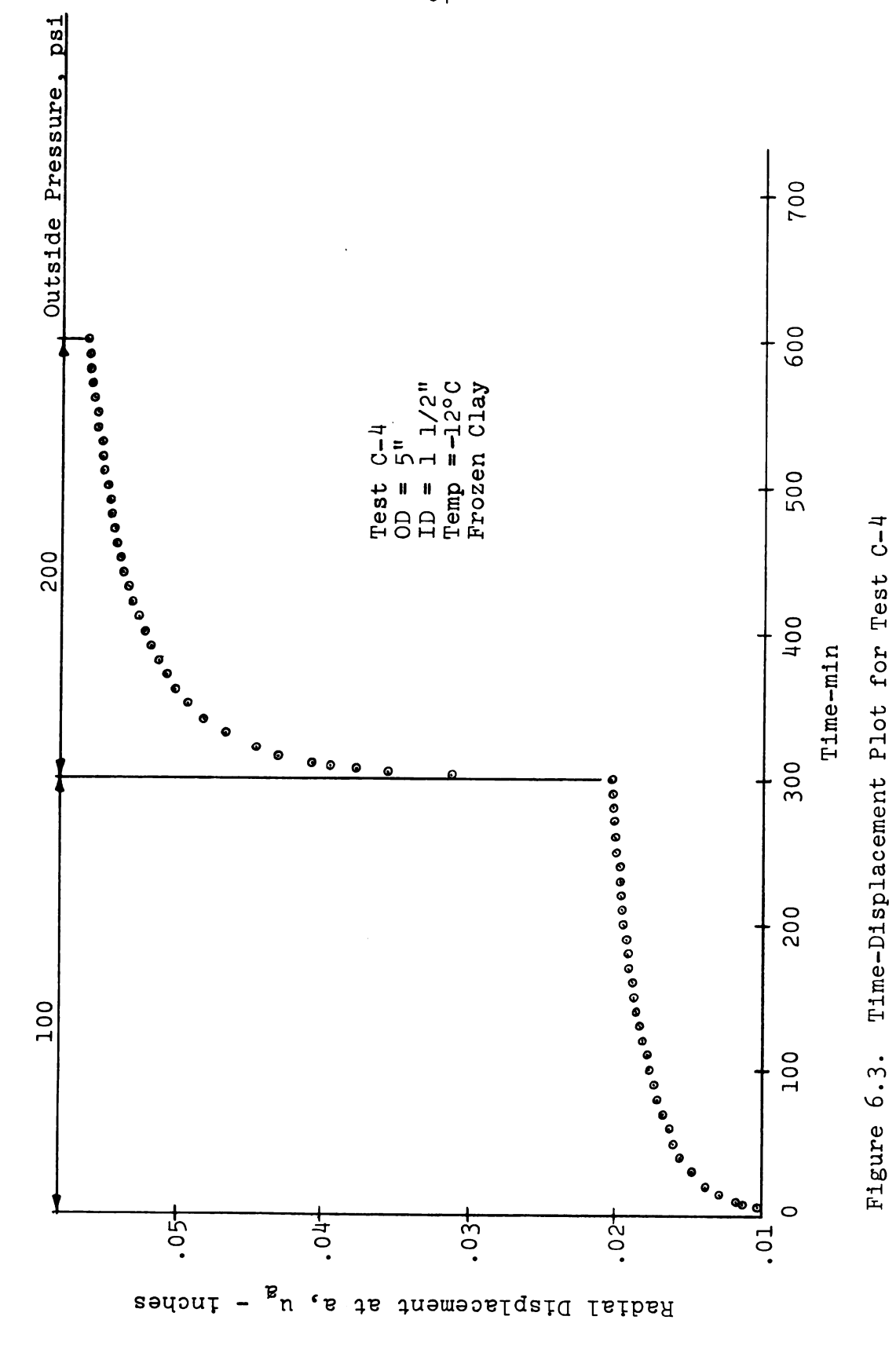
Pressure	Radial	kadiai displacement rate at inner surface, "a x 10" (in/minutes)								
p (ps1)	SA-4 OD=4" OD	SA-6 OD=3 1/2"	SA-4 SA-6 SA-7 SA-8 SA-9 SA-11 SA-12 SA-14 SA-16 SA-18 OD=4" OD=3 1/2" OD=3 1/2" OD=5" OD=5" OD=5"	SA-8 SA-9 OD=4" OD=4"	SA-9 OD=4"	SA-11 OD=3 1/2"	SA-12 OD=4 1/2"	SA-14 SA-16 SA-18 "OD=5" OD=5" OD=5"	SA-16 OD=5"	SA-18 OD=5"
00 †	1.30	1.24	2.65	2.12	2.12 2.07	1.28	2.25			
200	1.95	1.77	2.78	3.30	3.30 2.15	2.98	3.45	3.95	5.90 4.70	4.70
009	2.90	2.55	3.70	4.45	4.45 3.50	4.45	4.35	6.65	6.10	00.9
700	5.00	3.25	5.32	6.72	6.72 6.40	8.00	6.05	7.75	7.75 9.90	6.50
800	İ	1	9.90	9.45	9.45 9.75	10.55	8.20	11.30	11.30 13/30 11.20	11.20
006	1		27.00	17.00 14.30	14.30	16.45	10.75	16.00	16.00 21.00 17.60	17.60

TABLE 6.3 Summary of frozen clay tests

Test Designation	Height (inches)	Water Content (%)	Density (lbs/ft <sup>3</sup> )	Remarks
C-1	9 1/16	26.1	98.9	Membrane failed
C-2	9	25.5	98.9	Steady state creep not reached
C-3	9 1/4	26.2	97.3	
C-4	9 3/16	25.0	98.2	
C <b>-</b> 5	9 3/16	24.8	98.2	
C-6	9 1/8	24.8	99.1	Membrane failed

TABLE 6.4 Frozen clay displacement rate results

Outside Pressure	Radial dis at inner su	placemer rface, i (in/min)	ia x 10 <sup>-5</sup>
(psi)	C-3	C-4	C-5
100		0.815	
200	Constitution	1.48	1.56
300	2.42		1.77
400	***		



It is apparent from Figure 6.3 that the time-displacement characteristics of the frozen clay are quite different from those of the sand-ice material (Figures 6.1 and 6.2). The time required to reach steady state creep was approximately 150 minutes for each load increment, compared to 10 or 20 minutes for the sand-ice. In addition, the magnitude of the displacement during primary creep was considerably greater for the frozen clay. For this reason, the steady state displacement rates reported in Table 6.4 are smaller than those for the sand-ice tests. Pressures large enough to produce steady state displacement rates as large as those for the sand-ice would have caused the sample to become grossly distorted due to the large deformation during primary creep.

In Test C-1, a hydraulic oil was used as the fluid which transmitted the pressure to the sample. It was learned that this oil slowly expanded and penetrated the rubber membranes which encased the sample. When this was recognized, the hydraulic oil was replaced by the mixture of ethylene glycol and water.

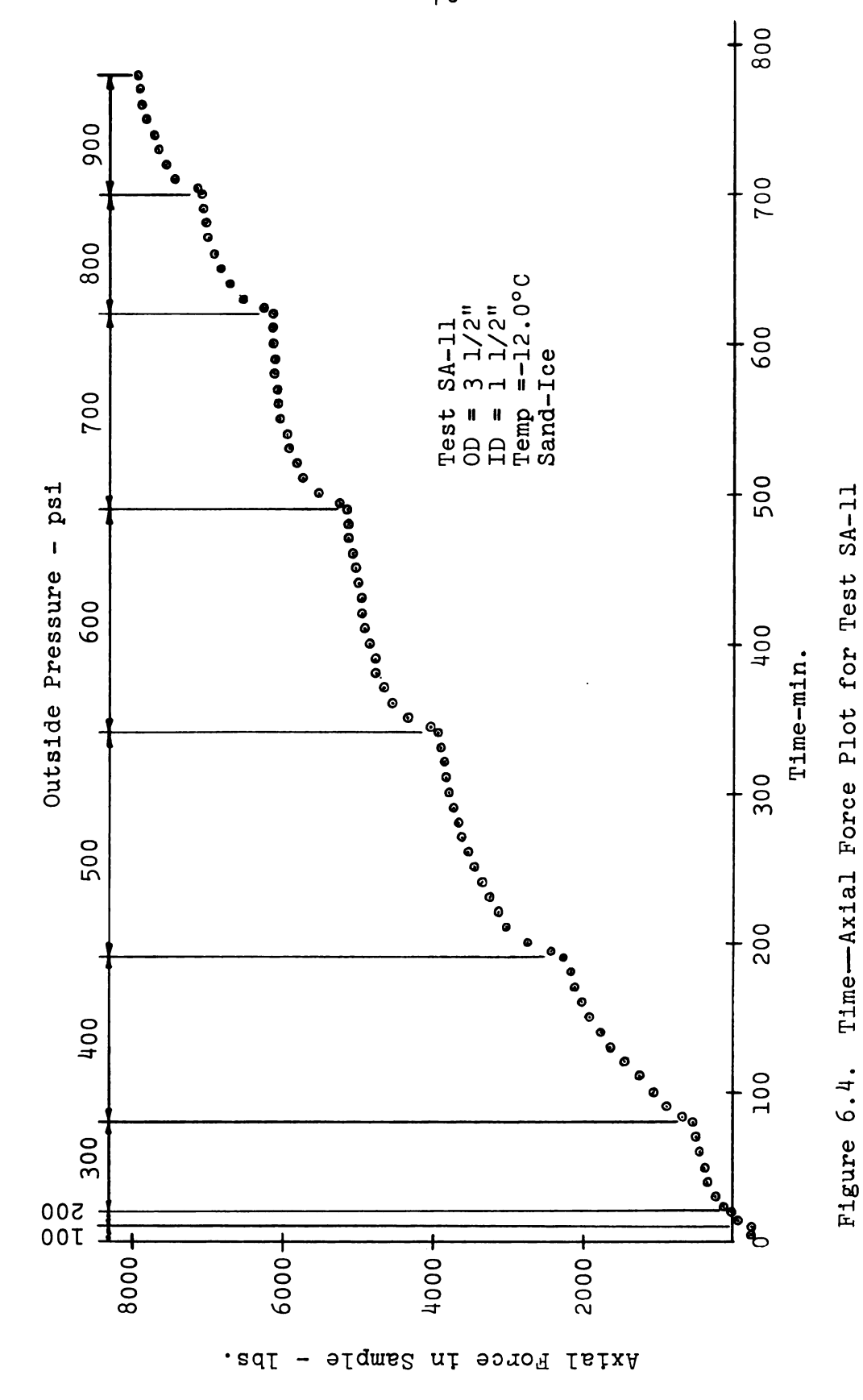
The length of time necessary to reach secondary creep was not known when Tests C-1 and C-2 were conducted.

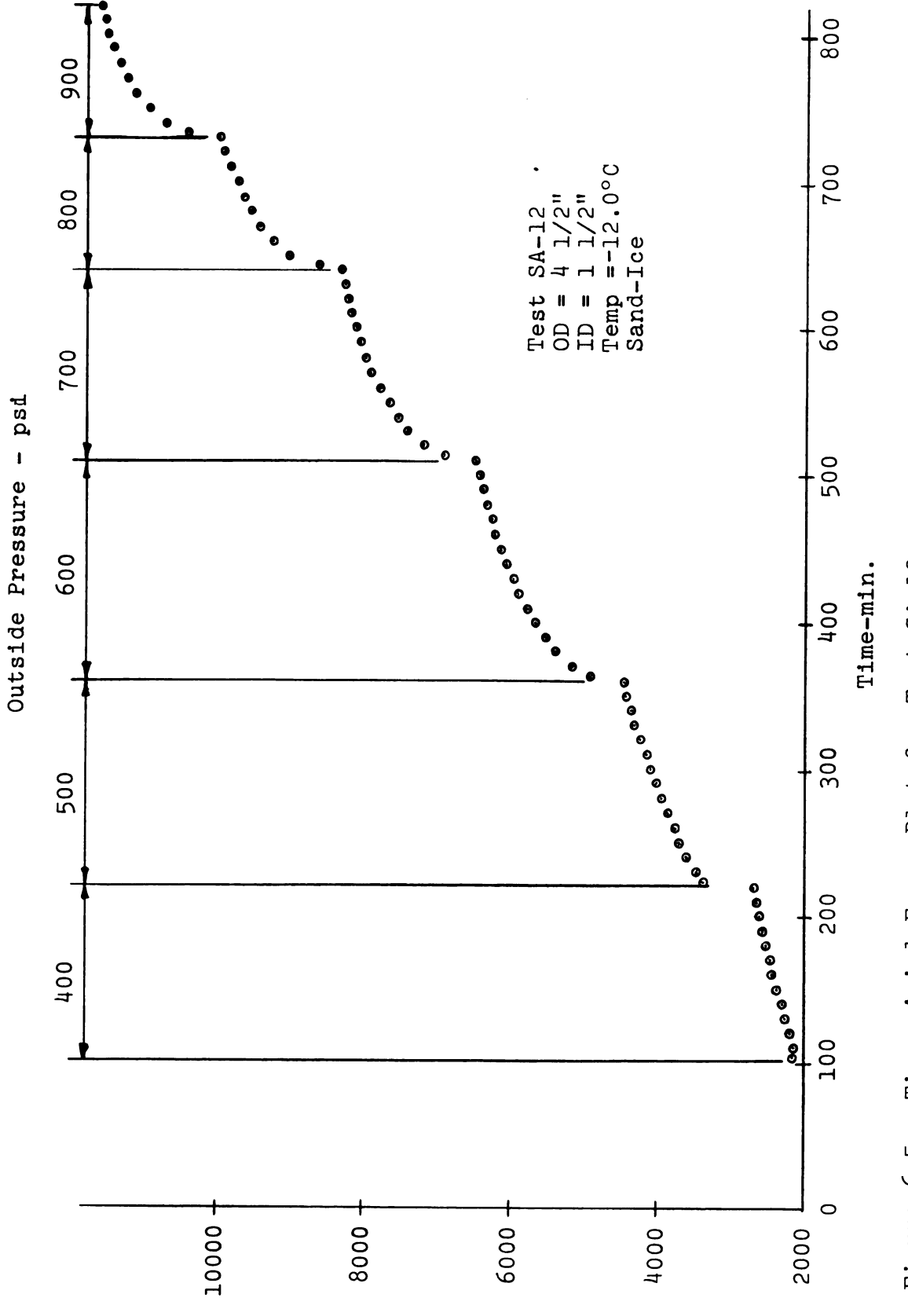
Therefore, the time used for each load increment was not sufficient to determine the displacement rate corresponding to this part of the creep curve. For subsequent tests, it was decided to apply each load increment for a period of 300 minutes, thus assuring approximately 150 minutes of steady state creep.

## 6.3 Axial Force Results

During each test, the total axial force in the sample was measured using the load cell mounted in the base of the testing cell. The force indicated by the load cell reading consisted of both the force due to the pressure acting on the exposed portion of the pedestal and the force in the sample. Since the pressure and the exposed area of the pedestal were known, the total axial force in the sample could be calculated. Details of the calculations are outlined in Appendix C, while calibration data for the load cell are given in Appendix B.

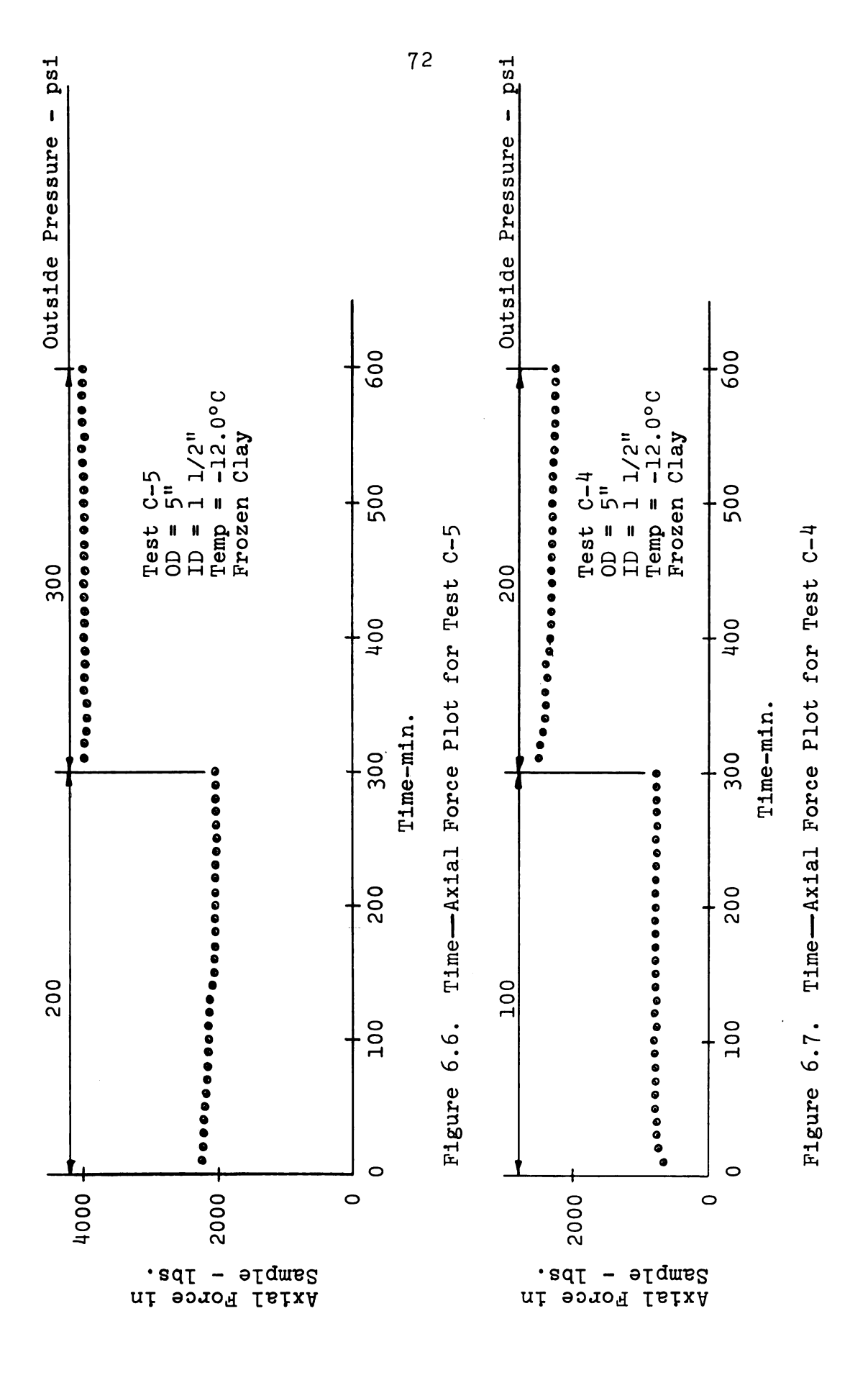
Figures 6.4 and 6.5 show the relationship between total axial force and time of loading for two tests on sand-ice samples. Figures 6.6 and 6.7 illustrate the same relationship for two clay samples. It can be seen that the time dependent behavior of the axial force differed for the two materials. In the case of the sand-ice samples, the total axial force continued to increase during the entire time of each load increment. Since the rate of this increase appears to decrease with time, it is probable that the axial force would approach a constant value after some period of time. By contrast, in the tests on clay samples, a constant value of axial force was reached almost immediately. Only minor fluctuations from this value occurred during the remainder of each load increment.





Axial Force in Sample - lbs.

Figure 6.5. Time -- Axial Force Plot for Test SA-12



#### CHAPTER VII

#### DISCUSSION AND INTERPRETATION OF RESULTS

## 7.1 General

In this chapter, the experimental results given in Chapter VI are discussed and compared with analytical results based on the theoretical considerations presented in Chapter V. As a consequence of these comparisons, modifications are proposed for the analyses in order that they may provide results more consistent with those experimentally measured.

The experimental parameters used for the sand-ice material and the frozen Ontonagon clay are those reported by AlNouri (1969). As far as possible, it was attempted in this study to duplicate the preparation techniques used by AlNouri. Materials, moisture content, density, and temperature history were as identical as conditions would permit. Further, strain rates were chosen to fall within or near the range used by AlNouri in his triaxial creep tests. This is illustrated in Figures 7.1 and 7.2 where the range of axial strain rates measured by AlNouri are shown adjacent to the circumferential strain rates found for the frozen soil cylinders.

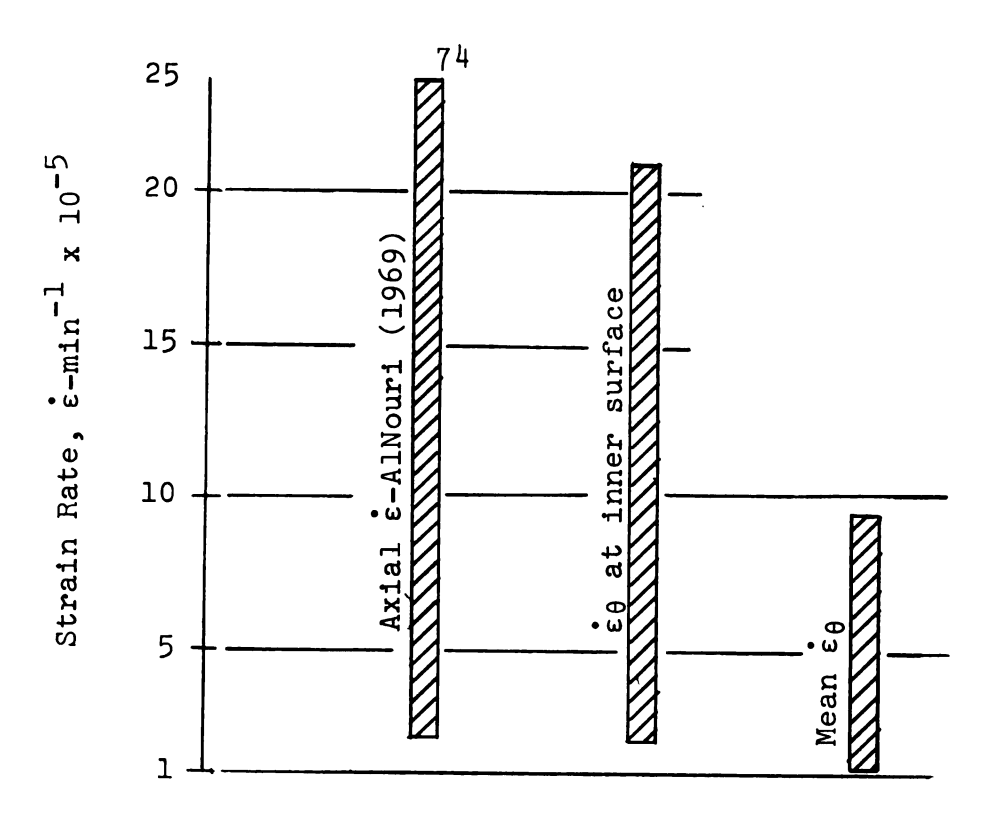


Figure 7.1. Range of Strain Rates, Sand-Ice

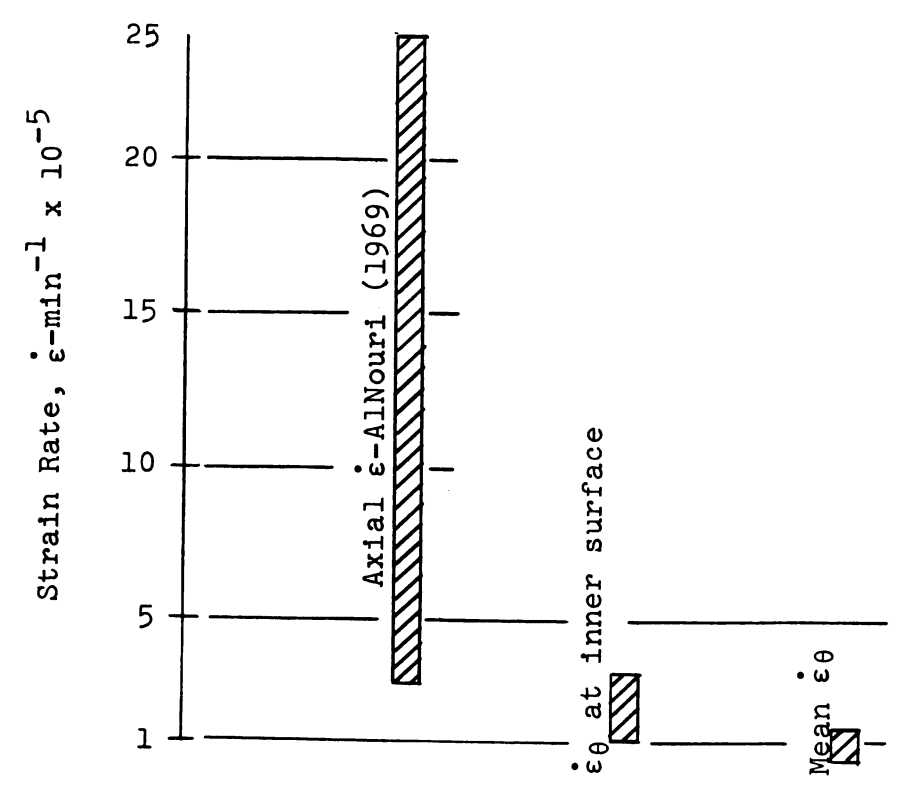


Figure 7.2. Range of Strain Rates, Frozen Clay

It should be noted here that the value of comparisons presented in this chapter must not be overestimated. The amount of available experimental data, both regarding evaluation of experimental parameters as well as results on hollow cylindrical models, are limited. The experimental equipment and procedures used in this study are new and can doubtless be improved upon. Thus, while the forms of Equation (2.6) and the equations proposed in Chapter V appear to be valid, and a comparison with experimental results is appropriate, the actual numerical values remain open to question.

The two materials used in this study are discussed separately below. Both analyses presented in Chapter V are compared with the experimental results on the sand-ice system. Since data regarding time dependent strength parameters for the frozen clay are unavailable, only the creep equation approach is discussed for this material.

# 7.2 Sand-Ice

# 7.2.1 Comparison With Creep Equation Analysis

In order to compare the rate of radial displacement predicted by Equation (5.23) with that measured experimentally, the following values for experimental parameters were taken from the results of AlNouri (1969) for the sand-ice material at  $-12.0^{\circ}$ C.:

$$C = 9.103 \times 10^{-6}$$
 min<sup>-1</sup>  
 $N = 8.08 \times 10^{-3}$  in<sup>2</sup>/1b  
 $m = 1.206 \times 10^{-2}$  in<sup>2</sup>/1b

Using these parameters to calculate the rate of radial displacement at the inner surface for a cylinder with an inner diameter of 1 1/2 inches and an outer diameter of 5 inches, the resulting equation is

$$\ddot{\mathbf{u}}_{a} = 3.96 \times 10^{-6} \exp \left[ 0.1608 + \frac{(1.206 \times 10^{-2}) \text{p} - 2.408}{3.53 \times 10^{6}} \right]$$

where p is the radial outside pressure in p.s.i. It is apparent from this expression that pressure has a negligible effect on the displacement rate. Since this neither appears to be reasonable nor is it confirmed by the experimental results, it is necessary to modify the analysis in some manner.

In Equation (5.9), the effect of the deviatoric part of the stress  $(\overline{\sigma})$  is separated from the hydrostatic portion  $(\sigma_m)$ . The relative effect of these portions on deformation is not well understood. In fact, it has often been assumed that creep is completely independent of the hydrostatic stress. It is, therefore, proposed that an adjustment be made in the relative contributions of the two parts of the stress.

This adjustment can be made in two ways. First, the  ${f hy}$ drostatic component can be allowed to remain as in

Equation (5.9) while the deviatoric portion is adjusted.

After doing this, Equation (5.23) becomes

$$\dot{u} = \frac{\sqrt{3}Ca^{2}}{2r} exp \left\{ \frac{2Q'}{m} + \left[ \frac{pm + 2 \ln \left( \frac{a}{b} \right)}{\frac{m}{Q'} - \frac{m}{Q'}} \right] \right\}$$
(b) (a) -1 (5.23')

where Q' = XN-m/2. The value of X, which was  $\sqrt{3}/2$  in the original formulation, can then be chosen to fit the experimental data.

In order to aid in the selection of an X value, a program was written for the CDC 3600 computer. This allowed a large number of possibilities to be tried with a minimum computation time.

The results of these computations for various values of X are given in Table 7.1. Also listed in Table 7.1 are experimental values for displacement rates from corresponding test results. The experimental results given are those from the tests which appear to be most reliable.

Since Equation (5.23') yields a straight line when the natural logarithm of the displacement rate is plotted against the applied pressure, such a plot is useful for comparison purposes. This is shown in Figure 7.3 for three sizes of cylinders at varying pressures. The straight lines represent the relationship of Equation (5.23') for the indicated values of X. Experimental values are plotted for several different pressures from each of three tests.

Summary of displacement rate comparisons using Equation (5.23'), sand-ice TABLE 7.1

		1.64	5.34 7.87 11.59 17.06 25.12 37.00		3.91 6.99 6.99 12.51 16.73		3.23 4.06 5.10 6.41 8.06
5 (in/min)		1.62	4.99 7.23 10.48 15.18 21.99		3.69 4.87 6.42 8.48 11.20 14.78		3.06 4.74 7.33 9.12
10-	# ×	1.60	4.66 6.65 9.48 13.51 27.47		3.48 4.53 5.91 7.70 10.03		865.448 2014.45 2014.45
sce, ua x	analysis,	1.58	4.35 6.11 8.58 12.04 16.89 23.71		86.23 6.99 11.599		2.77 3.37 4.10 4.99 6.07
inner surfa	By a	1.56	4.07 5.62 7.77 10.73 14.83		3.10 5.00 6.35 8.07		3.17 3.17 3.82 4.60 5.53
e a t		1.54	3.80 5.17 7.04 9.58 13.02 17.72		2.93 4.61 7.78 9.15		65.05 00.05 01.05 01.05
cement rat		1.52	3.56 4.77 6.38 8.55 11.45		86.57 86.57 86.57 86.57		7 4 3 3 5 5 5 6 1 1 5 6 1 1 5 6 1 1 5 6 1 1 5 6 1 1 5 6 1 1 5 6 1 1 5 6 1 1 5 6 1 1 5 6 1 1 5 6 1 1 5 6 1 1 5 6 1 1 5 6 1 1 5 6 1 1 5 6 1 1 5 6 1 1 5 6 1 1 5 6 1 1 5 6 1 1 5 6 1 1 5 6 1 1 5 6 1 1 5 6 1 1 5 6 1 1 5 6 1 1 5 6 1 1 5 6 1 1 5 6 1 1 5 6 1 1 5 6 1 1 5 6 1 1 5 6 1 1 5 6 1 1 5 6 1 1 5 6 1 1 5 6 1 1 5 6 1 1 5 6 1 1 5 6 1 1 5 6 1 1 5 6 1 1 5 6 1 1 5 6 1 1 5 6 1 1 5 6 1 1 5 6 1 1 5 6 1 1 5 6 1 1 5 6 1 1 5 6 1 1 5 6 1 1 5 6 1 1 5 6 1 1 5 6 1 1 5 6 1 1 5 6 1 1 5 6 1 1 5 6 1 1 5 6 1 1 5 6 1 1 5 6 1 1 5 6 1 1 5 6 1 1 5 6 1 1 5 6 1 1 5 6 1 1 5 6 1 1 5 6 1 1 5 6 1 1 5 6 1 1 5 6 1 1 5 6 1 1 5 6 1 1 5 6 1 1 5 6 1 1 5 6 1 1 5 6 1 1 5 6 1 1 5 6 1 1 5 6 1 1 5 6 1 1 5 6 1 1 5 6 1 1 5 6 1 1 5 6 1 1 5 6 1 1 5 6 1 1 5 6 1 1 5 6 1 1 5 6 1 1 5 6 1 1 5 6 1 1 5 6 1 1 5 6 1 1 5 6 1 1 5 6 1 1 5 6 1 1 5 6 1 1 5 6 1 1 5 6 1 1 5 6 1 1 5 6 1 1 5 6 1 1 5 6 1 1 5 6 1 1 5 6 1 1 5 6 1 1 5 6 1 1 5 6 1 1 5 6 1 1 5 6 1 1 5 6 1 1 5 6 1 1 5 6 1 1 5 6 1 1 5 6 1 1 5 6 1 1 5 6 1 1 5 6 1 1 5 6 1 1 5 6 1 1 5 6 1 1 5 6 1 1 5 6 1 1 5 6 1 1 5 6 1 1 5 6 1 1 5 6 1 1 5 6 1 1 5 6 1 1 5 6 1 1 5 6 1 1 5 6 1 1 5 6 1 1 5 6 1 1 5 6 1 1 5 6 1 1 5 6 1 1 5 6 1 1 5 6 1 1 5 6 1 1 5 6 1 1 5 6 1 1 5 6 1 1 5 6 1 1 5 6 1 1 5 6 1 1 5 6 1 1 5 6 1 1 5 6 1 1 5 6 1 1 5 6 1 1 5 6 1 1 5 6 1 1 5 6 1 1 5 6 1 1 5 6 1 1 5 6 1 1 5 6 1 1 5 6 1 1 5 6 1 1 5 6 1 1 5 6 1 1 5 6 1 1 5 6 1 1 5 6 1 1 5 6 1 1 5 6 1 1 5 6 1 1 5 6 1 1 5 6 1 1 5 6 1 1 5 6 1 1 5 6 1 1 5 6 1 1 5 6 1 1 5 6 1 1 5 6 1 1 5 6 1 1 5 6 1 1 5 6 1 1 5 6 1 1 5 6 1 1 5 6 1 1 5 6 1 1 5 6 1 1 5 6 1 1 5 6 1 1 5 6 1 1 5 6 1 1 5 6 1 1 5 6 1 1 5 6 1 1 5 6 1 1 5 6 1 1 5 6 1 1 5 6 1 1 5 6 1 1 5 6 1 1 5 6 1 1 5 6 1 1 5 6 1 1 5 6 1 1 5 6 1 1 5 6 1 1 5 6 1 1 5 6 1 1 5 6 1 1 5 6 1 1 5 6 1 1 5 6 1 1 5 6 1 1 5 6 1 1 5 6 1 1 5 6 1 1 5 6 1 1 5 6 1 1 5 6 1 1 5 6 1 1 5 6 1 1 5 6 1 1 5 6 1 1 5 6 1 1 5 6 1 1 5 6 1 1 5 6 1 1 5 6 1 1 5 6 1 1 5 6 1 1 5 6 1 1 5 6 1 1 5 6 1 1 5 6 1 1 5 6 1 1 5 6 1 1 5 6 1 1 5 6 1 1 5 6 1 1 5 6 1 1 5 6 1 1 5 6 1 1 5 6 1 1 5 6 1 1 5 6 1 1 5 6 1 1 5 6 1 1 5 6 1 1 5 6 1 1 5 6 1 1 5 6 1 1 5 6 1 1 5 6 1 1 5 6 1 1 5
Radial displace	Measured	AVG SA-11 & 7	2.00 2.88 4.07 6.76 10.22 21.72	AVG SA-9 & 8	2.09 3.97 6.56 9.60 15.65		
	Me	SA-11	1.28 4.98 8.45 10.55	SA-9	2.07 3.50 6.40 14.30	SA-12	2.25 3.45 4.35 6.05 8.20
Outsid	Pressure (ps1)	OD=3 1/2"	400 500 700 800 900	υ η=QO	4 500 500 700 900 900	OD=4 1/2"	400 500 700 800 900

Note: Q' = XN-m/2

It can be seen from Table 7.1 and Figure 7.3 that no single value of X provides strain rates which are consistent with experimental results for all sizes of cylinders. However, certain values of X give strain rates which are in reasonable agreement with experimental results for a given size over the range of pressures form 700 to 900 p.s.i. It was found that a better fit was obtained between the analysis and the measured values when the value  $\sqrt{3}/2$  in the coefficient of the exponential in Equation (5.23') was changed to 1/2. This produces the same result as changing the coefficient 2/9 in the expression for  $\frac{1}{6}$  (5.11). This is illustrated in the graphical comparison shown in Figure 7.4.

A second way of modifying Equation (5.9) is to reduce the hydrostatic component by a factor Y. This results in the following expression for the rate of radial displacement:

$$\dot{\mathbf{u}} = \frac{\sqrt{3} \operatorname{Ca}^{2}}{2 \operatorname{r}} \exp \left\{ \frac{2 \operatorname{Q}^{"}}{\operatorname{Ym}} + \left[ \frac{\operatorname{Ypm} + 2 \ln \left( \frac{\operatorname{a}}{\operatorname{b}} \right)}{\operatorname{Ym}} - \frac{\operatorname{Ym}}{\operatorname{Q}^{"}} - 1 \right] \right\}$$
(5.23")

where  $Q'' = (\sqrt{3}/2)N-Ym/2$ . Displacements calculated according to Equation (5.23") are compared with experimental data in Table 7.2 and Figure 7.5. Again, no single value of Y produces results which fit the experimental data for cylinders of all sizes. Certain values of Y give displacement rates which compare to measured values over a range of pressures

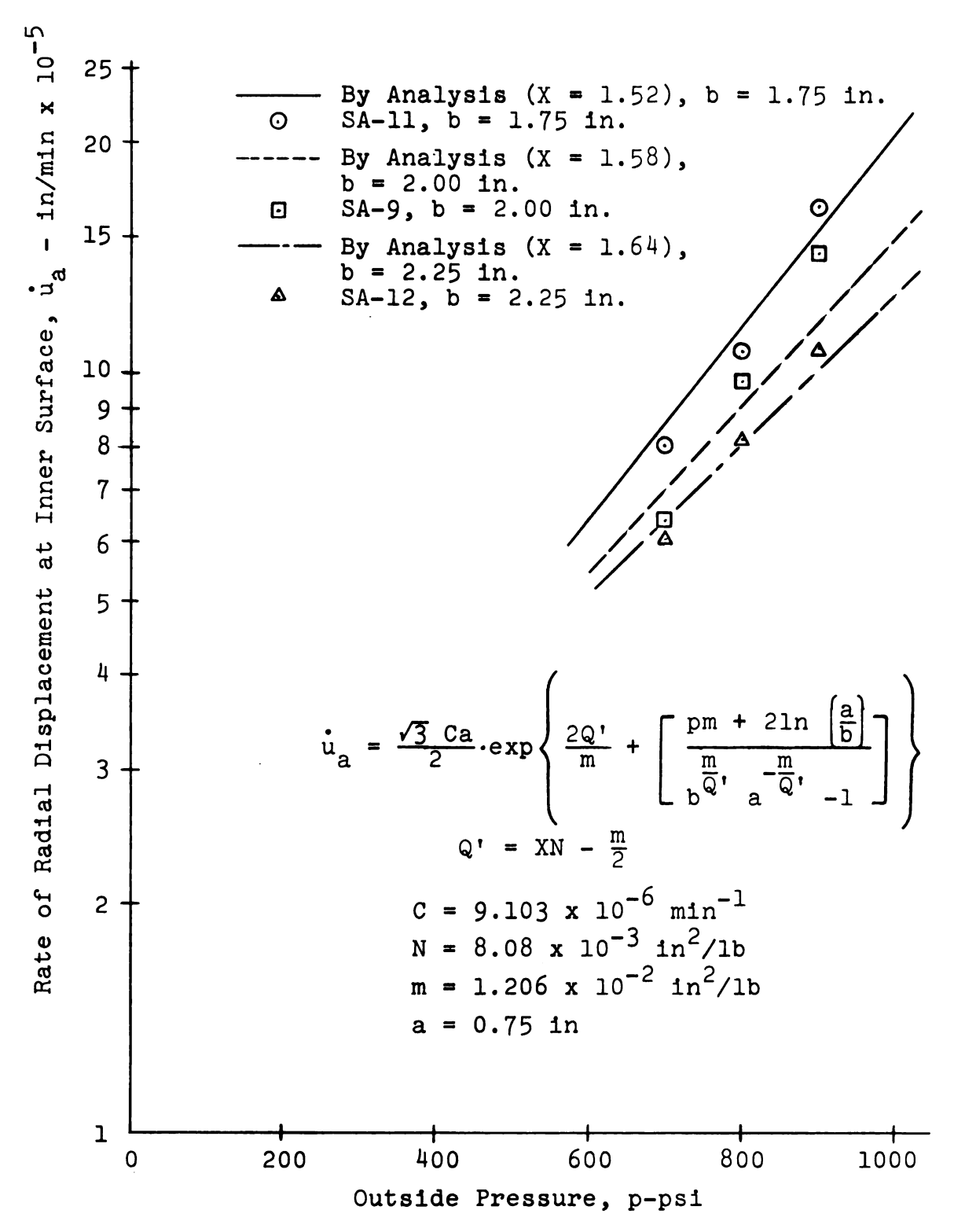


Figure 7.3. Graphical Comparison, Sand-Ice, Equation (5.23')

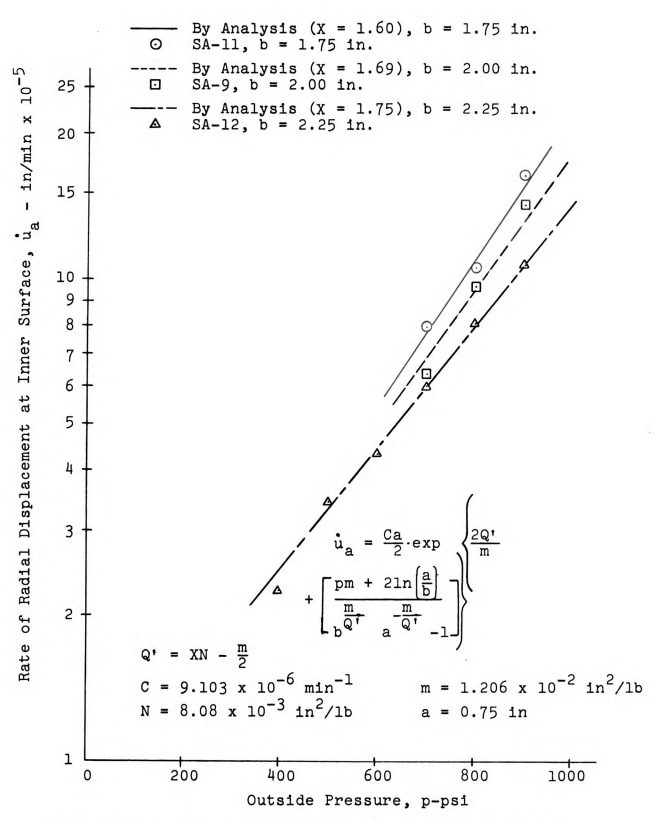


Figure 7.4. Graphical Comparison, Sand-Ice, Equation (5.23') (Modified)

Summary of displacement rate comparisons using Equation (5.23"), sand-ice TABLE 7.2

sid		Radial displa	lacement rat	te at inner	surface,	ua x 10 <sup>-5</sup>	5 (in/min)	
Pressure (ps1)	2	Measured		By	Analysis,	¥ =		
OD=3 1/2"	SA-11	AVG SA-11 & 7	0,40	0.41	0.42	0.43	ተተ•0	0.45
400 600 700 800 900	1.28 2.98 4.45 8.00 10.55	2.00 2.88 4.07 6.76 10.22 21.72	4.66 6.52 9.11 12.74 17.82 24.92	4.00.14 8.14 11.75 16.25	4.23 7.92 10.84 14.84	4.0.03 10.03 13.55	3.85 6.91 12.39 16.00	3.67 4.87 6.45 11.33 15.03
0D=4"	SA-9	AVG SA-9 & 8						
600 600 600 600 600 600	2.07 2.15 3.50 6.40 9.75	2.09 2.72 3.97 6.56 15.65	3.89 6.63 8.66 11.31	3.72 4.81 6.22 8.05 10.41	12.55 12.55 12.55 12.55 12.55	3.4.0 8.9.4.0 11.86.9 22.4.0 22.4.0	3.26 65.16 10.26 10.26	9.40.00 9.00.00 9.00.00 9.00.00
OD=4 1/2"	SA-12							
400 500 700 800 900	2.25 3.45 4.35 6.05 8.20		3.50 4.37 5.45 8.80 10.60	43.35 7.14 7.86 7.36 7.3	3.22 4.83 7.94 8.94 94	3.09 3.75 4.57 6.75 8.22	2.96 4.31 6.27 7.57	2.84 3.40 4.007 5.83 6.93

Note:  $Q^n = (\sqrt{3}/2)N-Ym/2$ 

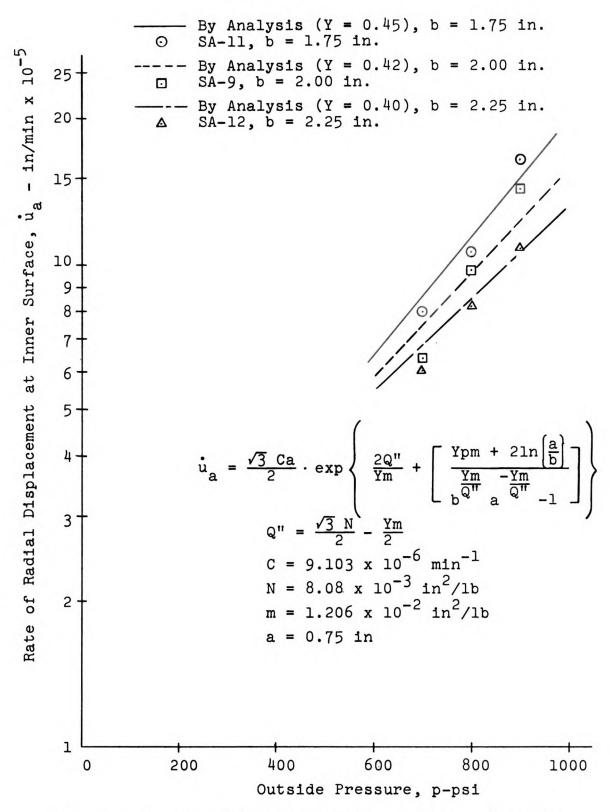


Figure 7.5. Graphical Comparison, Sand-Ice, Equation (5.23")

for each size tested. Figure 7.6 shows that much better agreement is obtained when the value  $\sqrt{3}/2$  in the coefficient to the exponential in Equation (5.23") is changed to 1/2.

Figure 7.7 shows a plot of  $\sigma_r$  and  $\sigma_\theta$  across the section according to Equations (5.22a) and (5.22b) for the sand-ice material. The plot is for a cylinder with outside diameter of 4 1/2 inches, inside diameter of 1 1/2 inches, and a pressure of 700 p.s.i.

The data given in Figures 6.4 and 6.5 show that the total axial force in the sample is not constant but varies with time. It follows from this that the stresses in the sample also vary with time. Thus, the implied assumption that the stresses are time independent is not correct for the sand-ice samples, at least during the initial stages of creep. It appears probable, however, that the stresses reach a constant value at some point during the deformation process.

The total axial force in the sample is a linear combination of the summations across the section of the radial and circumferential stresses. Therefore, by examining the development of the distribution of the radial stress, insight may be gained with regard to explaining this phenomenon. Consider the radial stress distributions illustrated in Figure 7.8. The radial stresses at the inner and outer surfaces of the cylinder are boundary conditions and, therefore, must remain constant under constant loading. It is proposed that the distribution across the section proceeds as shown

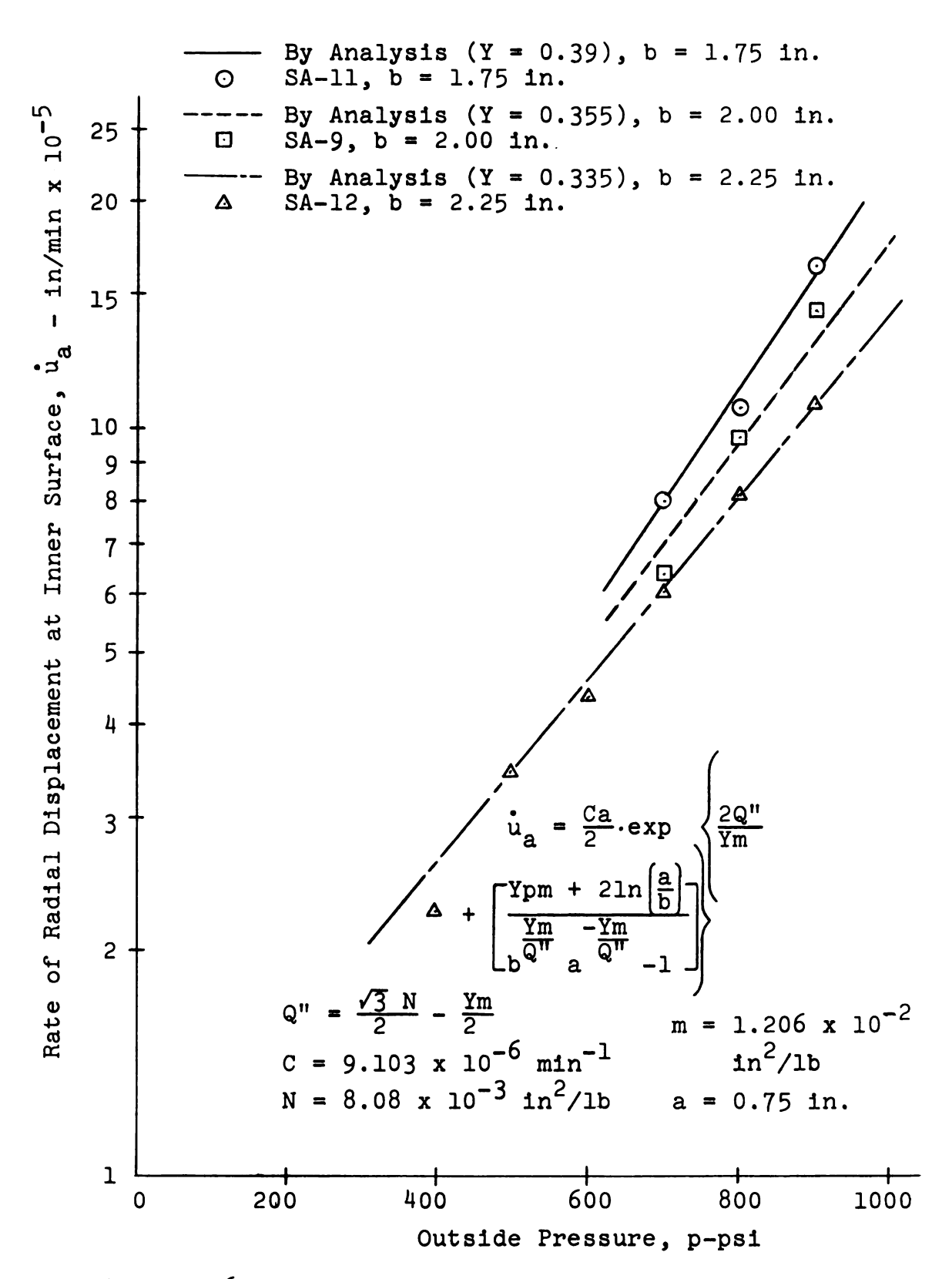


Figure 7.6. Graphical Comparison, Sand-Ice, Equation (5.23") (Modified)



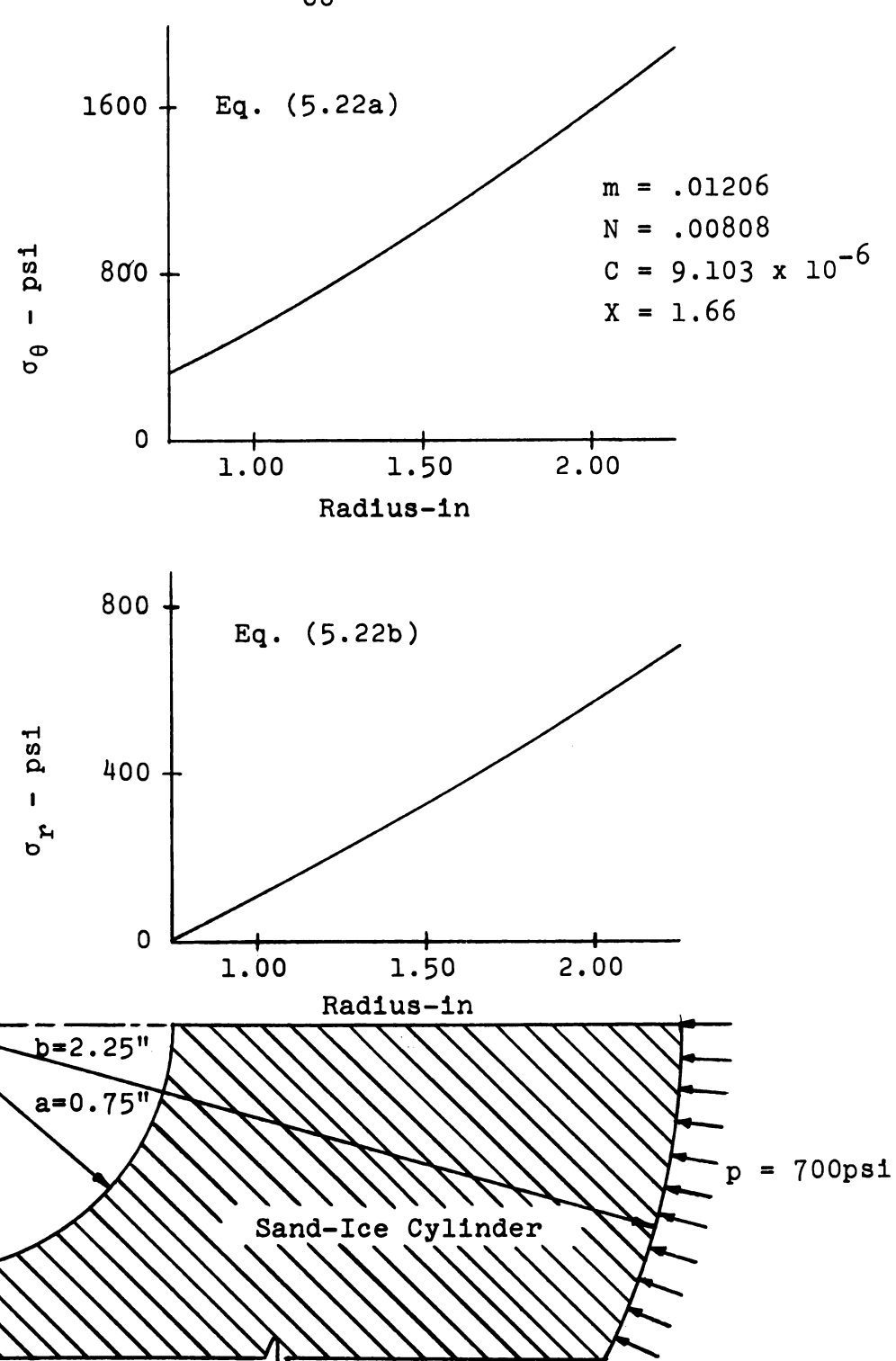


Figure 7.7. Distribution of  $\sigma_r$  and  $\sigma_\theta$  According to Equations (5.22a) and (5.22b)

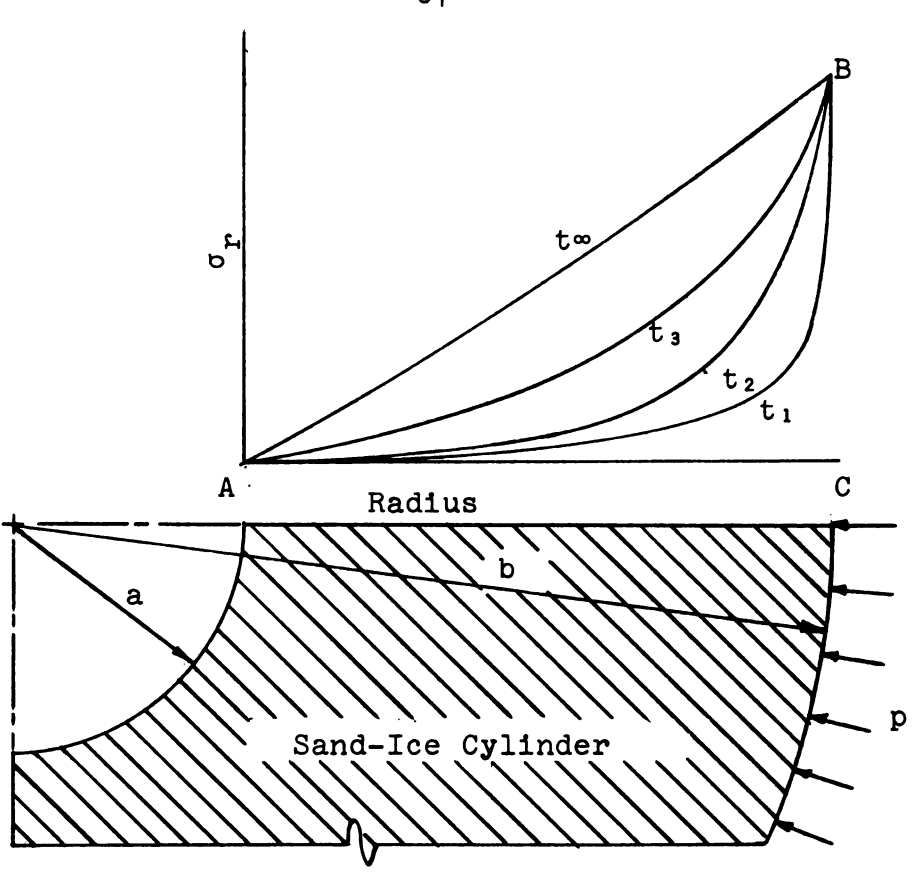


Figure 7.8. Sketch Showing Development of Radial Stress Distribution

Table 7.3. Results of Total Axial Force Calculations

Outside Pressure, p (psi)	Total Axial Force, (lbs), by Eqn (5.22c)	
500	6810	
600	7680	
700	8828	
800	10018	
900	11025	

m = 0.01206

N = 0.00808

 $c = 9.103 \times 10^{-6}$ 

X = 1.66

a = 0.75 in

b = 4.50 in

in the figure. At the earliest time,  $t_1$ , the summation of the radial stresses across the section, represented by the area under the curve, is small. As time passes, this area becomes larger until the distribution stabilizes at some time indicated by  $t_{\infty}$ . Since a similar increase with time may occur for the summation of the circumferential stresses, this would account for the increase in the total axial force with time in the early stages of creep.

In order to check the assumption that the axial stress is equal to one half the sum of the radial and circumferential stresses, the total axial force was calculated for several cases and compared with those experimentally measured. This was done by integrating the equation

$$\sigma_{z} = \frac{1}{m} \left[ 1 - \ln \left( \frac{a}{r} \right)^{2} \right] + \left[ \left( \frac{r}{a} \right)^{\frac{m}{Q}} \left( 1 + \frac{m}{2Q'} \right) - \right] \left[ \frac{p + \left( \frac{2}{m} \right) \ln \left( \frac{a}{b} \right)}{\frac{m}{Q'} - \frac{m}{Q'}} \right] (5.22c')$$

(where Q' = XN-m/2) over the cross section of the cylinder. (See Appendix C for details of the calculations). Results of these calculations are given in Table 7.3. Comparing these values with those shown in Figure 6.5, it can be seen that they fall within or near the range of the axial forces measured. In most cases, the measured values appear to be asymptotically approaching the calculated ones. Thus, the assumption that  $\sigma_z = \frac{1}{2}(\sigma_r + \sigma_\theta)$  appears to be reasonable for the advanced stages of creep.

### 7.2.2 Comparison With c-o Analysis

Equation (5.29) was used to compare the analysis based on time dependent strength parameters with experimental results. For a given measured strain rate, values of c and φ were determined based on data reported by AlNouri (1969). The pressure was then calculated according to Equation (5.29) and compared with the actual pressure that produced the strain rate.

Values of  $\alpha$  for 5 different axial strain rates measured by AlNouri are given in Table 7.4. The corresponding value of  $\phi$  as determined from the series of differential creep tests is 35.2°. A series of constant strain rate tests ( $\dot{\epsilon}$  = 3 x 10<sup>-3</sup> min<sup>-1</sup>) produced a friction angle of 25°.

Since the strain rate varies across the transverse section of the cylinder, it was necessary to determine what strain rate would give the proper value of  $\alpha$  before carrying out the calculations. It was assumed that the average value of  $\dot{\epsilon}_{\theta}$  would approximate AlNouri's axial strain rate. (See Appendix C for details of calculations). Values of  $\alpha$  were selected from the  $\dot{\epsilon}$  vs  $\alpha$  plot shown in Figure 7.9. Values of c were calculated according to the formula  $c = \alpha/\cos \phi$  (Lambe and Whitman, 1969) for the two values of  $\phi$ . Results of the calculations of c from measured displacement rates are summarized in Table 7.5.

A comparison of pressures calculated according to Equation (5.29) from measured strain rates and the actual pressures that produced these strain rates is given in Table

Table 7.4. Values of a (From AlNouri, 1969)

$(\min^{-1}x \ 10^{-5})$	α (psi)
4	79
6	96
8	112
10	125
20	155

 $\phi = 35.2^{\circ}$  (Creep test)

 $\phi = 25^{\circ}$  (Constant strain rate test,  $\dot{\epsilon} = 3 \times 10^{-3} \text{ min}^{-1}$ , c = 443 psi)

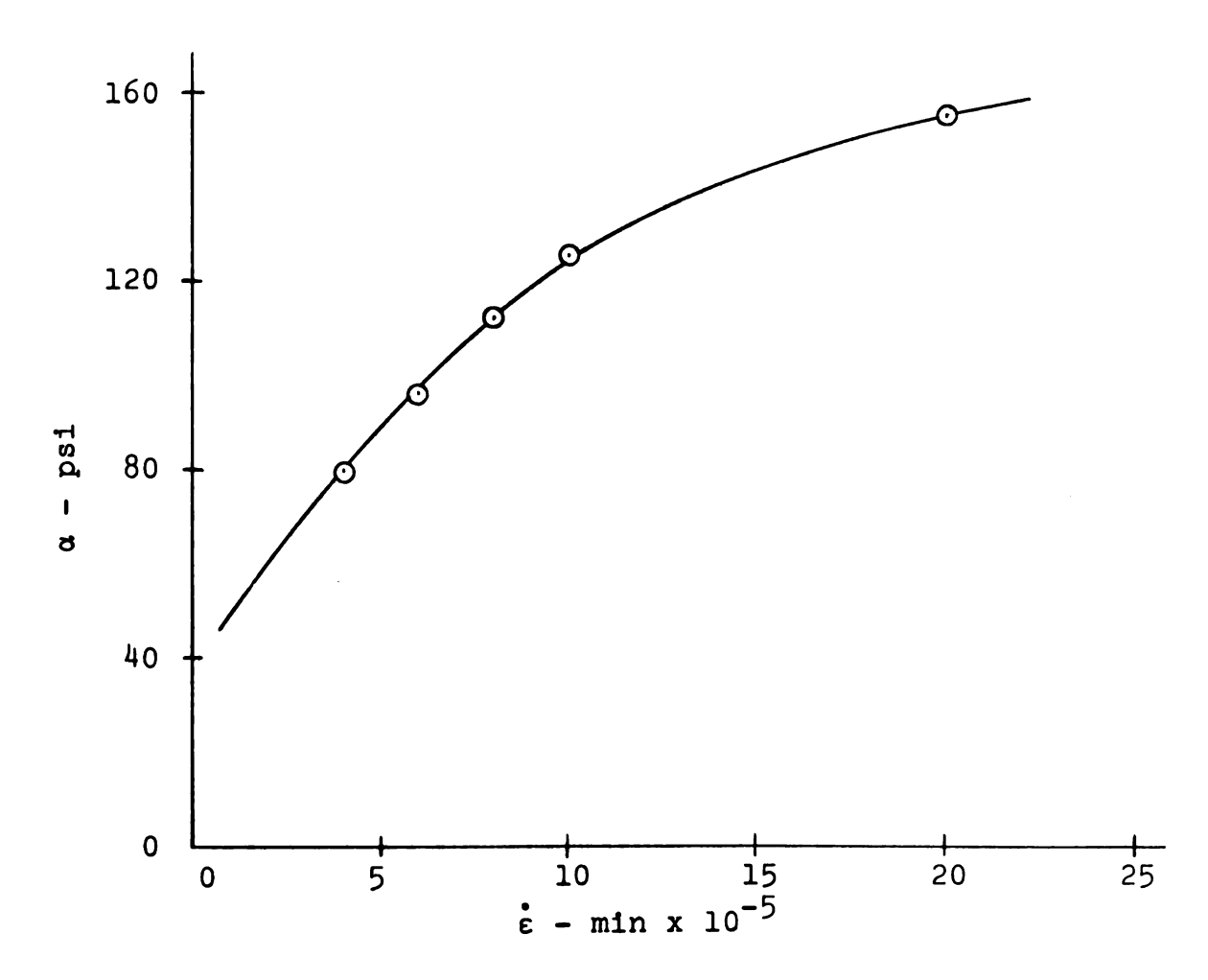


Figure 7.9. Plot of  $\dot{\epsilon}$  vs  $\alpha$ 

TABLE 7.5 Data for c-\phi analysis

				Alexander of the second se	
Outside Pressure (psi)	500	600	700	800	900
$(in/\min^{u} x \ 10^{-5})$	2.98	4.45	8.00	10.55	16.45
$\lim_{t \to \infty} (\min_{t \to \infty} \frac{\varepsilon}{t} \theta a + 10^{-5})$ $\lim_{t \to \infty} (\min_{t \to \infty} \frac{\varepsilon}{t} \theta m + 10^{-5})$	3.98	5.94	10.67	14.08	20.9
$\sum_{\kappa=0}^{\infty} (\min^{-1} \frac{\varepsilon}{x} 10^{-5})$	1.70	2.54	4.57	6.03	9.40
(psi)	57	65	84	97	122
<ul> <li>c, φ=35.2°</li> <li>(psi)</li> <li>c, φ=25°</li> </ul>	69.8	79.6	102.7	118.7	149.3
(psi)	63.0	71.7	92.7	107.0	134.8
u <sub>a</sub> (in/min x 10 <sup>-5</sup> )	2.15	3.50	6.40	9.75	14.30
$(\min_{x \in \Theta} x = 10^{-5})$ $(\min_{x \in \Theta} x = 10^{-5})$ $(\min_{x \in \Theta} x = 10^{-5})$	2.87	4.67	8.54	13.00	19.07
$\lim_{\varepsilon \to \infty} (\min^{-1} \frac{\theta m}{x} 10^{-5})$	1.08	1.75	3.20	4.87	7.15
n (psi)	50	58	71	87	106
Oc, $\phi = 35.2^{\circ}$ (psi)	61.2	71.0	87.0	106.4	129.8
c, φ=25 <sup>0</sup> (psi)	55.1	69.0	78.4	96.0	117.0
$\widehat{a}^{(in/\min^{i} a} \times 10^{-5})$	3.45	4.35	6.05	8.20	10.75
$\Psi_{\mathcal{O}}^{t}(\min^{-\frac{\varepsilon}{1}} \mathbf{x} \ 10^{-5})$	4.60	5.80	8.07	10.92	14.33
$\frac{(psi)}{u}$ $\frac{1}{\sqrt{(in/\min^2 x 10^{-5})}}$ $\frac{1}{\sqrt{(min^{-1} x 10^{-5})}}$ $\frac{1}{\sqrt{(min^{-1} x 10^{-5})}}$ $\frac{1}{\sqrt{(min^{-1} x 10^{-5})}}$	1.53	1.93	2.69	3.64	4.77
α (psi) "c, φ=35.2°	55	59	67	76	87
(psi) c, φ=25°	67.4	72.2	82.0	93.0	106.4
(psi)	60.7	65.1	74.0	83.9	96.0

 $<sup>\</sup>dot{\mathbf{u}}_{q}$  = rate of radial displacement at  $\mathbf{r} = \mathbf{a}$ 

 $<sup>\</sup>varepsilon_{\theta a}$  = circumferential strain rate at r = a

 $<sup>\</sup>epsilon_{\theta m}$  = mean value of circumferential strain rate

7.6. It can be seen that the predicted pressures are from  $1 \frac{1}{2}$  to nearly 3 times the actual pressures when the value  $35.2^{\circ}$  is used for  $\phi$ . For the constant strain rate friction angle of  $25^{\circ}$ , the agreement is considerably better.

The distribution of  $\sigma_r$  and  $\sigma_\theta$  as calculated by Equations (5.28) and (5.25'), respectively, is shown in Figure 7.10 for a cylinder with an outside diameter of 4 1/2 inches and an inside diameter of 1 1/2 inches. The value of c used was 74.0 p.s.i. This value was calculated using a displacement rate at the inner surface of 6.05 x  $10^{-5}$  in/min, the measured value for an outside pressure of 700 p.s.i. Note the close agreement between this distribution and that predicted by Equations (5.22a) and (5.22b) (See Figure 7.7).

# 7.3 Frozen Clay

Although the amount of experimental data is less for the frozen clay, a comparison of the analytical and experimental results similar to the one given for the sand-ice material was attempted. The following values for experimental parameters were taken from the results of AlNouri (1969):

$$C = 2.77 \times 10^{-4} \text{ min}^{-1}$$
  
 $N = 2.68 \times 10^{-3} \text{ in}^2/\text{lb}$   
 $m = 1.049 \times 10^{-2} \text{ in}^2/\text{lb}$ 

As shown in Figure 7.2, the strain rates measured in this study are at the lower end of the range used by AlNouri. This is due to the relatively large deformation which

TABLE 7.6 Summary of comparisons for c-\phi analysis

, <del>, , , , , , , , , , , , , , , , , , </del>	Actual Pressure (psi)	<sup>u</sup> a (in/min x 10 <sup>-5</sup> )	$\epsilon_{\theta m}$ (min <sup>-1</sup> x 10 <sup>-5</sup> )	Predict Pressure $\phi = 35.2^{\circ}$	(psi)
	500	2.98	1.70	801	331
1/5	600	4.45	2.54	914	376
3 1	700	8.00	4.57	1179	487
D = (SA-	800	10.55	6.03	1363	562
0	900	16.45	9.40	1714	708
	500	2.15	1.08	1035	379
<b>±</b>	600	3.50	1.75	1201	440
7 = 7	700	6.40	3.20	1471	539
OD :	. 800	9.75	4.87	1799	660
	900	14.30	7.15	2195	844
	500	3.45	1.53	1575	519
/5"	600	4.35	1.93	1687	557
4 1	700	6.05	2.69	1916	633
D = (SA-	800	8.20	3.64	2173	717
0	900	10.75	4.77	2487	821

 $<sup>\</sup>dot{u}_a$  = rate of radial displacement at r = a

 $<sup>\</sup>dot{\epsilon}_{\theta m}$  = mean value of circumferential strain rate

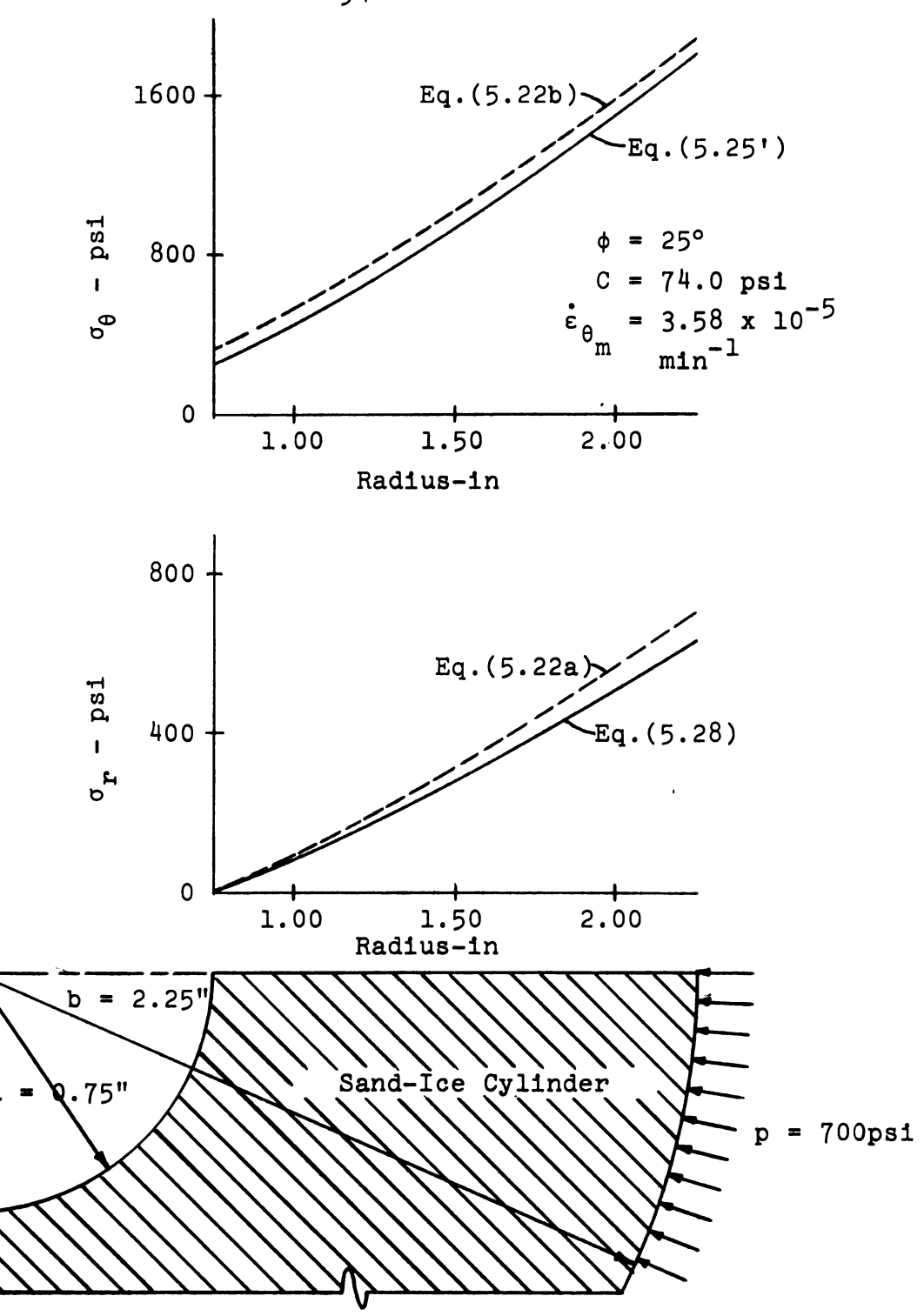


Figure 7.10. Distribution of  $\sigma_{\bf r}$  and  $\sigma_{\theta}$  According to Equations (5.28) and (5.25')

occurred during primary creep. This made it impossible to obtain larger steady state displacement rates before the total deformation became excessive.

Using the parameters given above, direct calculations according to Equation (5.23) produce displacement rates considerably larger than those measured. It was, therefore, necessary to modify Equation (5.23) by adjusting the relative contributions of the deviatoric and hydrostatic parts of the stress as in Section 7.2.1 for the sand-ice. Using Equation (5.23') with an X value of 6.40, and dividing the coefficient to the exponential by 100, the comparison illustrated in Figure 7.11 was obtained. It was not possible to fit the experimental data by using Equation (5.23") which varies the hydrostatic portion.

Figures 6.6 and 6.7 show that the total axial force in the frozen clay samples remained nearly constant for each load increment. Thus, it is probable that, unlike the sandice samples, the stresses are constant throughout the deformation process. This tends to indicate that the development of the stress distribution illustrated in Figure 7.8 for the sand-ice material occurs much more rapidly in the case of frozen clay.

The difference in axial force development between the two materials may be explained by considering the difference in the deformation characteristics of them. The small primary creep deformation observed in the case of the sand-ice

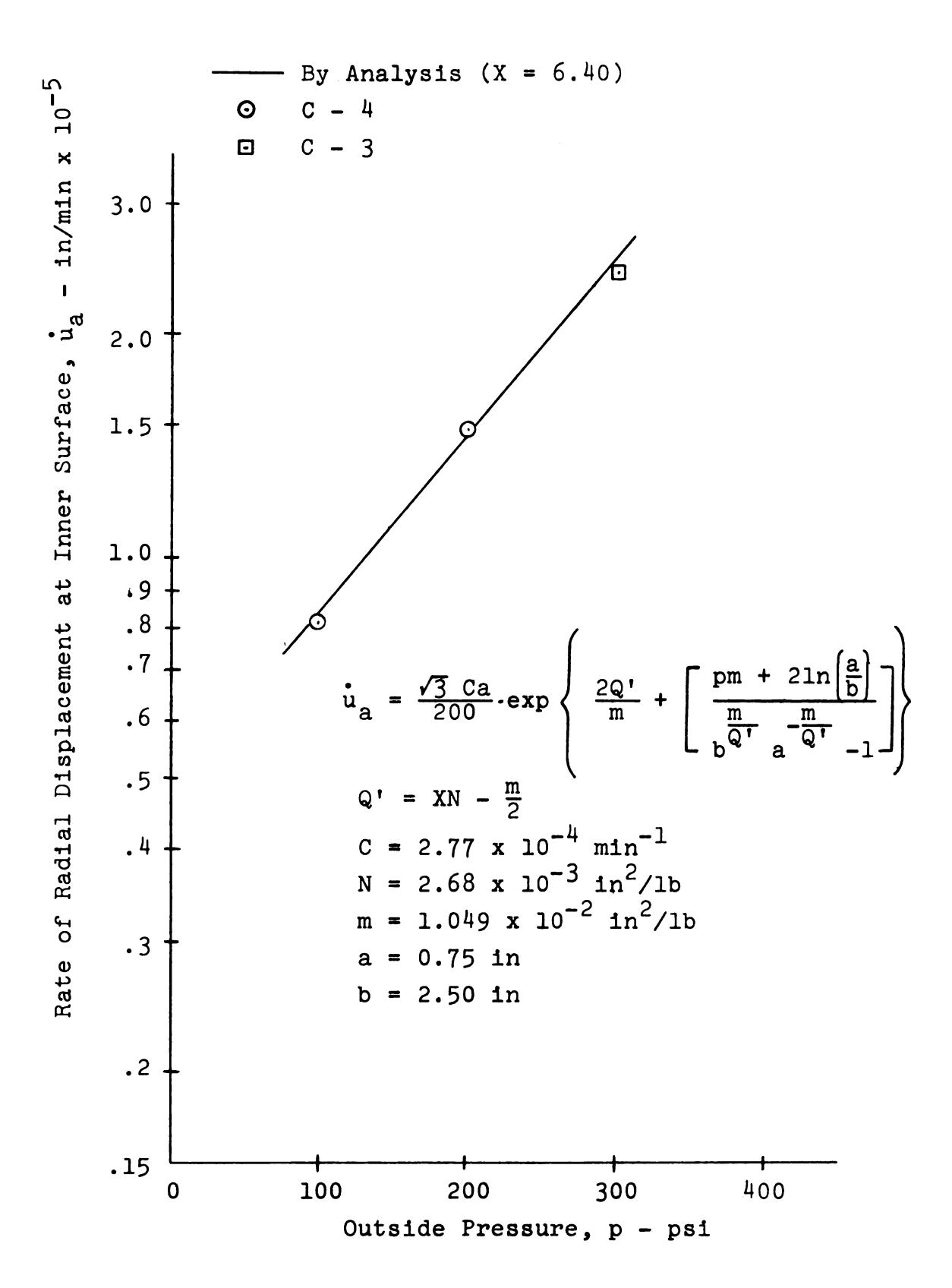


Figure 7.11. Graphical Comparison, Frozen Clay, Equation (5.23') (Modified)

indicates that this material is quite stiff and, thus, is slow in reacting to a change in external pressure. On the other hand, the frozen clay exhibited relatively large deformation during primary creep. This tends to indicate that the material flows more readily, reacts more quickly to an external change in pressure and, thus, reaches a final state of stress more rapidly.

A related result was reported by Goughnour (1967). found that, in constant strain rate tests, the peak stress was reached at approximately 2.5% strain for sand-ice samples; whereas, in the case of frozen clay the peak stress was not approached until a strain of 10% or greater had been realized. This tends to substantiate the argument given above regarding the relative stiffness and flow characteristics of the two materials. This may be explained by considering the development of the frictional component of shearing resistance. Indications are that in the case of the sand-ice material, the sand particles are initially either in contact with one another or very nearly so. allows the frictional component to be mobilized almost immediately. However, for clay, where the particles are widely dispersed, the frictional component cannot be fully developed until the occurrence of relatively large strains. This suggests the use of an analysis where  $\phi$  is taken as zero and a strain rate dependent cohesion used. There are, however, insufficient data available to verify this.

In order to check the values of total axial force measured, Equation (5.22c') was integrated across the section. Using the experimental parameters given above for the frozen clay and X = 6.40, the values for total axial force were found to be 1958, 3925, and 5888 pounds for outside pressures of 100, 200, and 300 p.s.i., respectively. Comparing these with the measured values illustrated in Figures 6.6 and 6.7, it can be seen that the calculated ones are higher in each case. One possible explanation for this discrepancy, as well as for the inconsistency in displacement results, is that the experimental parameters may be strain rate depen-Therefore, since it was impossible to achieve the range of strain rates for which the parameters were established (See Figure 7.2), the use of these parameters may not be justified. A second explanation concerns the fact that the constitutive equation used was established for steady state creep. Since this stress distribution appears to have developed during primary creep, it may be improper to use the constitutive relationship for this case.

#### CHAPTER VIII

# CONCLUSIONS AND RECOMMENDATIONS FOR FURTHER RESEARCH

## 8.1 Summary of Conclusions

Based on the experimental results for the two frozen soils used and their comparison with analytical calculations, the following conclusions can be drawn with regard to hollow frozen soil cylinders, loaded by an outside pressure:

- 1. Displacement rates calculated according to Equation (5.23), which is an extension of a creep equation suggested by AlNouri (1969), do not agree with actual displacement rates when experimental parameters reported by AlNouri are used. After modifying this approach by the introduction of additional parameters, the analytically predicted displacement rates compare favorably with those experimentally measured. Therefore, it can be concluded that, while the form of Equations (5.22), (5.23), and (5.24) appears to be valid, more experimental data are required to elucidate the nature and the use of the experimental parameters.
- 2. The relationship presented in Section 5.3 based on time dependent strength parameters (AlNouri, 1969) appears to be valid for the sand-ice material, provided the

correct value of friction angle is used. The friction angle which provided the best check with experimental data in this study was that determined from constant strain rate tests, rather than the value from creep tests. Since this result is unexpected and difficult to explain, no generalization regarding it can be made without further experimental work.

- 3. The deformation characteristics of sand-ice cylinders under constant radial load differ considerably from those of frozen clay, although both are time dependent. In the case of the sand-ice material, the magnitude of the deformation during primary creep is small, the length of time necessary to reach secondary creep is small, and the steady state portion of the creep curve is well defined. For frozen clay, both the length of time and the amount of deformation are much greater for primary creep and the steady state part of the creep curve is less well defined.
- 4. The behavior of the total axial force in hollow frozen soil cylinders under conditions of plane strain also differs for the two materials used in this study. The axial force in sand-ice cylinders is time dependent. It increases during the early stages of creep and then approaches a constant value. This increase in axial force is probably due to a continuing redistribution of stresses during the time immediately following loading. As creep continues, the stress distribution stabilizes, producing a constant axial force.

By contrast, the total axial force in the frozen clay cylinders reaches a constant value shortly after loading.

Thus, any redistribution of stresses occurs rapidly.

- 5. The phenomena discussed in Conclusions 4 and 5 appear to be compatible. They can be explained by considering the relative stiffness and flow characteristics of the two materials. The stiffer sand-ice exhibits little deformation during primary creep, reacts slowly to an external load, and, therefore, experiences considerable delay in reaching its final state of stress. The frozen clay, however, shows a greater ability to flow by its large primary creep deformation and is able to reach its final stress state more quickly.
- 6. The total axial force, as calculated by integrating Equation (5.22c') across the section, was in reasonable agreement with the actual axial force for most cases involving the sand-ice material. This supports the approximation that the axial stress is equal to one half the sum of the major and minor principal stresses. The above relationship is based on the argument that frozen soil is incompressible during the deformation process, at least for the advanced stages of creep. These results are in agreement with Vialov (1965b).

Discrepancies occurred regarding the total axial force in the frozen clay samples. Calculated values (Equation 5.22c') were 50 to 100% higher than those measured. This may

be due to a difference between the strain rates used in this study and the ones from which AlNouri (1969) determined the experimental parameters.

## 8.2 Suggestions For Further Research

This study represents a small contribution toward the understanding of the stress-deformation characteristics of soil-ice barriers used in shaft sinking. Many areas require further study before the complete problem can be solved. Several of these areas are listed in the following paragraphs:

- 1. Further investigation is required into the nature of the experimental parameters used in the analyses. Several of these were well established by AlNouri (1969) for a certain range of strain rates and for the uniform stress condition existing in a triaxial test. It is yet unclear how they should be extended for use in situations where stresses are non uniform. More information is also necessary regarding the parameters X and Y introduced in this study.
- 2. Studies similar to this one should be carried out on different soil types at varying temperatures to determine the general application of the conclusions drawn above.
- 3. The temperature was uniform throughout the frozen soil models tested in this study. Under actual field conditions where freeze pipes are used, such a condition would

be impossible to achieve. Therefore, it would be desirable to conduct a model study in which a more realistic approximation of temperature distribution is used.

**BIBLIOGRAPHY** 

### **BIBLIOGRAPHY**

- AlNouri, I. "Time Dependent Strength Behavior of Two Soil Types at Lowered Temperatures", Ph.D. Thesis, Michigan State University, East Lansing, Michigan, 1969.
- Andersland, O. B., and W. Akili, "Stress Effect on Creep Rates of a Frozen Clay Soil", Geotechnique, Vol. XVII, No. 1, March 1967, pp 27-39.
- Brace, J. H., "Freezing as an Aid to Excavation in Unstable Material", <u>Transactions</u>, ASCE, Vol. 52, pp 365-436, 1904.
- Cross, B., "Liquid Gas Freezes Bad Soil", Construction Methods and Equipment, July, 1964.
- Goughnour, R. R. "The Soil-Ice System and the Shear Strength of Frozen Soils", Ph.D. Thesis, Michigan State University, East Lansing, Michigan, 1967.
- Goughnour, R. R. and O. B. Andersland. "Mechanical Properties of a Sand-Ice System", <u>Journal of the Soil Mechanics and Foundations Division</u>, ASCE, Vol. 94, No. <u>SM4</u>, July, 1968.
- "Freezing Makes Shaft Sinking Easier", Construction Methods and Equipment, Oct., 1964.
- Lambe, T. W. and R. V. Whitman. Soil Mechanics. John Wiley &Sons, Inc., N. Y., 1969.
- Latz, J. E. "Freezing Method Solves Problem in Carlsbad N. M. Shaft", Mining Engineering, Oct., 1952.
- Low, G. J. "Soil Freezing to Reconstruct a Railway Tunnel", Journal of the Construction Division, ASCE, Vol. 86, No. CO3, Nov., 1960.
- Sanger, F. J. "Ground Freezing in Construction", <u>Journal of</u> the Soil Mechanics and Foundations Division, ASCE, Vol. 94, No. SM1, Jan., 1968.
- Silinsh, J. "Freezing Keeps Shaft Dry and Holds Dirt in Place", Construction Methods and Equipment, Jan., 1960.
- Stewart, G. C., W. K. Gildersleeve, S. Janpole, and J. E. Connolly. "Freezing Aids Shaft Sinking", Civil Engineering, ASCE, April, 1963.

- Tsytovich, N. A. "Instability of Mechanical Properties of Frozen and Thawing Soils", Proceedings of the Permafrost International Conference, National Academy of Sciences—National Research Council Publication No. 1287, pp 325-331, 1963.
- Tsytovich, N. A., and K. R. Khakimov. "Ground Freezing Applied to Mining and Construction", <u>Proceedings of the Fifth International Conference on Soil Mechanics and Foundation Engineering</u>, Vol. 2, pp 737-741, 1961.
- Vialov, S. S. "Plasticity and Creep of a Cohesive Medium", <u>Proceedings of the Sixth International Conference on Soil Mechanics and Foundation Engineering</u>, Vol. 1, <u>University of Toronto Press</u>, 1965.
- Vialov, S. S. Rheological Properties and Bearing Capacity of Frozen Soils, Cold Regions Research and Engineering Laboratory Translation 74, Hanover, New Hampshire, 1965a.
- Vialov, S. S. "Rheology of Frozen Soils", <u>Proceedings of the Permafrost International Conference</u>, National Academy of Sciences—National Research Council Publication No. 1287, pp 332-337, 1963.
- Vialov, S. S. (Ed). The Strength and Creep of Frozen Soils and Calculations for Ice-Soil Retaining Structures, Cold Regions Research and Engineering Laboratory Translation 76, Hanover, New Hampshire, 1965b.
- Yong, R. N. "Soil Freezing Considerations in Frozen Soil Strength", Proceedings of the Permafrost International Conference, National Academy of Sciences—National Research Council Publication No. 1287, pp 315-319, 1963.

APPENDIX A
TEST DATA

TABLE A-1. Test data, SA-4

Material—Ottawa Sand
Sand Density—64% by Volume
Water Content—20.6%
Test Temperature—-12.0°C.
Date of Test—7 Jan 69

Initial Sample Dimensions
Outside Diam. 4"
Inside Diam. 1 1/2"
Height 9 5/16"

Time (min)	Outside Pressure (psi)	Change in Diameter (in)	Total Axial Force (lb)
0	0	. 0	0
5	100	0.00038	-132*
10	100	0.00038	-122*
12	200	0.00038	<b>-</b> 75 <b>*</b>
30	200	0.00072	-64*
33	303	0.00072	408
35 38	303	0.00081	408
38	304	0.00128	418
45 55 65	305	0.00140	472
55	307	0.00174	483
05 75	308	0.00202	526
<b>75</b>	309	0.00212	568
90	310	0.00246	633 1284
93 96	398 398	0.00302 0.00319	1294
110	400	0.00319	1434
125	402	0.00451	1563
135	404	0.00494	1638
145	405	0.00794	1713
155	406	0.00562	1788
165	407	0.00587	1863
175	408	0.00625	1906
185	409	0.00647	1981
196	409	0.00685	2045
206	410	0.00723	2099
216	411	0.00748	2153
226	411	0.00766	2206
236	412	0.00792	2260
246	413	0.00817	2303
256	405	0.00851	2367
266	405	0.00864	2410
276	405	0.00885	2464
286	405 1105	0.00898	2496 2530
300	405 503	0.00936	2539 <b>2825</b>
303 305	503 503	0.00978 <b>0.</b> 00987	2911 ·
305 315	504	0.01047	3125
325	505	0.01098	3276
ر عر	707	0.01090	2510

<sup>\*</sup>Apparent negative force probably due to shifting of the sample.

TABLE A-1 Continued

Time	Outside Pressure	Change in	Total Axial
(min)	(psi)	Diameter (in)	Force (lb)
335	505	0.01145	3383
345 355	506 506	0.01187 0.01230	3469 3544
367	508	0.01280	3619
375	508	0.001310	3673
385	509 500	0.01349	3726 3813
395 405	509 510	0.01434 0.01434	3812 3812
415	510	0.01455	3866
425	511	0.01502	3909
435	511	0.01528	3962
445 455	511 512	0.01566 0.01604	4005 4048
465	512	0.01638	4091
467	601	0.01668	4301
475	603	0.01796	4623
485 495	605 605	0.01868 0.01932	4805 4945
505	605	0.02000	5052
515	606	0.02051	5149
525	606	0.02124	5234
535 545	606 606	0.02182 0.02240	5294 5374
555	606	0.02298	5385
564	606	0.02351	5428
574 584	605	0.02404	5470 5613
594	604 603	0.02485 0.02520	5613 5567
604	602	0.02573	5599
718	547	0.03023	5478
720 720	604 606	0.03036	5428 5642
729 739	605	0.03114 0.03173	5749
749	604	0.03236	5803
759	603	0.03295	5846
762 766	709 711	0.03350 0.03445	5810 6057
769	711	0.03491	6175
779	711	0.03623	6422
789	711	0.03750	6572
799 809	711 710	0.03860 0.03964	6636 6711
819	710 710	0.04068	6776
829	710	0.04164	6829
839	709	0.04268	6872

TABLE A-1 Continued

Time	Outside Pressure	Change in	Total Axial
(min)	(psi)	Diameter (in)	Force (lb)
849	709	0.04372	6915
859	709	0.04468	6947
869	709	0.04564	6980
879	709	0.04660	7001
889	709	0.04760	7023
899	709	0.04869	7044
909	708	0.04968	7055
919	707	0.05073	7055
929	707	0.05164	7065

TABLE A-2 Test data, SA-6

Material—Ottawa Sand Initial Sample Dimensions Sand Density—64% by Volume Outside Diam. 3 1/2" Water Content—20.2% Inside Diam. 1 1/2" Test Temperature—-12.0°C. Height 9" Date of Test—30 Jan 69

Time (min)	Outside Pressure (psi)	Change in Diameter (in)
0	0	0
5	101	0.00004
10	101	0.00004
<b>1</b> 5	200	0.00013
20	200	0.00030
30	200	0.00043
40	200	0.00055
50	200	0.00072
60	200	0.00081
65	300	0.00132
70	300	0.00153
80	300	0.00183
90	300	0.00217
100	300	0.00243 0.00264
110 120	300 300	0.00285
130	299	0.00205
140	299	0.00323
145	401	0.00383
150	402	0.00409
160	401	0.00460
170	401	0.00502
180	400	0.00528
190	400	0.00562
200	400	0.00587
210	400	0.00621
220	400	0.00643
230	399	0.00672
240	399	0.00689
250	399	0.00715
260	399	0.00736
270	399	0.00757
280	399	0.00779
290	399 500	0.00800 0.00872
295 300	500 500	0.00672
310	500	0.00900
320	500	0.01993
) £ 0	<b>J</b> 00	0.01000

TABLE A-2 Continued

Time (min)	Outside Pressure (psi)	Change in Diameter (in)
330 340	500 500	0.01038 0.01081
350	500	0.01001
360	500	0.01157
370	500	0.01191
380	500	0.01223
390	500	0.01260
400	500	0.01289
410	500	0.01323
420	500	0.01357
430 440	500 500	0.01387 0.01417
445	600	0.01417
450	600	0.01557
460	600	0.01617
470	600	0.01677
480	599	0.01740
490	599	0.01796
500	599	0.01855
510	599	0.01906
520	599	0.01953
530	599 500	0.02004 0.02098
550 560	599 599	0.02090
5 <b>7</b> 0	599	0.02191
580	598	0.02244
590	598	0.02289
595	703	0.02356
600	703	0.02404
610	703	0.02502
620	703	0.02591
630 640	703 703	0.02676 0.02760
650	703 703	0.02844
660	703	0.02916
670	703	0.02982
680	703	0.03050
690	702	0.03118
700	702	0.03186
710	702	0.03250
720	702	0.03314
730	702 703	0.03373 0.03432
740	702	0.03434

Note: Sand was reused for this test. Contaminated sand may have influenced results.

TABLE A-3 Test data, SA-7

Material-Ottawa Sand	Initial Sample Dim	ensions:
Sand Density—64% by Volume	Outside Diam.	3 1/2"
Water Content-21.0%	Inside Diam.	1 1/2"
Test Temperature—-12.0°C.	Height	9 1/8"
Date of Test-13 Feb 69	•	

Outside Pressure (psi)	Change in Diameter (in)	Total Axial Force (lb)
0 100 100 205 205 301 302 302 302 302 302 302 302 300 400 400 400 400 400 400 400 399 399 399 399 399 399 399 399 399 3	0 0 0 0 0 0 0.00013 0.00013 0.00042 0.00081 0.00123 0.00157 0.00196 0.00221 0.00251 0.00277 0.00315 0.00379 0.00451 0.00574 0.00511 0.00574 0.00634 0.00719 0.00766 0.00830 0.00868 0.00953 0.01034 0.01123 0.01157 0.01255	0 -122* -122* -61* 167 173 200 232 253 280 275 301 328 355 744 760 819 878 936 1066 1136 1211 1286 1393 1495 1559 1618 1683 1964
500 500 500 500 499	0.01311 0.01362 0.01434 0.01502 0.01570	2103 2296 2436 2554 2661
	(psi) 0 100 100 205 205 301 302 302 302 302 302 302 302 309 400 400 400 400 399 399 399 399 399 399 399 399 399 3	(ps1)         Diameter (in)           0         0           100         0           205         0           205         0           301         0.00013           302         0.00042           302         0.00081           302         0.00123           302         0.00157           302         0.00251           302         0.00277           400         0.00315           400         0.00451           400         0.00574           399         0.00634           399         0.00634           399         0.00888           399         0.00868           399         0.00868           399         0.01034           399         0.01064           399         0.0125           500         0.0125           500         0.0131           500         0.01362           500         0.01434           500         0.01502

<sup>\*</sup>Apparent negative axial force probably due to shift-ing of the sample.

TABLE A-3 Continued

Time	Outside Pressure	Change in	Total Axial
(min)	(psi)	Diameter (in)	Force (lb)
320	499	0.01613	2758
330	499	0.01677	2849
340	499	0.01740	2929
350	499	0.01813	3004
360	499	0.01847	3063
370	499	0.01911	3133
380	499	0.01974	3184
390	499	0.02004	3230
400	499	0.02076	3273
410	499	0.02138	3315
413	602	0.02191	3543
420	600	0.02271	3843
430	599	0.02400	3993
440	602	0.02507	4025
450	601	0.02618	4127
460	600	0.02702	4229
470	600	0.02782	4320
480	600	0.02844	4379 4444
490 500	600 600	0.02924	4444 4497
510	600	0.03005 0.03073	4497 4551
520	600	0.03155	4583
530	600	0.03218	4626
540	600	0.03295	4648
550	600	0.03368	4685
560	600	0.03441	4712
563	700	0.03486	4929
570	700	0.03600	5198
580	699	0.03736	5369
590	698	0.03836	5477
600	703	0.03955	5 <b>4</b> <u>7</u> .7
610	703	0.04077	5584
620	703	0.04200	
630	702	0.04291	
640	702	0.04386	
650	701 700	0.04468	
660 670	700 700	0.04573	· · · · · · · · · · · · · · · · · · ·
680	700 700	0.04682 0.04800	
690	699	0.04932	
<b>7</b> 00	699	0.05047	
710	699	0.05163	
713	804	0.05284	6648
720	804	0.05377	6304
730	802	0.05581	
. •	<del></del>		

TABLE A-3 Continued

Time (min)	Outside Pressure	Change in	Total Axial
	(psi)	Diameter (in)	Force (lb)
740 750 760 770 773 780 790 800 810 820 830 840	801 800 800 800 905 905 905 905 905 905	0.05772 0.05972 0.06186 0.06372 0.06465 0.06772 0.07177 0.08095 0.08667 0.09156 0.09698 0.10215	6747

TABLE A-4 Test data, SA-8

Material—Ottawa Sand Sand Density—64% by Volume Water Content—21.6%	Initial Sample Dimer Outside Diam. Inside Diam.	4" 1 1/2"
Test Temperature—-12.0°C. Date of Test—20 Feb 69	Height	9 5/16"

(min)         (psi)         Diameter (in)         Force (lb)           0         0         0         0           3         100         0.00013         14           10         100         0.00021         14           13         200         0.00055         97           20         200         0.00077         140           30         200         0.00094         172           33         301         0.00145         1062           40         301         0.00200         1062           50         299         0.00247         1148           60         299         0.00289         1201           70         299         0.00336         1244           80         299         0.00336         1244           80         299         0.00396         1330           100         299         0.00493         1373           110         299         0.00498         1448           130         299         0.00498         1448           130         299         0.00498         1448           130         299         0.00579         2153	Time	Outside Pressure	Change in	Total Axial
3       100       0.00021       14         10       100       0.00021       14         13       200       0.00055       97         20       200       0.00077       140         30       200       0.00094       172         33       301       0.00145       1062         40       301       0.00200       1062         50       299       0.00247       1148         60       299       0.00289       1201         70       299       0.00366       1287         90       299       0.00366       1287         90       299       0.00396       1330         100       299       0.00498       1448         120       299       0.00498       1448         130       299       0.00498       1448         130       299       0.00579       2153         140       399       0.00634       2217         150       399       0.00689       2324         160       399       0.00689       2324         170       399       0.00804       2475         180       399 <t< th=""><th></th><th></th><th></th><th></th></t<>				
3       100       0.00021       14         10       100       0.00021       14         13       200       0.00055       97         20       200       0.00077       140         30       200       0.00094       172         33       301       0.00145       1062         40       301       0.00200       1062         50       299       0.00247       1148         60       299       0.00289       1201         70       299       0.00366       1287         90       299       0.00366       1287         90       299       0.00396       1330         100       299       0.00498       1448         120       299       0.00498       1448         130       299       0.00498       1448         130       299       0.00579       2153         140       399       0.00634       2217         150       399       0.00689       2324         160       399       0.00689       2324         170       399       0.00804       2475         180       399 <t< td=""><td>0</td><td>^</td><td>^</td><td>^</td></t<>	0	^	^	^
10       100       0.00021       14         13       200       0.00055       97         20       200       0.00077       140         30       200       0.00094       172         33       301       0.00145       1062         40       301       0.00200       1062         50       299       0.00247       1148         60       299       0.00289       1201         70       299       0.00366       1287         90       299       0.00366       1287         90       299       0.00396       1330         100       299       0.00430       1373         110       299       0.00464       1405         120       299       0.00498       1448         130       299       0.00579       2153         140       399       0.00634       2217         150       399       0.00689       2324         160       399       0.00753       2410         170       399       0.00804       2475         180       399       0.00804       2475         180       399	0			
13       200       0.00055       97         20       200       0.00077       140         30       200       0.00094       172         33       301       0.00145       1062         40       301       0.00200       1062         50       299       0.00247       1148         60       299       0.00289       1201         70       299       0.00336       1244         80       299       0.00366       1287         90       299       0.00396       1330         100       299       0.00464       1405         120       299       0.00464       1405         120       299       0.00498       1448         130       299       0.00511       1470         133       400       0.00579       2153         140       399       0.00689       2324         160       399       0.00689       2324         160       399       0.00689       2324         160       399       0.00804       2475         180       399       0.00902       2604         200       399	3 10			
20       200       0.00074       140         30       200       0.00094       172         33       301       0.00145       1062         40       301       0.00200       1062         50       299       0.00247       1148         60       299       0.00289       1201         70       299       0.00366       1287         90       299       0.00366       1287         90       299       0.00430       1373         110       299       0.00440       1405         120       299       0.00498       1448         130       299       0.00498       1448         130       299       0.00511       1470         133       400       0.00579       2153         140       399       0.00689       2324         160       399       0.00689       2324         160       399       0.00804       2475         180       399       0.00804       2475         180       399       0.00902       2604         200       399       0.00902       2604         200       399 <td></td> <td></td> <td></td> <td></td>				
30       200       0.00094       172         33       301       0.00145       1062         50       299       0.00247       1148         60       299       0.00289       1201         70       299       0.00336       1244         80       299       0.00366       1287         90       299       0.00396       1330         100       299       0.00430       1373         110       299       0.00440       1405         120       299       0.00464       1405         120       299       0.00498       1448         130       299       0.00511       1470         133       400       0.00579       2153         140       399       0.00634       2217         150       399       0.00689       2324         160       399       0.00753       2410         170       399       0.00804       2475         180       399       0.00804       2475         210       399       0.00902       2604         200       399       0.01038       2754         230       399<				140
33       301       0.00145       1062         40       301       0.00200       1062         50       299       0.00247       1148         60       299       0.00289       1201         70       299       0.00336       1244         80       299       0.00366       1287         90       299       0.00430       1373         110       299       0.00464       1405         120       299       0.00440       1448         130       299       0.00511       1470         133       400       0.00579       2153         140       399       0.00634       2217         150       399       0.00689       2324         170       399       0.00689       2324         170       399       0.00804       2475         180       399       0.00855       2539         190       399       0.00902       2604         200       399       0.00906       2711         220       399       0.01038       2754         230       399       0.01204       2947         240       399				
40       301       0.00200       1062         50       299       0.00247       1148         60       299       0.00289       1201         70       299       0.00336       1244         80       299       0.00366       1287         90       299       0.00430       1373         110       299       0.00464       1405         120       299       0.00464       1475         120       299       0.00511       1470         133       400       0.00579       2153         140       399       0.00689       2324         150       399       0.00689       2324         170       399       0.00689       2324         170       399       0.00804       2475         180       399       0.00855       2539         190       399       0.00902       2604         200       399       0.00949       2657         210       399       0.01038       2754         230       399       0.0123       2861         250       399       0.01204       2947         270       399				
60         299         0.00289         1201           70         299         0.00336         1244           80         299         0.00396         1330           100         299         0.00430         1373           110         299         0.00464         1405           120         299         0.00498         1448           130         299         0.00511         1470           133         400         0.0579         2153           140         399         0.00634         2217           150         399         0.00689         2324           160         399         0.00753         2410           170         399         0.00804         2475           180         399         0.00855         2539           190         399         0.00992         2604           200         399         0.00996         2711           220         399         0.01038         2754           230         399         0.01080         2807           240         399         0.01204         2947           270         399         0.01243         2990 </td <td>40</td> <td>301</td> <td>0.00200</td> <td></td>	40	301	0.00200	
70       299       0.00336       1244         80       299       0.00366       1287         90       299       0.00396       1330         100       299       0.00430       1373         110       299       0.00464       1405         120       299       0.00498       1448         130       299       0.00511       1470         133       400       0.00579       2153         140       399       0.00634       2217         150       399       0.00689       2324         160       399       0.00753       2410         170       399       0.00855       2539         190       399       0.00855       2539         190       399       0.00902       2604         200       399       0.00996       2711         220       399       0.01038       2754         230       399       0.01080       2807         240       399       0.0123       2861         250       399       0.01243       2904         260       399       0.01243       2990         280	50			
80       299       0.00366       1287         90       299       0.00396       1330         100       299       0.00430       1373         110       299       0.00464       1405         120       299       0.00498       1448         130       299       0.00511       1470         133       400       0.00579       2153         140       399       0.00634       2217         150       399       0.00689       2324         160       399       0.00753       2410         170       399       0.00804       2475         180       399       0.00855       2539         190       399       0.00902       2604         200       399       0.00949       2657         210       399       0.01038       2754         230       399       0.01080       2807         240       399       0.01123       2861         250       399       0.01204       2947         270       399       0.01243       2990         283       500       0.01374       3319         290 <t< td=""><td></td><td></td><td></td><td></td></t<>				
90       299       0.00396       1330         100       299       0.00430       1373         110       299       0.00464       1405         120       299       0.00498       1448         130       299       0.00511       1470         133       400       0.00579       2153         140       399       0.00634       2217         150       399       0.00689       2324         160       399       0.00753       2410         170       399       0.00804       2475         180       399       0.00855       2539         190       399       0.00902       2604         200       399       0.00949       2657         210       399       0.01038       2754         230       399       0.01080       2807         240       399       0.01123       2861         250       399       0.01204       2947         270       399       0.01243       2990         283       500       0.01243       3990         283       500       0.01374       3319         290       <				
100       299       0.00430       1373         110       299       0.00464       1405         120       299       0.00498       1448         130       299       0.00511       1470         133       400       0.00579       2153         140       399       0.00634       2217         150       399       0.00689       2324         160       399       0.00753       2410         170       399       0.00804       2475         180       399       0.00855       2539         190       399       0.00902       2604         200       399       0.00996       2711         220       399       0.01038       2754         230       399       0.01080       2807         240       399       0.0123       2861         250       399       0.01204       2947         270       399       0.01243       2990         280       399       0.01243       2990         283       500       0.01243       3517         300       501       0.01532       3716         310       <				
110       299       0.00464       1405         120       299       0.00498       1448         130       299       0.00511       1470         133       400       0.00579       2153         140       399       0.00634       2217         150       399       0.00689       2324         160       399       0.00753       2410         170       399       0.00804       2475         180       399       0.00855       2539         190       399       0.00902       2604         200       399       0.00949       2657         210       399       0.01038       2754         230       399       0.01038       2754         230       399       0.01080       2807         240       399       0.01123       2861         250       399       0.0124       2947         270       399       0.0124       2947         270       399       0.01243       2990         283       500       0.01374       3319         290       501       0.01443       3517         300 <t< td=""><td></td><td></td><td></td><td></td></t<>				
120       299       0.00498       1448         130       299       0.00511       1470         133       400       0.00579       2153         140       399       0.00634       2217         150       399       0.00689       2324         160       399       0.00753       2410         170       399       0.00804       2475         180       399       0.00855       2539         190       399       0.00902       2604         200       399       0.00949       2657         210       399       0.00996       2711         220       399       0.01038       2754         230       399       0.01080       2807         240       399       0.01123       2861         250       399       0.01123       2861         250       399       0.01243       2990         280       399       0.01281       3022         283       500       0.01243       2990         280       399       0.01243       3990         290       501       0.01443       3517         300				
130       299       0.00511       1470         133       400       0.00579       2153         140       399       0.00634       2217         150       399       0.00689       2324         160       399       0.00753       2410         170       399       0.00804       2475         180       399       0.00855       2539         190       399       0.00902       2604         200       399       0.00949       2657         210       399       0.01038       2754         230       399       0.01080       2807         240       399       0.0123       2861         250       399       0.01123       2861         250       399       0.01204       2947         270       399       0.01243       2990         280       399       0.01243       2990         283       500       0.01374       3319         290       501       0.01443       3517         300       501       0.01532       3716         310       500       0.01613       3844				
133       400       0.00579       2153         140       399       0.00634       2217         150       399       0.00689       2324         160       399       0.00753       2410         170       399       0.00804       2475         180       399       0.00855       2539         190       399       0.00902       2604         200       399       0.00949       2657         210       399       0.01038       2754         230       399       0.01080       2807         240       399       0.01123       2861         250       399       0.01170       2904         260       399       0.01204       2947         270       399       0.01243       2990         280       399       0.01281       3022         283       500       0.01374       3319         290       501       0.01443       3517         300       501       0.01532       3716         310       500       0.01613       3844				
140       399       0.00634       2217         150       399       0.00689       2324         160       399       0.00753       2410         170       399       0.00804       2475         180       399       0.00855       2539         190       399       0.00902       2604         200       399       0.00949       2657         210       399       0.01038       2754         230       399       0.01080       2807         240       399       0.01123       2861         250       399       0.01170       2904         260       399       0.01204       2947         270       399       0.01243       2990         280       399       0.01281       3022         283       500       0.01374       3319         290       501       0.01443       3517         300       501       0.01532       3716         310       500       0.01613       3844				
150       399       0.00689       2324         160       399       0.00753       2410         170       399       0.00804       2475         180       399       0.00855       2539         190       399       0.00902       2604         200       399       0.00949       2657         210       399       0.01038       2754         230       399       0.01080       2807         240       399       0.01123       2861         250       399       0.01170       2904         260       399       0.01204       2947         270       399       0.01243       2990         280       399       0.01281       3022         283       500       0.01374       3319         290       501       0.01443       3517         300       501       0.01532       3716         310       500       0.01613       3844	140			
160       399       0.00753       2410         170       399       0.00804       2475         180       399       0.00855       2539         190       399       0.00902       2604         200       399       0.00949       2657         210       399       0.00996       2711         220       399       0.01038       2754         230       399       0.01080       2807         240       399       0.01123       2861         250       399       0.01170       2904         260       399       0.01204       2947         270       399       0.01243       2990         280       399       0.01281       3022         283       500       0.01374       3319         290       501       0.01443       3517         300       501       0.01532       3716         310       500       0.01613       3844				
180       399       0.00855       2539         190       399       0.00902       2604         200       399       0.00949       2657         210       399       0.00996       2711         220       399       0.01038       2754         230       399       0.01080       2807         240       399       0.01123       2861         250       399       0.01170       2904         260       399       0.01204       2947         270       399       0.01243       2990         283       500       0.01281       3022         283       500       0.01374       3319         290       501       0.01443       3517         300       501       0.01532       3716         310       500       0.01613       3844				2410
190       399       0.00902       2604         200       399       0.00949       2657         210       399       0.00996       2711         220       399       0.01038       2754         230       399       0.01080       2807         240       399       0.01123       2861         250       399       0.01170       2904         260       399       0.01204       2947         270       399       0.01243       2990         280       399       0.01281       3022         283       500       0.01374       3319         290       501       0.01443       3517         300       501       0.01532       3716         310       500       0.01613       3844				
200       399       0.00949       2657         210       399       0.00996       2711         220       399       0.01038       2754         230       399       0.01080       2807         240       399       0.01123       2861         250       399       0.01170       2904         260       399       0.01204       2947         270       399       0.01243       2990         280       399       0.01281       3022         283       500       0.01374       3319         290       501       0.01443       3517         300       501       0.01532       3716         310       500       0.01613       3844				
210       399       0.00996       2711         220       399       0.01038       2754         230       399       0.01080       2807         240       399       0.01123       2861         250       399       0.01170       2904         260       399       0.01204       2947         270       399       0.01243       2990         280       399       0.01281       3022         283       500       0.01374       3319         290       501       0.01443       3517         300       501       0.01532       3716         310       500       0.01613       3844				
220       399       0.01038       2754         230       399       0.01080       2807         240       399       0.01123       2861         250       399       0.01170       2904         260       399       0.01204       2947         270       399       0.01243       2990         280       399       0.01281       3022         283       500       0.01374       3319         290       501       0.01443       3517         300       501       0.01532       3716         310       500       0.01613       3844				
230       399       0.01080       2807         240       399       0.01123       2861         250       399       0.01170       2904         260       399       0.01204       2947         270       399       0.01243       2990         280       399       0.01281       3022         283       500       0.01374       3319         290       501       0.01443       3517         300       501       0.01532       3716         310       500       0.01613       3844				
240       399       0.01123       2861         250       399       0.01170       2904         260       399       0.01204       2947         270       399       0.01243       2990         280       399       0.01281       3022         283       500       0.01374       3319         290       501       0.01443       3517         300       501       0.01532       3716         310       500       0.01613       3844				
250       399       0.01170       2904         260       399       0.01204       2947         270       399       0.01243       2990         280       399       0.01281       3022         283       500       0.01374       3319         290       501       0.01443       3517         300       501       0.01532       3716         310       500       0.01613       3844				
260       399       0.01204       2947         270       399       0.01243       2990         280       399       0.01281       3022         283       500       0.01374       3319         290       501       0.01443       3517         300       501       0.01532       3716         310       500       0.01613       3844			<del>-</del>	
270       399       0.01243       2990         280       399       0.01281       3022         283       500       0.01374       3319         290       501       0.01443       3517         300       501       0.01532       3716         310       500       0.01613       3844				
280       399       0.01281       3022         283       500       0.01374       3319         290       501       0.01443       3517         300       501       0.01532       3716         310       500       0.01613       3844				
283       500       0.01374       3319         290       501       0.01443       3517         300       501       0.01532       3716         310       500       0.01613       3844		399		
290       501       0.01443       3517         300       501       0.01532       3716         310       500       0.01613       3844		500		
300 501 0.01532 3716 310 500 0.01613 3844				
310 500 0.01613 3844				3716
320 500 0.01681 3962				3844
	320	500	0.01681	3962



TABLE A-4 Continued

Time (min)	Outside Pressure (psi)	Change in Diameter (in)	Total Axial Force (lb)
330 340	500 500	0.01753 0.01826	4059 4145
<b>3</b> 50	500	0.01889	4220
360 370	500 500	0.01962 0.02031	4295 4395
380	500	0.02084	4413
390 400	500 500	0.02138 0.02213	4477 4509
410	500	0.02276	4564
420	500	0.02347	4606
430 433	500 604	0.02404 0.02444	4649 4880
440	603 ′	0.02533	5116
450	603	0.02658	5331
460 470	603 603	0.02769 0.02876	5492 5610
480	603	0.02978	5707
490 500	603	0.03077	5792 5857
500 510	604 604	0.03168 0.03259	5857 5932
520	604	0.03350	5895
530 540	604 604	0.03436 0.03523	6039 6082
550	604	0.03614	6146
560 5 <b>7</b> 0	604	0.03695	6168
5 <b>7</b> 0 580	604 604	0.03759 0.03850	6189 6232
583	701	0.03900	6465
590 600	704 703	0.04018 0.04182	6701 6894
610	704	0.04318	7023
620	704	0.04455	7119
630 640	705 705	0.04600 0.04727	7216 7280
650	705	0.04863	7345
660	705	0.04995	7409
680 690	705 705	0.05270 0.05395	7495 7538
700	705	0.05530	7580
<b>71</b> 0 <b>7</b> 20	705 <b>7</b> 05	0.05665 0.05781	7602 7634
730	705	0.05761	7656
<b>7</b> 35	800	0.06060	8017
740 750	800 800	0.06172 0.06377	8156 8339
760	800	0.06586	8457

TABLE A-4 Continued

Time (min)	Outside Pressure	Change in	Total Axial
	(psi)	Diameter (in)	Force (lb)
770 780 790 800 810 820 825 830 840 850 860 870 880 890 910	800 800 800 800 800 800 903 903 903 903 903 902 902 902	0.06786 0.06977 0.07163 0.07349 0.07535 0.07725 0.07949 0.08133 0.08471 0.08810 0.09146 0.09488 0.09488 0.09829 0.10165 0.10510	8553 8608 8682 —————————————————————————————————

TABLE A-5 Test data, SA-9

Material—Ottawa Sand Sand Density—64% by Volume Water Content—21.2% Test Temperature—-120°C. Date of Test—6 Mar 69 Initial Sample Dimensions
Outside Diam. 4"
Inside Diam. 1 1/2"
Height 9 3/16"

Outside Pressure (psi)	Change in Diameter (in)	Total Axial Force (lb)
0	0	0
	<del>-</del>	-
		697
		688
	_	735
		794
		842
	_	890
		933
		976
		1019
		1051
		1563
		1659
		1740
		1809
		1901
		1981
		2056
		2121
400		2174
400		2217
400	0.01042	2271
400	0.01081	2324
400	0.01119	2367
399	0.01153	2416
399	0.01187	2459
399	0.01213	2496
501	0.01268	2782
501	0.01327	3034
501	0.01417	3222
501	0.01495	3361
500	0.01561	3469
500	0.01621	3571
500	0.01676	3662
	(psi)  0 100 100 201 200 200 302 301 301 300 399 299 298 297 401 401 401 401 400 400 400 400 400 400	(psi)         Diameter (in)           0         0           100         0.00004           100         0.00009           201         0.00009           200         0.00064           302         0.00077           301         0.00200           301         0.00246           300         0.00332           299         0.00370           299         0.00396           298         0.00425           297         0.00451           401         0.00545           401         0.00621           401         0.00621           401         0.00621           401         0.00758           401         0.00817           400         0.00916           400         0.00916           400         0.01042           400         0.01042           400         0.01081           400         0.01187           399         0.01187           399         0.01213           501         0.01268           501         0.01495           501         0.01495           500

TABLE A-5 Continued

Time (min)	Outside Pressure (psi)	Change in Diameter (in)	Total Axial Force (lb)
340	500	0.01741	3742
350	500	0.01741	3842
360	500	0.01703	3876
370	500	0.01872	3941
380	499	0.01911	4000
390	499	0.01953	4059
400	499	0.01996	4113
410	499	0.02040	4166
420	499	0.02085	4214
423	601	0.02209	4462
430	601	0.02267	4719
440	601	0.02355	4934
450 460	601 601	0.02413 0.02485	5084 5208
470	601	0.02556	5310
480	600	0.02618	5295
490	600	0.02689	5481
500	600	0.02752	5551
510	600	0.02809	5615
520	600	0.02894	5674
530	600	0.02956	5723
540	600	0.03073	5776
550	600	0.03109	5825
560	600	0.03168	5867
570	600	0.03225	5900
573	702 701	0.03304	6100 6406
580 590	701 701	0.03577 0.03727	6615
600	701	0.03864	6802
610	701	0.03978	6878
620	701	0.04082	6969
630	701	0.04227	7006
640	703	0.04359	7087
650	703	0.04486	7151
660	703	0.04636	7200
670	703	0.04736	7253
680	703	0.04863	7302
690 700	703 703	0.04986 0.05116	7334 7366
710	703 703	0.05251	7403
720	703	0.05363	7430
723	802	0.05740	1609
730	802	0.05916	7909
740	802	0.06098	8124
<b>7</b> 50	802	0.06279	8253
760	802	0.06502	8339
770	802	0.06684	8414

TABLE A-5 Continued

Time	Outside Pressure	Change in	Total Axial
(min)	(psi)	Diameter (in)	Force (1b)
780 790 793 800 810 820 830 840 850 860	802 802 904 900 900 900 900 900	0.06842 0.07070 0.07391 0.07581 0.07893 0.08176 0.08500 0.08728 0.08990	8467 8510 8753 9118 9311 9435 9521 9590 9633

TABLE A-6 Test data, SA-11

Material—Ottawa SAnd	Initial Sample Dim	ensions
Sand Density-64% by Volume	Outside Diam.	3 1/2"
Water Content-21.4%	Inside Diam.	1 1/2"
Test Temperature—-12.0°C	Height	9 1/8"
Date of Test-20 Mar 69	<b>G</b>	

<del></del>	· · · · · · · · · · · · · · · · · · ·	
Outside Pressure (psi)	Change in Diameter (in)	Total Axial Force (lb)
(psi)  0 100 102 200 200 303 300 300 300 300 300 401 401 401 401 401 401 401 401 401 4	Diameter (in)  0 0.00009 0.00009 0.00013 0.00196 0.00226 0.00247 0.00251 0.00251 0.00353 0.00374 0.00383 0.00404 0.00421 0.00460 0.00498 0.00519 0.00549 0.00574 0.00600 0.00706 0.00706 0.00706 0.00706 0.00706 0.00902 0.00970 0.01081 0.01102	Force (1b)  0 -254* -234* -71* -26* 125 243 334 452 500 554 699 1264 1457 1634 1779 1908 2015 2117 2198 2283 2428 2758 3144 3267 3376
500 500 500 500 500 500 500	0.01208 0.01230 0.01315 0.01391 0.01472 0.01485 0.01532	3541 3621 3680 3734 3788 3830 3873 3906
	(psi)  0 100 102 200 200 303 300 300 300 300 300 401 401 401 401 401 401 401 401 401 4	(psi)         Diameter (in)           0         0           100         0           102         0.00009           200         0.00013           303         0.00196           300         0.00243           300         0.00247           300         0.00251           300         0.00251           300         0.00251           401         0.00353           401         0.00374           401         0.00383           401         0.00404           401         0.00404           401         0.00404           401         0.00404           401         0.00519           401         0.00519           401         0.00549           401         0.00549           401         0.00549           401         0.00549           401         0.00600           500         0.00762           500         0.00970           500         0.0181           500         0.01208           500         0.01208           500         0.01391           500

<sup>\*</sup>Apparent negative force probably due to shifting of sample.

TABLE A-6 Continued

343       601       0.0         350       601       0.0         360       601       0.0	1549 1664 1751 1864 1983 2062 2178	3943 4053 4348 4552 4690 4788
350 601 0.0 360 601 0.0	1751 1864 1983 2062	4348 4552 4690
360 601 0.0	1864 1983 2062	4552 4690
	1983 2062	4690
3/0	2062	
		4700
		4798
	2253	4873
	2316	4938
	2396	4938
	2506	4959
	2573	5002
	2622	5034
	2 <b>711</b> 2 <b>7</b> 91	5088 5120
	2889	5120
	2973	5142
	3068	5262
- <del>-</del>	3195	5519
510 702 0.0	3332	5713
	3477	5782
	3618	5906
	3741	5970
	3886 4032	6045
	4155	6077 6099
	4255	6110
	4382	6110
	4518	6120
610 702 0.0	4627	6142
	4759	6142
	4895	6283
	5079	6541
	530 <b>7</b> 5502	6712 6820
	5726	6906
	5916	6916
	6116	6927
	6335	6948
700 803 0.0	6530	6959
· · ·	6712	7133
	6977	7444
	7372	7573
. •	7702 8010	7680
	8295	7712

TABLE A-6 Continued

Time (min)	Outside Pressure (psi)	Change in Diameter (in)	Total Axial Force (lb)
760	903	0.08629	***
770	903	0.08905	<del></del>
780	902	0.09205	***************************************

TABLE A-7 Test data, SA-12

Material—Ottawa Sand	Initial Sample Dimen	sions
Sand Density-64% by Volume	Outside Diam.	4 1/2"
Water Content-21.0%	Inside Diam.	1 1/2"
Test Temperature—-12.0°C.	Height	9 3/16"
Date of Test-27 Mar 69	· ·	

Outside Pressure (psi)	Change in Diameter (in)	Total Axial Force (lb)
(ps1)  0 100 99 200 200 300 300 300 299 2998 298 298 298 298 400 400 400 400 400 400 399 399 399 399 399 399 501 501 501	Diameter (in)  0 0.00026 0.00051 0.00191 0.00247 0.00591 0.00779 0.00842 0.00894 0.00983 0.01013 0.01060 0.01076 0.01319 0.01502 0.01583 0.01660 0.01715 0.01770 0.01847 0.01940 0.02004 0.02004 0.02089 0.02138 0.02302 0.02342 0.02413 0.02493 0.02618	Force (1b)  0 -45* -40* 204 247 1151 1087 1087 1114 1140 1173 1199 1226 1258 2157 2146 2187 2243 2297 2356 2409 2463 2511 2565 2602 2645 2688 3372 3496 3614 3710 3796
501 501 501 500 500	0.02707 0.02755 0.02849 0.02933 0.03005	3887 3957 4032 4102 4172
	(ps1) 0 100 99 200 300 300 300 299 2998 298 400 400 400 400 400 399 399 399 399 501 501 501 501 501 500	(psi)       Diameter (in)         0       0         100       0.00026         99       0.00051         200       0.00247         300       0.00591         300       0.00779         299       0.00842         299       0.00894         299       0.00983         298       0.01013         298       0.01060         298       0.01076         400       0.01319         400       0.01502         400       0.01502         400       0.01715         400       0.01775         399       0.01847         399       0.02080         399       0.02080         399       0.02089         399       0.02089         399       0.02138         501       0.02302         501       0.02493         501       0.02707         501       0.02755         501       0.02849         500       0.02933

<sup>\*</sup>Apparent negative force probably due to shifting of sample.

TABLE A-7 Continued

Time (min)				
330         500         0.03100         4311           340         500         0.03214         4376           350         500         0.03286         4440           360         500         0.03486         4931           370         601         0.03486         4931           370         601         0.03695         5414           390         601         0.03791         5564           400         600         0.03914         5693           410         600         0.03977         5800           420         600         0.04068         5907           430         600         0.04191         5993           440         600         0.04300         6079           450         600         0.04144         6159           450         600         0.044300         6079           450         600         0.044300         6079           450         600         0.04430         6079           460         600         0.04430         6218           470         600         0.04530         6218           480         600         0.04431         6454				
330         500         0.03100         4311           340         500         0.03214         4376           350         500         0.03286         4440           360         500         0.03486         4931           370         601         0.03486         4931           370         601         0.03695         5414           390         601         0.03791         5564           400         600         0.03914         5693           410         600         0.03977         5800           420         600         0.04068         5907           430         600         0.04191         5993           440         600         0.04300         6079           450         600         0.04300         6079           450         600         0.04414         6159           460         600         0.04486         6218           470         600         0.04595         6282           480         600         0.0471         6401           500         600         0.0471         6401           500         600         0.04813         6454	320	500	0 02018	h 2 h 1
340         500         0.03214         4376           350         500         0.03286         4440           360         500         0.03341         4494           363         601         0.03486         4931           370         601         0.03695         5414           390         601         0.03791         5564           400         600         0.03914         5693           410         600         0.03977         5800           420         600         0.04068         5907           430         600         0.04191         5993           440         600         0.04300         6079           450         600         0.04191         5993           440         600         0.04300         6079           450         600         0.04486         6218           470         600         0.04486         6218           470         600         0.04595         6282           480         600         0.04741         6401           500         600         0.04813         6454           510         600         0.04813         6454				
350         500         0.03286         4440           360         500         0.03341         4494           363         601         0.03486         4931           370         601         0.03568         5199           380         601         0.03791         5564           400         600         0.03791         5564           400         600         0.03977         5800           420         600         0.04068         5907           430         600         0.04191         5993           440         600         0.04300         6079           450         600         0.04300         6079           450         600         0.04414         6159           460         600         0.04486         6218           470         600         0.04595         6282           480         600         0.04668         6342           490         600         0.04741         6401           500         600         0.04936         6503           510         600         0.04936         6503           513         701         0.05163         7203		<u>=</u>		
360         500         0.03341         4494           363         601         0.03486         4931           370         601         0.03568         5199           380         601         0.03695         5414           390         601         0.03791         5564           400         600         0.03914         5693           410         600         0.03977         5800           420         600         0.04968         5907           430         600         0.04191         5993           440         600         0.04300         6079           450         600         0.04300         6079           450         600         0.04486         6218           470         600         0.04595         6282           480         600         0.04741         6401           500         600         0.04741         6401           500         600         0.04741         6401           510         600         0.04813         6454           510         600         0.04936         6503           513         701         0.05140         6908				
363         601         0.03486         4931           370         601         0.03568         5199           380         601         0.03695         5414           390         601         0.03791         5564           400         600         0.03914         5693           410         600         0.04068         5907           430         600         0.04191         5993           440         600         0.04300         6079           450         600         0.04300         6079           450         600         0.04300         6079           450         600         0.04300         6079           450         600         0.04486         6218           470         600         0.04595         6282           480         600         0.04595         6282           480         600         0.04741         6401           500         600         0.04741         6401           510         600         0.04936         6503           513         701         0.05163         7223           520         701         0.05163         7223				
370         601         0.03568         5199           380         601         0.03695         5414           390         601         0.03791         5564           400         600         0.03914         5693           410         600         0.04068         5907           420         600         0.04068         5907           430         600         0.04191         5993           440         600         0.04300         6079           450         600         0.04300         6079           450         600         0.04414         6159           470         600         0.04595         6282           480         600         0.0468         6342           490         600         0.04741         6401           500         600         0.04741         6401           500         600         0.04936         6503           513         701         0.05140         6908           520         701         0.05140         6908           520         701         0.05140         6908           520         701         0.05133         7417				
380       601       0.03695       5414         390       601       0.03791       5564         400       600       0.03914       5693         410       600       0.03977       5800         420       600       0.04068       5907         430       600       0.04191       5993         440       600       0.04300       6079         450       600       0.04300       6079         450       600       0.04414       6159         460       600       0.04486       6218         470       600       0.04595       6282         480       600       0.04595       6282         490       600       0.04741       6401         500       600       0.04813       6454         510       600       0.04813       6454         510       600       0.04813       6454         513       701       0.05163       7203         530       701       0.05163       7203         540       701       0.05300       7417         550       701       0.05605       7697         560				
390         601         0.03791         5564           400         600         0.03914         5693           410         600         0.04068         5907           430         600         0.04191         5993           440         600         0.04300         6079           450         600         0.04414         6159           460         600         0.04486         6218           470         600         0.04595         6282           480         600         0.04688         6342           490         600         0.04688         6342           490         600         0.04936         6503           510         600         0.04936         6503           513         701         0.05140         6908           520         701         0.05140         6908           530         701         0.05442         7573           540         701         0.05442         7573           550         701         0.05442         7573           550         701         0.05605         7697           570         700         0.05860         7922				
400       600       0.03914       5693         410       600       0.03977       5800         420       600       0.04068       5907         430       600       0.04191       5993         440       600       0.04300       6079         450       600       0.04300       6079         460       600       0.04486       6218         470       600       0.04595       6282         480       600       0.04668       6342         490       600       0.04741       6401         500       600       0.04936       6503         513       701       0.05140       6908         520       701       0.05163       7203         530       701       0.05163       7203         550       701       0.05330       7417         540       701       0.05442       7573         550       701       0.05442       7573         550       701       0.05605       7697         560       700       0.05991       7986         570       700       0.05860       7922         580				
410       600       0.03977       5800         420       600       0.04068       5907         430       600       0.04191       5993         440       600       0.04300       6079         450       600       0.04414       6159         460       600       0.04486       6218         470       600       0.04568       6342         480       600       0.04668       6342         490       600       0.0471       6401         500       600       0.04813       6454         510       600       0.04936       6503         513       701       0.05163       7203         530       701       0.05163       7203         530       701       0.05163       7203         540       701       0.05492       7573         550       701       0.05142       7573         550       701       0.05726       7804         570       700       0.05726       7804         570       700       0.05860       7922         580       700       0.06372       8201         600       <				
420       600       0.04068       5907         430       600       0.04191       5993         440       600       0.04300       6079         450       600       0.04414       6159         460       600       0.04486       6218         470       600       0.04595       6282         480       600       0.04668       6342         490       600       0.04741       6401         500       600       0.04813       6454         510       600       0.04936       6503         513       701       0.05140       6908         520       701       0.05140       6908         520       701       0.05163       7203         530       701       0.05330       7417         540       701       0.05330       7417         540       701       0.05605       7697         560       700       0.05726       7804         570       700       0.05860       7922         580       700       0.05860       7922         580       700       0.06135       8061         600				5093
430       600       0.04191       5993         440       600       0.04300       6079         450       600       0.04414       6159         460       600       0.04486       6218         470       600       0.04595       6282         480       600       0.04668       6342         490       600       0.04741       6401         500       600       0.04813       6454         510       600       0.04936       6503         513       701       0.05163       7203         530       701       0.05163       7203         530       701       0.05330       7417         540       701       0.05442       7573         550       701       0.05442       7573         560       700       0.05726       7804         570       700       0.05860       7922         580       700       0.05991       7986         590       700       0.06135       801         600       700       0.06228       8136         610       700       0.06465       8244         630       <				
440       600       0.04300       6079         450       600       0.04414       6159         460       600       0.04486       6218         470       600       0.04595       6282         480       600       0.04668       6342         490       600       0.04741       6401         500       600       0.04936       6503         513       701       0.05140       6908         520       701       0.05163       7203         530       701       0.05330       7417         540       701       0.05330       7417         540       701       0.05442       7573         550       701       0.05605       7697         560       700       0.05726       7804         570       700       0.05860       7922         580       700       0.05860       7922         580       700       0.06135       8061         600       700       0.06372       8201         620       700       0.06465       8244         630       700       0.06605       8297         640				
450       600       0.04414       6159         460       600       0.04486       6218         470       600       0.04595       6282         480       600       0.0468       6342         490       600       0.04741       6401         500       600       0.04813       6454         510       600       0.04936       6503         513       701       0.05140       6908         520       701       0.05163       7203         530       701       0.05163       7203         530       701       0.05422       7573         550       701       0.05422       7573         550       701       0.05605       7697         560       700       0.05726       7804         570       700       0.05860       7922         580       700       0.05991       7986         590       700       0.06135       8061         600       700       0.06228       8136         610       700       0.06372       8201         620       700       0.06465       8244         630       <				
460       600       0.04486       6218         470       600       0.04595       6282         480       600       0.04668       6342         490       600       0.04741       6401         500       600       0.04813       6454         510       600       0.04936       6503         513       701       0.05140       6908         520       701       0.05163       7203         530       701       0.05330       7417         540       701       0.0542       7573         550       701       0.05605       7697         560       700       0.05726       7804         570       700       0.05860       7922         580       700       0.05860       7922         580       700       0.05991       7986         590       700       0.06135       8061         600       700       0.06228       8136         610       700       0.06428       8136         640       700       0.06405       8244         630       700       0.06405       8244         630       <				
470       600       0.04595       6282         480       600       0.04668       6342         490       600       0.04741       6401         500       600       0.04813       6454         510       600       0.04936       6503         513       701       0.05140       6908         520       701       0.05163       7203         530       701       0.05330       7417         540       701       0.05442       7573         550       701       0.05605       7697         560       700       0.05726       7804         570       700       0.05860       7922         580       700       0.05860       7922         580       700       0.05860       7922         580       700       0.06135       8061         600       700       0.06228       8136         610       700       0.06228       8136         610       700       0.06465       8244         630       700       0.06605       8297         640       700       0.06605       8297         640				
480       600       0.04668       6342         490       600       0.04741       6401         500       600       0.04813       6454         510       600       0.04936       6503         513       701       0.05140       6908         520       701       0.05163       7203         530       701       0.05330       7417         540       701       0.05442       7573         550       701       0.05605       7697         560       700       0.05726       7804         570       700       0.05860       7922         580       700       0.05860       7922         580       700       0.05991       7986         590       700       0.06135       8061         600       700       0.06228       8136         610       700       0.06228       8136         640       700       0.06465       8244         630       700       0.06721       8351         643       800       0.06707       8650         650       801       0.07028       9067         660				
490       600       0.04741       6401         500       600       0.04813       6454         510       600       0.04936       6503         513       701       0.05140       6908         520       701       0.05163       7203         530       701       0.05330       7417         540       701       0.05442       7573         550       701       0.05605       7697         560       700       0.05726       7804         570       700       0.05860       7922         580       700       0.05991       7986         590       700       0.06135       8061         600       700       0.06228       8136         610       700       0.06228       8136         610       700       0.06465       8244         630       700       0.06721       8351         643       800       0.06707       8650         650       801       0.07028       9067         660       800       0.07237       9293         670       800       0.07433       9459         680				
500         600         0.04813         6454           510         600         0.04936         6503           513         701         0.05140         6908           520         701         0.05163         7203           530         701         0.05330         7417           540         701         0.05442         7573           550         701         0.05605         7697           560         700         0.05726         7804           570         700         0.05860         7922           580         700         0.05991         7986           590         700         0.06135         8061           600         700         0.06228         8136           610         700         0.06372         8201           620         700         0.06465         8244           630         700         0.06605         8297           640         700         0.06721         8351           643         800         0.06707         8650           650         801         0.07028         9067           660         800         0.07237         9293				6)101
510       600       0.04936       6503         513       701       0.05140       6908         520       701       0.05163       7203         530       701       0.05330       7417         540       701       0.05442       7573         550       701       0.05605       7697         560       700       0.05726       7804         570       700       0.05860       7922         580       700       0.05860       7922         580       700       0.05991       7986         590       700       0.06135       8061         600       700       0.06228       8136         610       700       0.06372       8201         620       700       0.06465       8244         630       700       0.06605       8297         643       800       0.06721       8351         643       800       0.07028       9067         660       800       0.07237       9293         670       800       0.07433       9459         680       800       0.07605       9690         700				
513       701       0.05140       6908         520       701       0.05163       7203         530       701       0.05330       7417         540       701       0.05442       7573         550       701       0.05605       7697         560       700       0.05726       7804         570       700       0.05860       7922         580       700       0.05991       7986         590       700       0.06135       8061         600       700       0.06228       8136         610       700       0.06228       8136         610       700       0.06465       8244         630       700       0.06465       8244         630       700       0.06605       8297         643       800       0.06721       8351         643       800       0.07028       9067         660       800       0.07237       9293         670       800       0.07433       9459         680       800       0.07805       9690         700       800       0.07953       9777				
520       701       0.05163       7203         530       701       0.05330       7417         540       701       0.05442       7573         550       701       0.05605       7697         560       700       0.05726       7804         570       700       0.05860       7922         580       700       0.05991       7986         590       700       0.06135       8061         600       700       0.06228       8136         610       700       0.06372       8201         620       700       0.06465       8244         630       700       0.06605       8297         640       700       0.06721       8351         643       800       0.06707       8650         650       801       0.07028       9067         660       800       0.07237       9293         670       800       0.07433       9459         680       800       0.07619       9588         690       800       0.07953       9777				
530       701       0.05330       7417         540       701       0.05442       7573         550       701       0.05605       7697         560       700       0.05726       7804         570       700       0.05860       7922         580       700       0.05991       7986         590       700       0.06135       8061         600       700       0.06228       8136         610       700       0.06372       8201         620       700       0.06465       8244         630       700       0.06605       8297         640       700       0.06721       8351         643       800       0.06707       8650         650       801       0.07028       9067         660       800       0.07237       9293         670       800       0.07433       9459         680       800       0.07619       9588         690       800       0.07805       9690         700       800       0.07953       9777				7203
540       701       0.05442       7573         550       701       0.05605       7697         560       700       0.05726       7804         570       700       0.05860       7922         580       700       0.05991       7986         590       700       0.06135       8061         600       700       0.06228       8136         610       700       0.06372       8201         620       700       0.06465       8244         630       700       0.06605       8297         640       700       0.06721       8351         643       800       0.06707       8650         650       801       0.07028       9067         660       800       0.07237       9293         670       800       0.07433       9459         680       800       0.07805       9690         700       800       0.07953       9777				
550       701       0.05605       7697         560       700       0.05726       7804         570       700       0.05860       7922         580       700       0.05991       7986         590       700       0.06135       8061         600       700       0.06228       8136         610       700       0.06372       8201         620       700       0.06465       8244         630       700       0.06605       8297         640       700       0.06721       8351         643       800       0.06707       8650         650       801       0.07028       9067         660       800       0.07237       9293         670       800       0.07433       9459         680       800       0.07805       9690         700       800       0.07953       9777	540			
560       700       0.05726       7804         570       700       0.05860       7922         580       700       0.05991       7986         590       700       0.06135       8061         600       700       0.06228       8136         610       700       0.06372       8201         620       700       0.06465       8244         630       700       0.06605       8297         640       700       0.06721       8351         643       800       0.06707       8650         650       801       0.07028       9067         660       800       0.07237       9293         670       800       0.07433       9459         680       800       0.07619       9588         690       800       0.07805       9690         700       800       0.07953       9777	550			
570       700       0.05860       7922         580       700       0.05991       7986         590       700       0.06135       8061         600       700       0.06228       8136         610       700       0.06372       8201         620       700       0.06465       8244         630       700       0.06605       8297         640       700       0.06721       8351         643       800       0.06707       8650         650       801       0.07028       9067         660       800       0.07237       9293         670       800       0.07433       9459         680       800       0.07619       9588         690       800       0.07805       9690         700       800       0.07953       9777	560			
580       700       0.05991       7986         590       700       0.06135       8061         600       700       0.06228       8136         610       700       0.06372       8201         620       700       0.06465       8244         630       700       0.06605       8297         640       700       0.06721       8351         643       800       0.06707       8650         650       801       0.07028       9067         660       800       0.07237       9293         670       800       0.07433       9459         680       800       0.07619       9588         690       800       0.07805       9690         700       800       0.07953       9777				
590       700       0.06135       8061         600       700       0.06228       8136         610       700       0.06372       8201         620       700       0.06465       8244         630       700       0.06605       8297         640       700       0.06721       8351         643       800       0.06707       8650         650       801       0.07028       9067         660       800       0.07237       9293         670       800       0.07433       9459         680       800       0.07619       9588         690       800       0.07805       9690         700       800       0.07953       9777				
600       700       0.06228       8136         610       700       0.06372       8201         620       700       0.06465       8244         630       700       0.06605       8297         640       700       0.06721       8351         643       800       0.06707       8650         650       801       0.07028       9067         660       800       0.07237       9293         670       800       0.07433       9459         680       800       0.07619       9588         690       800       0.07805       9690         700       800       0.07953       9777				
610       700       0.06372       8201         620       700       0.06465       8244         630       700       0.06605       8297         640       700       0.06721       8351         643       800       0.06707       8650         650       801       0.07028       9067         660       800       0.07237       9293         670       800       0.07433       9459         680       800       0.07619       9588         690       800       0.07805       9690         700       800       0.07953       9777				
620       700       0.06465       8244         630       700       0.06605       8297         640       700       0.06721       8351         643       800       0.06707       8650         650       801       0.07028       9067         660       800       0.07237       9293         670       800       0.07433       9459         680       800       0.07619       9588         690       800       0.07805       9690         700       800       0.07953       9777			0.06372	
630       700       0.06605       8297         640       700       0.06721       8351         643       800       0.06707       8650         650       801       0.07028       9067         660       800       0.07237       9293         670       800       0.07433       9459         680       800       0.07619       9588         690       800       0.07805       9690         700       800       0.07953       9777				
640       700       0.06721       8351         643       800       0.06707       8650         650       801       0.07028       9067         660       800       0.07237       9293         670       800       0.07433       9459         680       800       0.07619       9588         690       800       0.07805       9690         700       800       0.07953       9777				
643       800       0.06707       8650         650       801       0.07028       9067         660       800       0.07237       9293         670       800       0.07433       9459         680       800       0.07619       9588         690       800       0.07805       9690         700       800       0.07953       9777	640			
650       801       0.07028       9067         660       800       0.07237       9293         670       800       0.07433       9459         680       800       0.07619       9588         690       800       0.07805       9690         700       800       0.07953       9777	643			8650
660       800       0.07237       9293         670       800       0.07433       9459         680       800       0.07619       9588         690       800       0.07805       9690         700       800       0.07953       9777				
670       800       0.07433       9459         680       800       0.07619       9588         690       800       0.07805       9690         700       800       0.07953       9777	660			
680       800       0.07619       9588         690       800       0.07805       9690         700       800       0.07953       9777				
690       800       0.07805       9690         700       800       0.07953       9777				
700 800 0.07953 9777				
710 800 0.08138 9861		800	0.08138	9861
720 800 0.8276 9936				
730 800 0.08438 10001		800	0.08438	10001

TABLE A-7 Continued

Time	Outside Pressure	Change in	Total Axial
(min)	(psi)	Diameter (in)	Force (lb)
733 740 750 760 770 780 790 800 810 820	900 901 901 901 901 901 901 901	0.08624 0.08767 0.09093 0.09341 0.09571 0.09790 0.10000 0.10210 0.10380 0.10625	10438 10728 10975 11146 11275 11382 11468 11532 11586 11640

TABLE A-8 Test data, SA-14

Material—Ottawa Sand Sand Density—64% by Volume Water Content—21.6% Test Temperature—-12.0°C. Date of Test—10 Apr 69	Initial Sample Dimensions Outside Diam. 5" Inside Diam. 1 1/2" Height 9 1/4"
----------------------------------------------------------------------------------------------------------------------	------------------------------------------------------------------------------

Time (min)	Outside Pressure (psi)	Change in Diameter (in)	Total Axial Force (1b)
0 3	0	0	0
3	100	0	70
10	100 200	0	38 763
13 20	200	0 0	763 739
23	300	Ö	1605
30	300	0	1573
40	300	0	1573
50 60	300	0	1573
60 <b>7</b> 0	299 299	0	1583 1594
80	299	Ö	1594
.83	400	0	3317
90	400	0	3478
100	400 401	0	3488
110 120	401	0.00013	3478 3478
130	401	0.00038	3488
140	401	0.00043	3499
143	500	0.00047	5565
150	500	0.00081	5629 5737
160 170	500 500	0.00174 0.00285	5737 5769
180	500	0.00366	5812
190	500	0.00472	5855
200	500	0.00574	5876
210	500	0.00677	5898
220 230	500 500	0.00766 0.00842	5908 5919
240	500	0.00915	5930
250	500	0.01009	5951
260	500	0.01068	5962
263	600	0.01234	8296
270 280	600 600	0.01268 0.01481	8221 8189
290	600	0.01655	8168
300	600	0.01706	8168
310	.600	0.01872	8168
320	600	0.02036	8168

TABLE A-8 Continued

Time (min)	Outside Pressure (psi)	Change in Diameter (in)	Total Axial Force (lb)
330	600	0.02253	8168 8168
340 350	600 600	0.02320 0.02542	8168
360	600	0.02569	8178
370	600	0.02715	8200
380	600	0.02898	8210
383	700	0.03036	10148
390	700	0.03177	10126
400 410	700 700	0.03250 0.03473	10094 10083
420	700	0.03723	10083
430	700	0.03895	10083
440	700	0.04045	10083
450	700	0.04205	10094
460	700	0.04341	10105
470	700	0.04482	10115
480 490	700 700	0.04650 0.04768	10126 10137
500	700	0.04968	10157
510	700	0.05074	10169
520	700	0.05256	10180
530	700	0.05395	10201
533	801	0.05637	11901
540	801 801	0.05712	11891 11880
550 560	801	0.05991 0.06233	11880
570	801	0.06456	11880
580	801	0.06698	11891
590	801	0.06856	11901
600	801	0.07116	11912
610	801	0.07270	11923
620 630	801 801	0.07544 0.07721	11944 11955
640	801	0.07958	11966
650	801	0.08200	11987
653	901	0.08424	13742
660	902	0.08610	13753
670	902	0.08933	13753
680	901	0.09239	13764 13764
690 <b>7</b> 00	901 901	0.09600 0.09917	13774
710	901	0.10240	13785
720	901	0.10535	13796
730	901	0.10835	13806
740	901	0.11235	13817
750	900	0.11535	13828
760	900	0.11850	13849

Note: Bottom portion of shaft slipped. This may have caused excessive axial force and deformation. It also may have allowed small amount of ethylene glycol to reach sample

TABLE A-9 Test data, SA-16

Material—Ottawa Sand Sand Density—64% by Volume Water Content—21.3% Test Temperature—-12.0°C Date of Test—24 Apr 69 Initial Sample Dimensions
Outside Diam. 5"
Inside Diam. 1 1/2"
Height 9 1/4"

Time (min)	Outside Pres <b>su</b> re (psi)	Change in Diameter (in)	Total Axial Force (lb)
0	0 100	0	0 49
10	100	ő	44
13	200	0	184
20	200	0	216
23	300	0	468
30	300	0	521 506
40 50	300 299	0	586 634
60	299	0	682
63	400	ŏ	940
70	400	0	1043
80	400	0	1160
90	400	0	1268
100	400	0	1375
110 120	400 400	0.00034	1461
123	500	0.00081 0.00136	1546 2035
130	500	0.00130	2196
140	500	0.00331	2400
150	500	0.00460	2582
160	500	0.00574	2754
170	500	0.00698	2915
180	500	0.00791	3046
190 200	500 500	0.00889 0.01004	3226 3371
210	500	0.01004	3371 3516
220	500	0.01306	3623
230	500	0.01404	<b>37</b> 30
240	500	0.01498	3838
243	599	0.01608	4520
250	600	0.01694	4777
260	600	0.01830	5035 5031
270 280	600 600	0.01953 0.02089	5271 5399
290	600	0.02280	5550
300	600	0.02400	5689
310	600	0.02529	5807
320	600	0.02644	5925

TABLE A-9 Continued

Time	Outside Pressure	Change in	Total Axial
(min)	(psi)	Diameter (in)	Force (lb)
330	600	0.02760	6032
340	600	0.02880	6038
350	600	0.02995	6204
360	600	0.03114	6290
363	700	0.03214	6940
370	700	0.03350	7283
380	700	0.03532	7530
390	700	0.03750	7701
400	700	0.03927	7852
410	700	0.04118	7959
420	700	0.04282	8045
430 440	700 700	0.04445 0.04623	8131 8216
450	700 700	0.04795	8281
460	700	0.04986	8345
470	700	0.05149	8410
480	700	0.05312	8474
485	800	0.05512	9176
490	800	0.05637	9380
500	802	0.05916	9573
510	799	0.06191	9831
520	798	0.06456	10002
530	796	0.06730	10110
540	798	0.07047	10170
550 560	796	0.07256	10271
560 570	798 708	0.07512	10271
570 580	798 797	0.07767 0.08029	10367 10442
590	796	0.08300	10496
593	902	0.08486	11038
600	902	0.08810	11403
610	901	0.09229	11682
620	900	0.09639	11854
630	900	0.10065	11940
640	900	0.10475	12036
650	900	0.10885	12096
660	899	0.11295	12165
670	898	0.11711	12219
680	896	0.12154	12272
690	903	0.12615	12261

Note: Small amount of ethylene glycol may have reached sample.

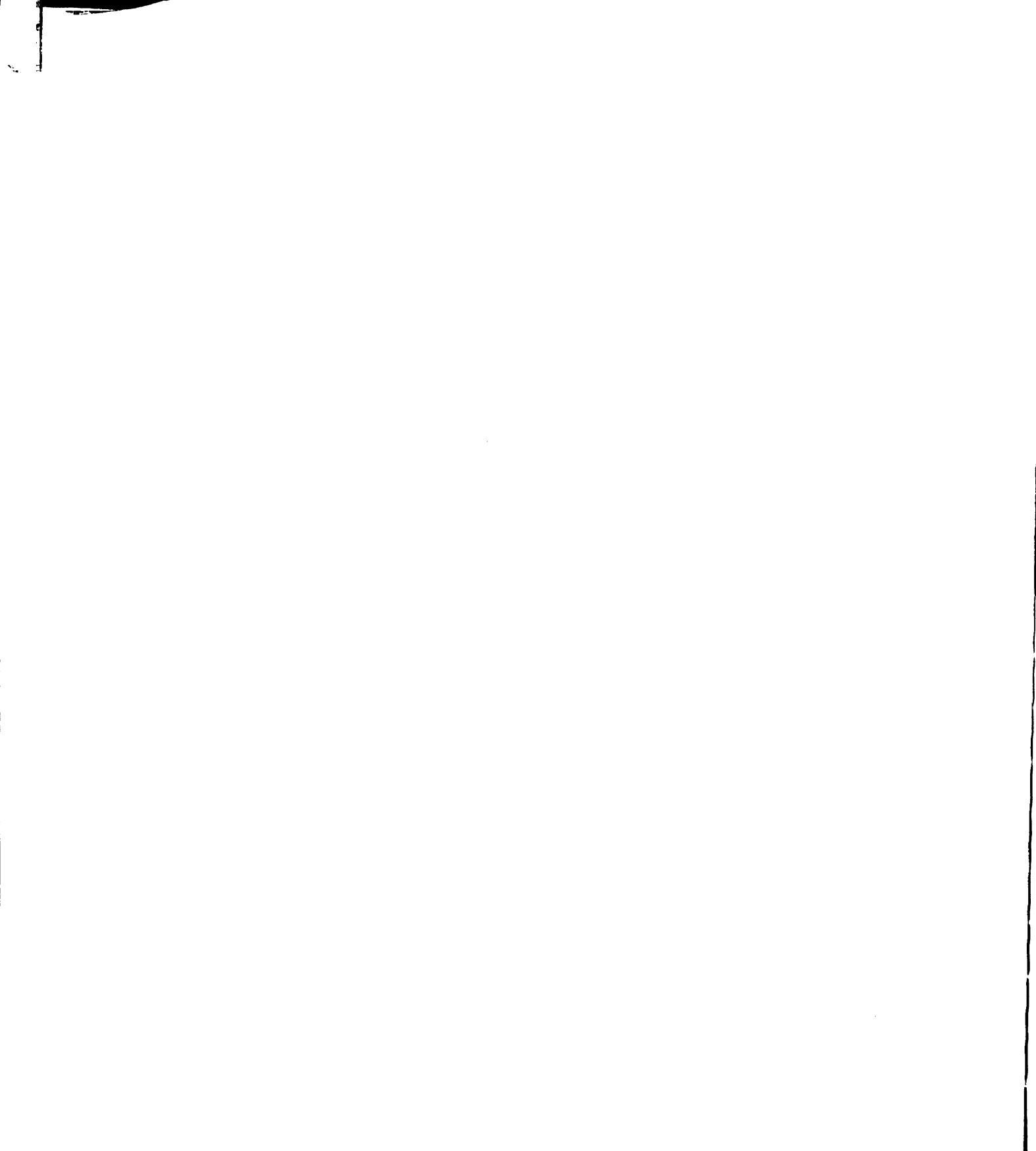


TABLE A-10 Test data, SA-18

Material-Ottawa Sand
Sand Density-64% by Volume
Water Content—21.4%
Test Temperature—-12.0°C.
Date of Test-9 May 69

Initial Sample Dimensions
Outside Diam. 5"
Inside Diam. 1 1/2"
Height 9"

Outside Pressure (psi)	Change in Diameter (in)	Total Axial Force (lb)
	(psi) 0 100 100 201 204 299 300 399 399 399 399 399 399 399 498 499 498 499 498 499 498 497 590 601 601 601 601 601	(ps1)         Diameter (in)           0         0           100         0           201         0           204         0           299         0           300         0           399         0           399         0           398         0           400         0           400         0           398         0           400         0           398         0           400         0           490         0           491         0           492         0           493         0           499         0           499         0           499         0           499         0           499         0           499         0           499         0           499         0           498         0           0         0           497         0           497         0           497         0           600         0           601

TABLE A-10 Continued

Time (min)	Outside Pressure	Change in	Total Axial
	(psi)	Diameter (in)	Force (lb)
590	899	0.09390	13506
600	898	0.09756	13603

Note: Small amount of ethylene glycol may have reached sample. Leak in cell caused fluctuations in pressure.

TABLE A-11 Test data, C-3

Material—Ontonagon Clay Initial Sample Dimensions
Density—97.3 lb/ft3 Outside Diam. 5"
Water Content—26.2% Inside Diam. 1 1/2"
Test Temperature—-12.0°C. Height 9 1/4"
Date of Test—21 Nov 68

Time (min)	Outside Pressure (psi)	Change in Diameter (in)
(min) 0486420864208864208864220864222222222222		Diameter (in)  0 0.1381 0.1586 0.1806 0.1924 0.2012 0.2075 0.2119 0.2159 0.2188 0.2212 0.2234 0.2253 0.2269 0.2281 0.2297 0.2309 0.2319 0.2338 0.2362 0.2369 0.2378 0.2384 0.2394 0.2406 0.2412 0.2419 0.2428 0.2431 0.2428 0.2431 0.2444 0.2444
288 296 304	300 300 300	0.2447 0.2453 0.2459

TABLE A-11 Continued

Time	Outside Pressure	Change in
(min)	(psi)	Diameter (in)
<u> </u>	(1932)	220
312	300	0.2462
320	300	0.2462
328	300	0.2469
336	300	0.2472
344	300	0.2475
352	300	0.2475
360	300	0.2478
368	300	0.2484
376	300	0.2484
384	300	0.2488
392	300	0.2488
400	300	0.2491
404	300	0.2494
408	400	0.2643
412	400	0.2721
420	400	0.2829
428	400	0.2911
436.	400	0.2970
444	400	0.3022
452	400	0.3063
460	400	0.3104
468	400	0.3135
476	400	0.3165
484	400	0.3192
492	400	0.3215

TABLE A-12 Test data, C-4

Material—Ontonagon Clay Density—98.2 lb/ft3 Water Content—25.0% Test Temperature—-12.0°C.	Initial Sample Dimensions Outside Diam. 5" Inside Diam. 1 1/2" Height 9 3/16"
Date of Test—12 May 69	2 3.

Time (min)	Outside Pressure (psi)	Change in Diameter (in)	Total Axial Force (lb)
(111)	(501)	prame oer (III)	10100 (10)
0	0	0	0
4	101	0.01838	5 <b>21</b>
10 15	100 100	0.02356 0.02578	682
20	100	0.02769	<b>730</b> 75 <u>7</u>
30	100	0.02964	778
40	100	0.03109	795
50	100	0.03209	800
60	100	0.03286	800
70	100	0.03364	790
80	100	0.03423	800
90 100	100 100	0.03495	<b>8</b> 00 805
110	100	0.03523 0.03582	778
120	100	0.03645	800
130	100	0.03682	789
140	100	0.03718	789
150	100	0.03764	789
160	100	0.03795	789
170	100	0.03818	795
180 190	100	0.03850 0.03877	800 800
200	100 100	0.03077	795
210	100	0.03927	795
220	100	0.03959	795
230	100	0.03973	795
240	100	0.03982	789
250	100	0.04014	789
260	100	0.04023	784
270 280	100 100	0.04036 0.04059	784 784
290	100	0.04068	789
300	100	0.04077	784
304	200	0.07126	250 <b>1</b>
310	200	0.08181	2522
315	200	0.08638	2511
320	200	0.08929	2501
330	200	0.09371	2479 2459
340	200	0.09668	2458

TABLE A-12 Continued

Time (min)	Outside Pressure	Change in	Total Axial
	(psi)	Diameter (in)	Force (lb)
570	200	0.11205	2286
580	200	0.11225	2286
590	200	0.11245	2286
600	200	0.11265	2286

TABLE A-13 Test data, C-5

Material—Ontonagon Clay Density—98.2 lb/ft3 Water Content—24.8% Test Temperature—-12.0°C. Date of Test—22 May 69	Initial Sample Dim Outside Diam. Inside Diam. Height	ensions 5" 1 1/2" 9 3/16"
------------------------------------------------------------------------------------------------------------------	---------------------------------------------------------------	------------------------------------

		<del></del>	
Time (min)	Outside Pressure (psi)	Change in Diameter (in)	Total Axial Force (1b)
0	0	0	0
4	200	0 0.06567	0 2190
10	200	0.08105	2275
15	200	0.08605	2254
20	200	0.08910	2254
30	200	0.09380	2233
40	200	0.09639	2222
50	200	0.09800	2211
60	200	0.09932	2195
70	200	0.10095	2179
80	200	0.10160	2168
90	200	0.10310	2168
100	200	0.10435	2157
110	200	0.10465	2157
120	200	0.10495	2136
130	200	0.10595	2125
140	200	0.10635	2093
150	200	0.10755	2082
160	200	0.10785	2082
170	200	0.10905	2072
180	200	0.10915	2061
190	200	0.10945	2050
200	200	0.10975	2050
210	200	0.10985	2050
220	200	0.11005	2050
230	200	0.11015	2039
240	200	0.11180	2029
250	200	0.11180	2029
260	200	0.11190	2029
270	200	0.11200	2039
280	200	0.11215	2039
290	200	0.11225	2039
300 304	200	0.11235	2039 3901
310	300 300	0.13316 0.14705	3998
315	300	0.15153	3998
320	300	0.15521	3998
330	300	0.15889	4008
340	300	0.16297	3976
<del>۱</del> ۰	300	0.10291	3310

TABLE A-13 Continued

Time (min)	Outside Pressure	Change in	Total Axial
	(psi)	Diameter (in)	Force (lb)
350	300	0.16546	3966
360	300	0.16584	3998
370 380	300	0.16622	3998 3987
390	300 300	0.16762 0.16789	3987
400	300	0.16940	3998
410	300	0.16973	3987
420	300	0.17081	3987
430	300	0.17097	3998
440	300	0.17130	3998
450	300	0.17151	3987
460	300	0.17184	3998
470	300	0.17331	3998
480	300	0.17319	3998
490	300	0.17351	3998
500	300	0.17373	3998
<b>510</b>	300	0.17395	3998
520	300	0.17497	3998
530	300	0.17503	4008
540	300	0.17503	4008
550	300	0.17513	3998
560	300	0.17535	4008
5 <b>7</b> 0	300	0.17557	4008
580	300	0.17562	4008
590	300	0.17573	4008
600	300	0.17703	4008

APPENDIX B

CALIBRATION DATA

#### B-1 CALIBRATION OF DEFORMATION MEASURING APPARATUS

The deformation measuring apparatus described in Section 4.2.1 was calibrated by placing it in a vertical position and moving the brass pieces by measured increments using a micrometer. The micrometer was secured in a vise and was re-centered periodically. The movement of the brass pieces caused movement of the vertical rod which was measured by a Linear Differential Transformer (Sanborn Linearsyn Differential Transformer Model No. 575 DT-500). The LDT was connected electronically to a two-channel recorder (Sanborn Recorder Model 7702B with a Sanborn Carrier Preamplifier Model 8805A). The left channel of the recorder was used with a calibration factor of 337. This provided for a stylus deflection of one division on the chart for each movement of 0.00025 inches through the LDT. Calibration data are given in Table B-1 and the calibration curve is shown in Figure B-1.

TABLE B-1 Calibration data for deformation measuring device

Hole Diameter (in)	Recorder Rdg (Divisions)	Hole Diameter (in)	Recorder Rdg (Divisions)
1.50 1.49 1.48 1.47 1.46 1.45 1.41 1.40 1.39 1.38 1.37 1.36 1.35 1.31 1.32 1.31 1.32 1.31 1.29 1.28 1.27 1.26 1.25	0 23.5 47.0 69.5 91.5 1135.0 156.0 199.0 219.5 239.5 279.0 298.0 317.0 336.5 373.0 391.0 391.0 405.5 425.5 4459.0 475.5	1.24 1.23 1.22 1.21 1.20 1.19 1.18 1.17 1.16 1.15 1.14 1.13 1.12 1.11 1.00 1.09 1.08 1.07 1.06 1.05 1.04 1.03 1.02 1.01 1.00	507.5 523.5 539.5 555.5 571.0 586.0 600.0 614.0 627.5 641.0 654.0 667.0 680.0 693.0 706.0 719.0 731.5 744.0 755.5 767.0 778.0 789.0 789.0 799.5 810.0 820.0

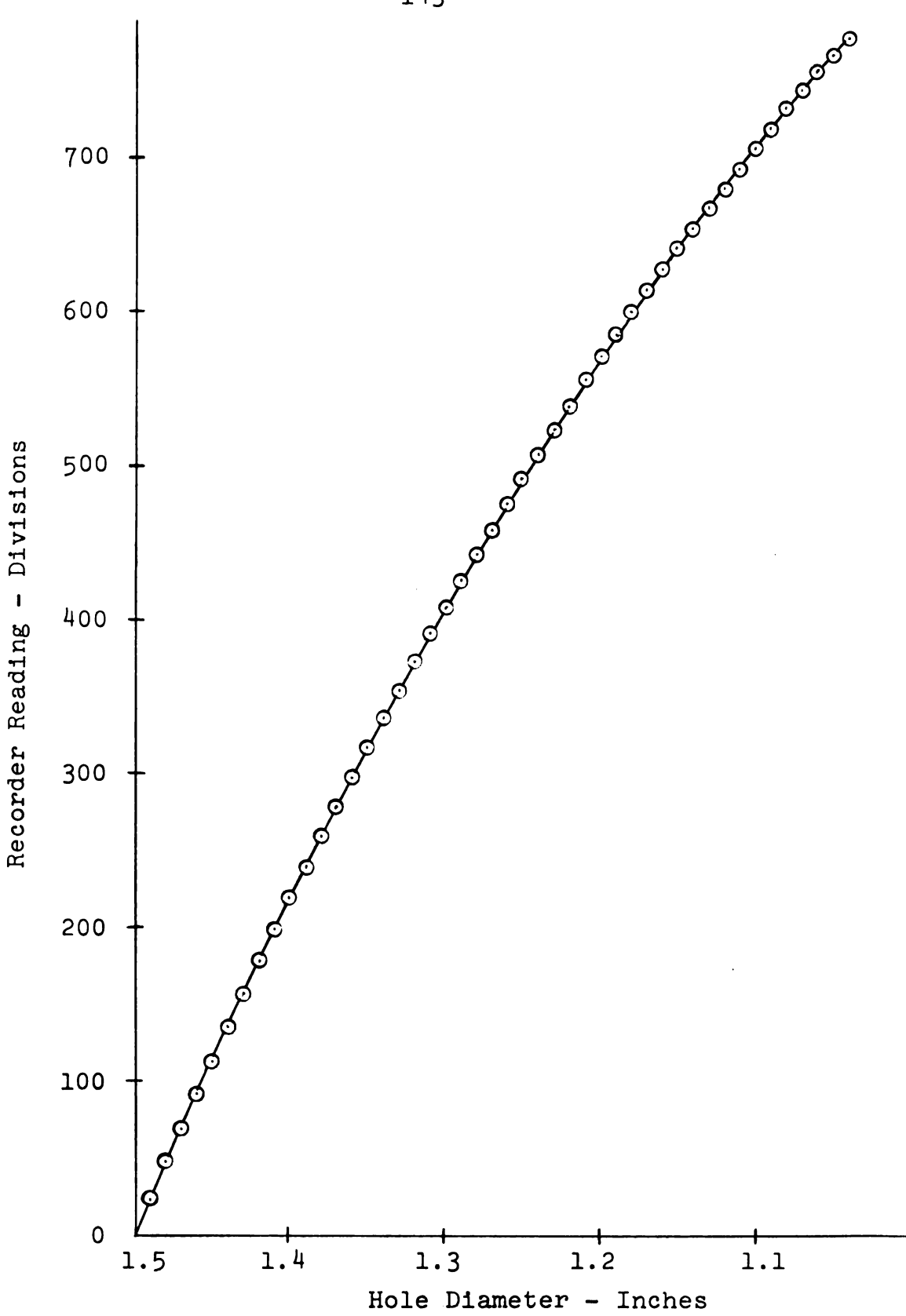


Figure B-l Calibration Curve for Deformation Measuring Device

## B-2 CALIBRATION OF LOAD CELL

The load cell (Strainsert Universal Flat Load Cell, 25000 lb. capacity) was calibrated by loading it in 1000 pound increments using a Tinius Olsen Testing Machine. The load cell was connected electronically to the right channel of the two channel recorder (calibration factor 123.5). Results of the calibration are presented in tabular form in Table B-2 and graphically in Figure B-2.

TABLE B-2 Calibration data for load cell

Load (1b)	Recorder Reading (Divisions)
0	0
1000	94.5
2000	186.0
3000	278.0
4000	372.0
5000	464.0
6000	558.0
7000	653.0
8000	745.0
9000	840.0
10000	931.0

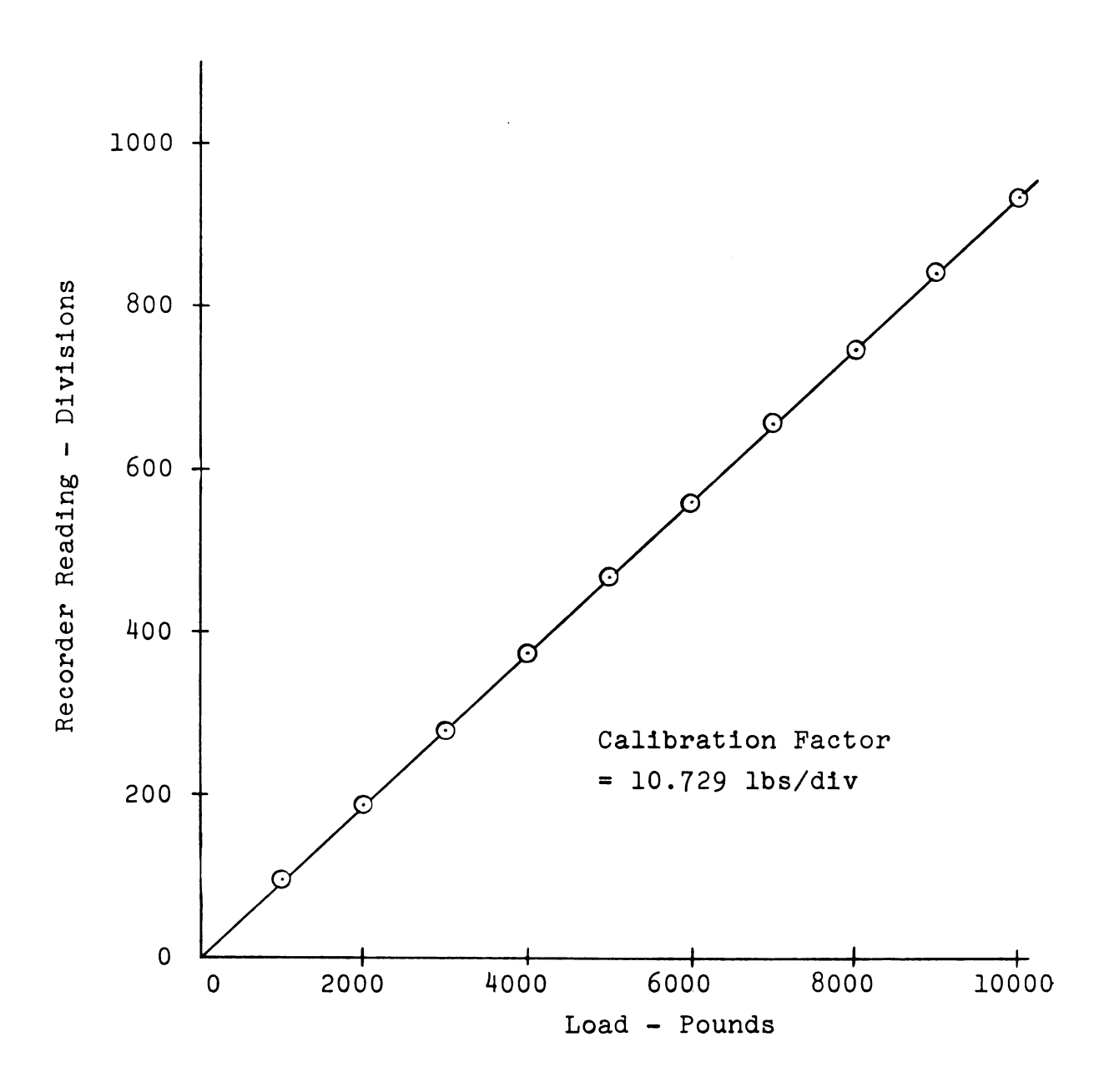


Figure B-2 Calibration Curve for Load Cell

## APPENDIX C

SAMPLE CALCULATIONS

C-1 CALCULATION OF  $\dot{u}_m$  AND  $\dot{\epsilon}_{\theta m}$ 

To find the mean rate of radial displacement from the measured value at the inner surface, recall from Equation (5.23) that

$$\dot{\mathbf{u}} = \frac{a\dot{\mathbf{u}}_{\mathbf{a}}}{r}$$

Thus, for a = 0.75

$$\dot{u}_{m} = \frac{.75\dot{u}_{a} \int_{.75\frac{dr}{r}}^{b}}{\int_{.75}^{b} .75^{dr}}$$

$$= \frac{.75\dot{\mathbf{u}}_{\mathbf{a}} \left[ \ln \mathbf{r} \right]_{.75}^{\mathbf{b}}}{\left[ \mathbf{r} \right]_{.75}^{\mathbf{b}}}$$

$$= \frac{.75\dot{u}_a \left[ ln \ b-ln.75 \right]}{b-.75}$$

$$= \frac{.75\dot{u}_a}{b-.75} \left[ \ln b-\ln.75 \right]$$

Similarly, from Equation (5.24a),

•

$$\dot{\varepsilon}_{\theta} = \frac{a\dot{u}_{a}}{r^{2}}$$

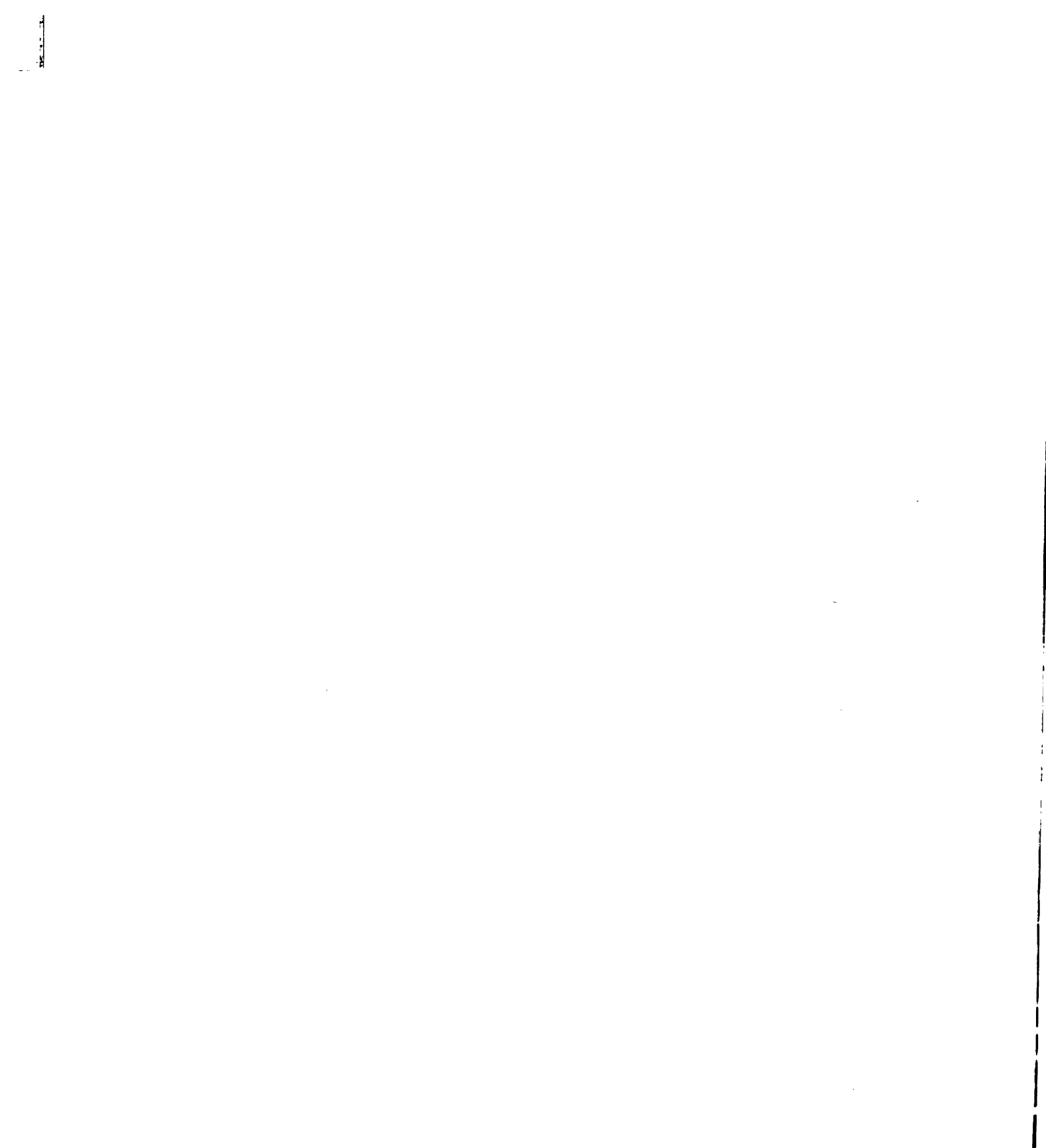
For a = 0.75

$$\varepsilon_{\theta} = \frac{.75\dot{u}_{a} \int_{.75}^{b} \frac{dr}{r^{2}}}{\int_{.75}^{b} dr} = \frac{.75}{b - .75} \begin{bmatrix} 1 \\ b \end{bmatrix} - 1.333 \dot{u}_{a}$$

Table C-1 gives values of  $\dot{u}_m$  and  $\dot{\epsilon}_{\theta m}$  for various values of b.

TABLE C-1 Values of  $\dot{u}_m$  and  $\dot{\epsilon}_{\theta m}$ 

Outside Radius, b (in)	Mean Rate of Radial Displacement, um(in/min)	Mean Rate of Tangential Strain, έ <sub>θm</sub> (min <sup>-1</sup> )
1.75	0.636ů <sub>a</sub>	0.571ů <sub>a</sub>
2.00	0.589ů <sub>a</sub>	0.500ů <sub>a</sub>
2.25	0.550u <sub>a</sub>	0.444ů <sub>a</sub>
2.50	0.515u <sub>a</sub>	0.400ů <sub>a</sub>



## C-2 CALCULATION OF u FROM TEST DATA

To find  $\dot{u}_a$  from test results, it was first necessary to calculate the displacements at the inner surface for the various times. This was done by using the calibration data given in Table B-1. The relationship between the change in hole diameter and the recorder reading was assumed to be linear between the measured values at 0.01 inch increments.

#### SAMPLE CALCULATION:

On Test SA-9, a recording reading of 73.2 would result in a change of diameter,  $\Delta$ , of

$$\Delta = 0.03 + \frac{3.7}{21.5}$$
 (.01) = 0.03168 in.

The radial movement at the inner surface,  $\dot{u}_a$ , was then found by halving this value. The value of  $\dot{u}_a$  was found by plotting  $u_a$  against time and measuring the slope.

#### C-3 CALCULATION OF TOTAL AXIAL FORCE FROM TEST DATA

To find the total axial force,  $F_z$ , from the load cell readings, first calculate the force on the pedestal due to the pressure in the test cell. This was done by computing the area on the bottom of the pedestal, subtracting the exposed area on the top for the size sample in question, and multiplying the result by the pressure. The difference between this result and the force on the load cell as computed according to the calibration data in Figure B-2 represents the total axial force in the sample.

#### SAMPLE CALCULATION:

For Test SA-12, at a time of 513 minutes, the load cell reading was 278.5. The pressure was 700 p.s.i. and the outer radius was 2.25 inches.

Force on Pedestal = 
$$700 \pi \left[ (2.5^2 - 1.5^2) - (2.5^2 - 2.25^2) \right]$$
  
= 9896 lbs.

Force on Load Cell = 278.5 div(10.7291bs/div)

= 2988 lbs.

Total Axial Force = 9896-2988

= 6908 lbs.

# C-4 CALCULATION OF $\dot{u}_a$ , $\sigma_r$ , and $\sigma_\theta$ BY EQUATIONS

The calculation of  $\dot{u}_a$ ,  $\sigma_r$ , and  $\sigma_\theta$ , according to Equations (5.23), (5.22a), and (5.22b), respectively was accomplished by merely substituting the appropriate values for the parameters, dimensions, and pressure directly into these expressions. Due to the long calculation time and the large number of operations, a computer program was written for the CDC 3600 computer to carry out the operations of Equation (5.23) for  $\dot{u}_a$ .

### C-5 CALCULATION OF TOTAL AXIAL FORCE BY EQUATION (5.22c)

The total axial force in the sample was calculated by integrating Equation (5.22c) across the section.

#### SAMPLE CALCULATION:

Take: p = 700 p.s.i.

a = 0.75 in

b = 2.25 in

m = 0.01206

N = 0.00808

 $C = 9.103 \times 10^{-6}$ 

X = 1.66

Substituting these values into Equation (5.22c'), the result is

$$\sigma_{z} = 27.4 + 166.0 \text{ ln r} + 300.3 \text{r}^{1.633}$$

$$F_{z} = \begin{cases} 2\pi \\ 0 \end{cases} \begin{cases} 2.25 \\ .75 \end{cases} [27.4 + 166.01n r + 300.3r^{1.633}] r dr d\theta$$

$$F_z = 2\pi \int_{.75}^{2.25} [27.4r + 166.0r \ln r + 300.3r^{2.633}] dr$$

$$= 2\pi \left[13.7r^{2} + 83.0r^{2}\ln r + 41.5r^{2} + 82.7r^{3.633}\right]^{2.25}.75$$

$$= 2\pi \left\{ 13.7(2.25^2 - .75^2) + 83.0 \left[ 2.25^2 (.811) - (.75)^2 (-.288) \right] + 41.5(2.25^2 - .75^2) + 82.7(14.6 - .4) \right\}$$

- $= 2\pi (1406)$
- = 8828 lbs.

#### C-6 CALCULATION OF PRESSURE BY EQUATION (5.29)

For a given measured  $\dot{u}_a$ , it was necessary to determine the proper  $\dot{\epsilon}$  value from which to choose a c value. This was done by calculating the value of  $\dot{\epsilon}_{\theta m}$  by the coefficients given in Table C-1. The value of  $\alpha$  was then taken from Figure 7.9 and the appropriate value of c calculated.

#### SAMPLE CALCULATION:

From Test SA-12,

a = .75 in

b = 2.25 in

p = 700 psi

 $\dot{u}_a = 6.05 \times 10^{-5} in/min$ 

$$\epsilon_{\theta m} = 6.05 \times 10^{-5} \text{ (.444)} = 3.58 \times 10^{-5} \text{min}^{-1}$$

 $\alpha = 67$  (From Figure 7.9)

For  $\phi = 25^{\circ}$ ,  $\cos \phi = 0.906$ 

$$C = \frac{67}{0.906} = 74.0$$

Substituting into Equation (5.29),

$$p = \frac{2(74.0)(1.570)}{2.46-1} \left[ \left( \frac{2.25}{.75} \right)^{1.46} - 1 \right]$$

= 633 p.s.i.

